

TAG

CG

CER-83/84-30

C. E. - R. R. COPY

COPY 2

WIND-TUNNEL STUDY OF CHIMNEY DOWNWASH  
 AT THE B.L. ENGLAND STATION OF THE  
 ATLANTIC CITY ELECTRIC COMPANY

(REPORT)

by  
 J. E. Cermak<sup>1</sup>, J. A. Peterka<sup>2</sup>  
 and J. A. Beatty<sup>3</sup>



**FLUID MECHANICS AND  
 WIND ENGINEERING PROGRAM**

**COLLEGE OF ENGINEERING**

**COLORADO STATE UNIVERSITY  
 FORT COLLINS, COLORADO**

Engineering Sciences

FEB 11 1985

Branch Library

CER 83-84 JEC-JAP-JAB 30

WIND-TUNNEL STUDY OF CHIMNEY DOWNWASH  
AT THE B.L. ENGLAND STATION OF THE  
ATLANTIC CITY ELECTRIC COMPANY

(REPORT)

by

J. E. Cermak<sup>1</sup>, J. A. Peterka<sup>2</sup>  
and J. A. Beatty<sup>3</sup>

prepared for

Stearns-Roger Engineering Corporation  
4500 Cherry Creek Drive  
Denver, Colorado 80217

Fluid Mechanics and Wind Engineering Program  
Fluid Dynamics and Diffusion Laboratory  
Colorado State University  
Fort Collins, Colorado 80523

June 1984

CER83-84JEC-JAP30

<sup>1</sup>Professor-in-Charge, Fluid Mechanics and Wind Engineering Program, and Director, Fluid Dynamics and Diffusion Laboratory, Colorado State University.

<sup>2</sup>Professor, Department of Civil Engineering, Colorado State University.

<sup>3</sup>Research Engineer, Department of Civil Engineering, Colorado State University.

## ABSTRACT

The Atlantic City Electric Company has measured SO<sub>2</sub> concentrations, downwind from one of their electrical power generating stations, which occasionally exceed regulatory limitations. The problem (suspected to be plume downwash induced by adjacent buildings) was referred to the Stearns-Roger Engineering Corporation for further study. The study included wind-tunnel simulation, which was subcontracted to Colorado State University.

Diffusion tests were subsequently conducted on a 1:300 scale model of the B. L. England Station (a coal and oil fired electrical power generation facility) in the CSU Meteorological Wind Tunnel. Their purpose was to confirm the downwash and to determine the effect of various changes in stack/site configuration upon plume behavior.

The model tests, conducted at pre-selected wind directions and velocities, included physical alterations in the station site, increases in momentum and buoyancy of the flue gases, increases in height of the existing stacks, and inspection of two new stacks - GEP and greater.

Data obtained included ground-level concentration measurements for all tests and visualization of selected configurations. The model tracer gas concentrations were converted to equivalent prototype SO<sub>2</sub> concentrations for comparison with any similar field data. The visualization studies were documented on 35 mm slides, B&W photos, and video cassette.

Evaluation of test results indicates that significant downwash is caused by the boiler buildings. The data further reveal that those configurations which increased the plume height above the building influence are practicable measures to mitigate the downwash phenomenon. Extension of the existing stacks when accompanied by flue gas reheat provide SO<sub>2</sub> reductions nearly equal to a GEP stack.

## TABLE OF CONTENTS

<u>Section</u>	<u>Page</u>
ABSTRACT . . . . .	i
LIST OF TABLES . . . . .	iii
LIST OF FIGURES . . . . .	v
LIST OF ABBREVIATIONS AND SYMBOLS . . . . .	ix
1.0 INTRODUCTION . . . . .	1
1.1 Historical Background . . . . .	1
1.2 Purpose . . . . .	1
1.3 Report Organization . . . . .	2
2.0 EXPERIMENTAL CONFIGURATION . . . . .	4
2.1 Wind Tunnel . . . . .	4
2.2 Model Environment . . . . .	4
2.3 Model Construction . . . . .	5
2.4 Velocity Data . . . . .	6
3.0 SIMILARITY REQUIREMENTS . . . . .	16
3.1 General . . . . .	16
3.2 Model Flexibility/Limitations . . . . .	18
3.3 Model Time Scale . . . . .	21
3.4 Scale Up/Scale Down . . . . .	21
3.5 Similarity Verification . . . . .	23
4.0 CONCENTRATION MEASUREMENTS . . . . .	28
4.1 General . . . . .	28
4.2 Tracer Gases . . . . .	28
4.3 Test Procedure . . . . .	29
4.4 Sample Concentration Calculation . . . . .	30
4.5 Data Analysis . . . . .	31
5.0 VISUALIZATION STUDY . . . . .	96
5.1 General . . . . .	96
5.2 Visualization Tests . . . . .	96
5.3 Data Analysis . . . . .	97
6.0 DISCUSSION AND CONCLUSIONS . . . . .	102
7.0 REFERENCES . . . . .	105
APPENDICES (SEPARATELY BOUND)	
Appendix A - CONCENTRATION DATA FOR BLES	
Appendix B - CONCENTRATION ISOPLETHS	

## LIST OF TABLES

<u>Table</u>	<u>Page</u>
4-1 Run Numbers and Model Parameters Used on BLES Wind Tunnel Tests . . . . .	33
4-2 Prototype Operating Conditions Used in Model Calculations . . . . .	45
4-3a Tabulation of SO <sub>2</sub> Concentrations (µg/m <sup>3</sup> ) and Percentage Change from Existing Configuration for a 8.94 m/s (20 mph) Wind Speed and Full Power Load . . . .	46
4-3b Tabulation of SO <sub>2</sub> Concentrations (µg/m <sup>3</sup> ) and Percentage Change from Existing Configuration for a 11.18 m/s (25 mph) Wind Speed and Full Power Load . . .	47
4-3c Tabulation of SO <sub>2</sub> Concentrations (µg/m <sup>3</sup> ) and Percentage Change from Existing Configuration for a 13.41 m/s (30 mph) Wind Speed and Full Power Load . . .	48
4-3d Tabulation of SO <sub>2</sub> Concentrations (µg/m <sup>3</sup> ) and Percentage Change from Existing Configuration for a 16.76 m/s (37.5 mph) Wind Speed and Full Power Load . .	49
4-3e Tabulation of SO <sub>2</sub> Concentrations (µg/m <sup>3</sup> ) and Percentage Change from Existing Configuration for a 20.12 m/s (45 mph) Wind Speed and Full Power Load . . .	50
4-4a Tabulation of SO <sub>2</sub> Concentrations (µg/m <sup>3</sup> ) and Percentage Change from Existing Configuration for a 8.94 m/s (20 mph) Wind Speed and Minimum Power Load . .	51
4-4b Tabulation of SO <sub>2</sub> Concentrations (µg/m <sup>3</sup> ) and Percentage Change from Existing Configuration for a 11.18 m/s (25 mph) Wind Speed and Minimum Power Load . .	52
4-4c Tabulation of SO <sub>2</sub> Concentrations (µg/m <sup>3</sup> ) and Percentage Change from Existing Configuration for a 13.41 m/s (30 mph) Wind Speed and Minimum Power Load . .	53
4-4d Tabulation of SO <sub>2</sub> Concentrations (µg/m <sup>3</sup> ) and Percentage Change from Existing Configuration for a 16.76 m/s (37.5 mph) Wind Speed and Minimum Power Load . .	54
4-4e Tabulation of SO <sub>2</sub> Concentrations (µg/m <sup>3</sup> ) and Percentage Change from Existing Configuration for a 20.12 m/s (45 mph) Wind Speed and Minimum Power Load . .	55

<u>Table</u>		<u>Page</u>
5-1	Identification Key for 35 mm Color Slides and Black and White Photos of B. L. England Station Wind-Tunnel Tests . . . . .	98
6-1	Tabulation of Percentage Reduction in SO <sub>2</sub> Concentrations for Specified Changes in Stack Operation/Configuration . . . . .	104

## LIST OF FIGURES

<u>Figure</u>		<u>Page</u>
2-1	Meteorological Wind Tunnel, Fluid Dynamics and Diffusion Laboratory, Colorado State University . . . . .	8
2-2	Schematic of MWT Test Section . . . . .	9
2-3	Prototype (a) and Model (b) Photos of the B. L. England Station . . . . .	10
2-4	Upwind (a) and Downwind (b) Views of the BLES Model Installed on MWT Turntable . . . . .	11
2-5	Extensions and Nozzles Used to Alter Configurations of Basic Model Stacks . . . . .	12
2-6	Comparison of Existing Stacks with a 385' Three-Flue Chimney . . . . .	12
2-7	Vertical Profiles of Mean Velocity and Turbulence Intensity for a Stack Height Velocity, $u_s = 1.32$ m/s . . .	13
2-8	Gas Chromatograph Output ( $C_2H_6$ only) for February 1984 and May 1984 Tests at Various Wind Speeds (mph) as a Function of Distance from the Source . . . . .	14
2-9	Comparison of February 1984 (original) to May 1984 (revised) Prototype Wind Speeds . . . . .	15
3-1	Predicted $SO_2$ Concentrations at Sampling Point #25 Based on Model Studies . . . . .	27
4-1	Location/Identification of Ground-level Sampling Grid Used in BLES Diffusion Study . . . . .	56
4-2	Photographs of (a) the Gas Sampling System, and (b) the HP Integrator and Chromatograph . . . . .	57
4-3a	Effect of Reheat on Ground-level $SO_2$ Concentrations Along Plume Centerline for a 30 mph/198° Wind and Full Power Load . . . . .	58
4-3b	Effect of Reheat on Ground-level $SO_2$ Concentrations Along Plume Centerline for a 25 mph/198° Wind and Full Power Load . . . . .	59
4-3c	Effect of Reheat on Ground-level $SO_2$ Concentrations Along Plume Centerline for a 20 mph/198° Wind and Full Power Load . . . . .	60

<u>Figure</u>	<u>Page</u>
4-3d Effect of Reheat on Ground-level SO <sub>2</sub> Concentrations at 2.7 km for a 30 mph/198° Wind and Full Power Load . . .	61
4-3e Effect of Reheat on Ground-level SO <sub>2</sub> Concentrations at 2.7 km for a 25 mph/198° Wind and Full Power Load . . .	62
4-3f Effect of Reheat on Ground-level SO <sub>2</sub> Concentrations at 2.7 km for a 20 mph/198° Wind and Full Power Load . . .	63
4-4a Effect of Reheat on Ground-level SO <sub>2</sub> Concentrations Along Plume Centerline for a 30 mph/198° Wind and Minimum Power Load . . . . .	64
4-4b Effect of Reheat on Ground-level SO <sub>2</sub> Concentrations Along Plume Centerline for a 25 mph/198° Wind and Minimum Power Load . . . . .	65
4-4c Effect of Reheat on Ground-level SO <sub>2</sub> Concentrations Along Plume Centerline for a 20 mph/198° Wind and Minimum Power Load . . . . .	66
4-4d Effect of Reheat on Ground-level SO <sub>2</sub> Concentrations at 2.7 km for a 30 mph/198° Wind and Minimum Power Load . . .	67
4-4e Effect of Reheat on Ground-level SO <sub>2</sub> Concentrations at 2.7 km for a 25 mph/198° Wind and Minimum Power Load . . .	68
4-4f Effect of Reheat on Ground-level SO <sub>2</sub> Concentrations at 2.7 km for a 20 mph/198° Wind and Minimum Power Load . . .	69
4-5a Effect of 50' Extensions on Ground-level SO <sub>2</sub> Concentrations Along Plume Centerline for a 30 mph/198° Wind and Full Power Load . . . . .	70
4-5b Effect of 50' Extensions on Ground-level SO <sub>2</sub> Concentrations Along Plume Centerline for a 25 mph/198° Wind and Full Power Load . . . . .	71
4-5c Effect of 50' Extensions on Ground-level SO <sub>2</sub> Concentrations Along Plume Centerline for a 20 mph/198° Wind and Full Power Load . . . . .	72
4-5d Effect of 50' Extensions on Ground-level SO <sub>2</sub> Concentrations at 2.7 km for a 30 mph/198° Wind and Full Power Load . . . . .	73
4-5e Effect of 50' Extensions on Ground-level SO <sub>2</sub> Concentrations at 2.7 km for a 25 mph/198° Wind and Full Power Load . . . . .	74
4-5f Effect of 50' Extensions on Ground-level SO <sub>2</sub> Concentrations at 2.7 km for a 20 mph/198° Wind and Full Power Load . . . . .	75

<u>Figure</u>	<u>Page</u>
4-6a Effect of 50' Extensions on Ground-level SO <sub>2</sub> Concentrations Along Plume Centerline for a 30 mph/198° Wind and Minimum Power Load . . . . .	76
4-6b Effect of 50' Extensions on Ground-level SO <sub>2</sub> Concentrations at 2.7 km for a 30 mph/198° Wind and Minimum Power Load . . . . .	77
4-7a Effect of Added Air on Ground-level SO <sub>2</sub> Concentrations Along Plume Centerline for a 30 mph/198° Wind and Full Power Load . . . . .	78
4-7b Effect of Added Air on Ground-level SO <sub>2</sub> Concentrations Along Plume Centerline for a 25 mph/198° Wind and Full Power Load . . . . .	79
4-7c Effect of Added Air on Ground-level SO <sub>2</sub> Concentrations Along Plume Centerline for a 20 mph/198° Wind and Full Power Load . . . . .	80
4-7d Effect of Added Air on Ground-level SO <sub>2</sub> Concentrations at 2.7 km for a 30 mph/198° Wind and Full Power Load . . . . .	81
4-7e Effect of Added Air on Ground-level SO <sub>2</sub> Concentrations at 2.7 km for a 25 mph/198° Wind and Full Power Load . . . . .	82
4-7f Effect of Added Air on Ground-level SO <sub>2</sub> Concentrations at 2.7 km for a 20 mph/198° Wind and Full Power Load . . . . .	83
4-8a Effect of Added Air on Ground-level SO <sub>2</sub> Concentrations Along Plume Centerline for a 30 mph/198° Wind and Minimum Power Load . . . . .	84
4-8b Effect of Added Air on Ground-level SO <sub>2</sub> Concentrations Along Plume Centerline for a 25 mph/198° Wind and Minimum Power Load . . . . .	85
4-8c Effect of Added Air on Ground-level SO <sub>2</sub> Concentrations Along Plume Centerline for a 20 mph/198° Wind and Minimum Power Load . . . . .	86
4-8d Effect of Added Air on Ground-level SO <sub>2</sub> Concentrations at 2.7 km for a 30 mph/198° Wind and Minimum Power Load . . . . .	87
4-8e Effect of Added Air on Ground-level SO <sub>2</sub> Concentrations at 2.7 km for a 25 mph/198° Wind and Minimum Power Load . . . . .	88

<u>Figure</u>	<u>Page</u>
4-8f Effect of Added Air on Ground-level SO <sub>2</sub> Concentrations at 2.7 km for a 20 mph/198° Wind and Minimum Power Load . . . . .	89
4-9a Effect of Wind Speed on Ground-level SO <sub>2</sub> Concentrations Along Plume Centerline with Full Power Load for Existing BLES Configuration . . . . .	90
4-9b Effect of Wind Speed on Ground-level SO <sub>2</sub> Concentrations at 2.7 km with Full Power Load for Existing BLES Configuration . . . . .	91
4-9c Effect of Wind Speed on Ground-level SO <sub>2</sub> Concentrations Along Plume Centerline with Minimum Power Load for Existing BLES Configuration . . . . .	92
4-9d Effect of Wind Speed on Ground-level SO <sub>2</sub> Concentrations at 2.7 km with Minimum Power Load for Existing BLES Configuration . . . . .	93
4-10a Effect of Wind Speed on Ground-level SO <sub>2</sub> Concentrations at Sampling Point #25 with a Full Power Load . . . . .	94
4-10b Effect of Wind Speed on Ground-level SO <sub>2</sub> Concentrations at Sampling Point #25 with a Minimum Power Load . . . . .	95
5-1 Flow Visualization at 45 mph, 198° Direction and Minimum Power for: (a) Basic, (b) 390° Reheat and, (c) 50' Extensions plus 390° Reheat Conditions . . . . .	99
5-2 Flow Visualization at 45 mph, 198° Direction and Full Power for: (a) Basic, (b) 390° Reheat and, (c) 50' Extensions plus 390° Reheat Conditions . . . . .	100
5-3 Flow Visualization at 45 mph, 198° Direction and Full Power for: (a) 50' Extensions at 260°, (b) Basic w/o Buildings and, (c) 425' Multiple Flue Stack . . . . .	101

## LIST OF ABBREVIATIONS AND SYMBOLS

<u>Abbreviations</u>	<u>Definitions</u>	<u>Units</u>
ABL	Atmospheric Boundary Layer	
ACL	Atlantic City Electric	
AGL	Above Ground Level	
B&W	Black and White	
BG	Background	
BLES	B. L. England Station	
CALFAC	Calibration Factor ( $\mu\text{v}\cdot\text{sec}/\text{ppm}$ )	
CSU	Colorado State University	
FDDL	Fluid Dynamics and Diffusion Laboratory	
GC	Gas Chromatograph	
GEP	Good Engineering Practice	
MWT	Meteorological Wind Tunnel	
S.F.	Scale Factor	
S.S.	Source Strength (ppm)	
Fr	Froude Number $\frac{u_s^2 \rho_a}{g\Delta\gamma D}$	
Re	Reynolds Number $\frac{u_s \rho_a B}{\mu_a}$	
Ro	Rossby Number $\frac{u_s}{H\Omega}$	
 <u>Symbol</u>		
A	cross-sectional area of stack exit	( $\text{m}^2$ )
B	building dimension	(m)
D	diameter of stack	(m)
g	gravitational acceleration	( $\text{m}/\text{sec}^2$ )
H	height of stack	(m)
Q	volume flow	( $\text{gm}/\text{sec}, \text{m}^3/\text{sec}$ )

<u>Symbol</u>	<u>Definition</u>	<u>Units</u>
t	time duration	(sec)
u	characteristic velocity	(m/sec)
$u_{ref}$	reference velocity	(m/sec)
$u_s$	wind velocity at stack height	(m/sec)
$\bar{u}$	mean velocity	(m/sec)
V	exit velocity of stack gas	(m/sec)
z	height	(m)
$z_{ref}$	reference height	(m)
$z_o$	aerodynamic roughness height	(m)
<u>Greek</u>		
$\gamma$	density ratio $(\rho_a - \rho_s)/\rho_a$	-
$\Delta$	difference in density	(kg/m <sup>3</sup> )
$\delta$	boundary layer thickness	(m)
$\theta$	angular direction	(rad)
$\mu$	dynamic viscosity	(kg/m·sec)
$\rho$	density	(kg/m <sup>3</sup> )
$\sigma$	standard deviation	-
$\Omega$	angular velocity	(rad/sec)
<u>Subscripts</u>		
a	ambient	
m	model	
o	reference	
p	prototype	
s	stack	

## 1.0 INTRODUCTION

### 1.1 Historical Background

The Atlantic City Electric Company (ACE) operates an electrical power generating facility in southern New Jersey, herein referred to as the B. L. England Station (BLES). The station is situated approximately 0.9 km west of the Garden State Parkway and upon the southerly shore of the Great Egg Harbor Bay, in Cape May County, N.J.

The facility consists of two coal-fired boilers and a third oil-fired boiler which have a combined emission rate of approximately 2220 grams of sulfur dioxide per second, when operating at full capacity, and 855 grams SO<sub>2</sub>/second, under minimum load conditions.

The operator, who maintains an SO<sub>2</sub> monitor at Somers Point Marina (~N18°E, 2.7 km from the BLES), has recorded SO<sub>2</sub> concentrations which are near, or exceed, federal-state imposed air-quality standards during certain meteorological conditions. Particular concern centered about winds from 195°-203° and above 20 mph.

Stearns-Roger Engineering Corporation, of Denver, Colorado was contracted to provide an "engineering fix" for the SO<sub>2</sub> concentration problem. Having established a need for an evaluation of potential solutions, the Stearns-Roger Corporation subsequently sub-contracted with the Fluid Dynamics and Diffusion Laboratory (FDDL), under the direction of Dr. J. E. Cermak, at Colorado State University, for a wind-tunnel study of a reasonable number of potential fixes on a scale model of the BLES.

### 1.2 Purpose

Since high levels of SO<sub>2</sub> concentration were recorded when the BLES chimneys were generally downwind of the boiler buildings, and when

ambient winds were in excess of 20 mph, it was surmised that an objectionable plume downwash was created in the building wake.

The downwash theory, although clearly credible, required substantiation. Some method for testing the relative effectiveness of potential changes is also desirable. The only reliable prediction technique is that of actual measurement, either at the prototype site, or on a properly scaled wind-tunnel model. Since field measurements and physical modifications are far too costly and impractical for consideration, wind-tunnel modelling provided both a practical and reasonable method for accomplishing the desired investigations.

Through the wind-tunnel study, in a simulated neutrally stable and isothermal atmosphere, the investigators sought to establish and document the effect of the boiler building complex upon ground-level concentration of stack effluents at selected wind directions-velocities and to rate the effectiveness of proposed solutions.

### 1.3 Report Organization

The remainder of this report contains documentation of the experimental configuration, similarity requirements, test methods, test parameters, data analysis, data presentation and conclusions. A generalized format follows:

- Chapter 2.0, EXPERIMENTAL CONFIGURATION, contains descriptions of the wind-tunnel, model assembly, model environment, model location, velocity profiles, and related information.
- Chapter 3.0, SIMILARITY REQUIREMENTS (MODEL/PROTOTYPE SCALING) contains a discussion of modelling flexibility/limitations, time scaling, modelling techniques, Reynolds number independence, velocity corrections and similar information.

- Chapter 4.0, CONCENTRATION DATA, contains tables of the test program, sample locations, measurement-analysis procedures, a sample calculation of the measured concentrations and graphs of selected data.
- Chapter 5.0, VISUALIZATION DATA, provides a key for identifying photos of documented airflows and pictorial presentation of selected studies.
- Chapter 6.0, DISCUSSION AND CONCLUSION, provides a synopsis of the study's validity and tabulated data results.
- Appendices A and B contain computer printouts of all test runs and isopleths of measured ground-level concentrations, respectively.

## 2.0 EXPERIMENTAL CONFIGURATION

### 2.1 Wind Tunnel

All BLES model studies were accomplished in the Meteorological Wind Tunnel (MWT) of the Fluid Dynamics and Diffusion Laboratory at Colorado State University. Elevation and plan views of the MWT are contained in Figure 2-1. This wind tunnel, specially designed to simulate atmospheric boundary layers (ABL), has an approximately 2 m square and 26 m long test section. Design and operation of the MWT are described in detail by Cermak (1).

The tunnel has a flexible roof which can be adjusted to maintain a zero pressure gradient along the test section. Adjustment was unnecessary for these studies since blockage created by the model was insignificant.

Thermal stratification in the MWT corresponded to a neutral stratification in the atmosphere since the airflow, without supplemental heating or cooling of the tunnel boundaries, was isothermal.

### 2.2 Model Environment

The area of the test section which was downwind from the BLES model was covered with smooth Masonite to simulate roughness of the Great Egg Harbor Bay water surface. That portion of the test section which was upstream from the model was also covered with a uniform roughness constructed from Masonite with  $\frac{1}{4}$ " holes and  $\frac{1}{4}$ " diameter x  $\frac{1}{2}$ " long dowels placed in a 2" x 8" pattern. The upwind roughness was selected to simulate terrain SW of the station.

Five evenly spaced 1.07 m tall spires and a 15 cm high trip were installed at the tunnel entrance to create the desired ABL within the

test section. Pertinent theories of ABL simulation are discussed in detail by Cermak (2,3).

Figure 2-2 provides documentation in the form of a schematic drawing of the entire test section length, which includes: spire and trip location, upwind roughness, turntable location, downwind roughness and pertinent dimensions. (The location of velocity profile measurements and velocity reference probes, discussed in Section 2.4, are also located on this schematic.)

### 2.3 Model Construction

The 1:300 scale model of the BLES used for the wind-tunnel tests was fabricated within the FDDL, with assistance from the Engineering Research Center, Machine Shop.

The BLES is comprised of three abutted boiler units and their attendant stacks, precipitators and generators. The site also contains a coal storage/handling complex, a crusher, several bulk storage tanks, and a large cooling tower, as well as administrative, maintenance, and related buildings used in the station's operation. The wind tunnel model consisted of a circular area 1.5 m (450 m prototype) in diameter, centered upon the number two stack. Nearby significant features, outside that circle, were also modelled.

The boiler buildings, which are approximately 150' AGL, and the three stacks, which rise to 250' above grade, were of primary interest, and therefore modelled in the most detail. The existing stacks, extensions, nozzles and GEP stacks were machined from brass and acrylic stock to obtain accurate modelling of heights, diameters and related critical dimensions. The stacks were aligned on a 135°-315° true azimuth axis. The boiler buildings were similarly oriented and situated

SW of the stacks. All remaining structures were modelled in the detail necessary to provide accurate wind flow patterns over the plant complex. Figures 2-3a and 2-3b provide pictorial comparisons of the prototype and model.

The completed model was affixed to an aluminum turntable (1.5 m diameter), to facilitate simulation of multiple wind directions, prior to installation in the MWT. The turntable was indexed to identify true azimuth wind directions. Figures 2-4a and 2-4b contain pictorial documentation of upwind and downwind views of the installed model.

The comparative size of the existing stacks with the extensions, nozzles and GEP stack are illustrated in Figures 2-5 and 2-6.

#### 2.4 Velocity Data

Velocity profiles of mean velocity,  $\bar{u}$ , and longitudinal turbulence intensity were obtained on the tunnel center-line at positions indicated on Figure 2-2, for a wind speed at stack height,  $u_s = 1.32$  m/s.

Instrumentation used to document the velocity profile and to set the tunnel velocity included: 1) a Datametrics Model 880-LV linear velocimeter and 2) a MKS Baratron Pressure meter.

The mean velocity and turbulence intensity profiles are presented on Figure 2-7. If the boundary layer thickness,  $\delta$ , is defined to be the point where the profiles flatten out, the observed value of  $\delta$  is at least one meter, for a comparable 300 m prototype boundary, corresponding well with the atmospheric boundary layer. Consideration of the terrain near the BLES site suggested that the atmospheric approach flow would be well-described by

$$\frac{u}{u_{\text{ref}}} = \left( \frac{z}{z_{\text{ref}}} \right)^n$$

with a value of  $n = .14$ , and the same value for this exponent was achieved in the wind tunnel, assuring that  $\left(\frac{z_o}{H}\right)_m = \left(\frac{z_o}{H}\right)_p$ . Since  $\left(\frac{\delta}{H}\right)_m = \left(\frac{\delta}{H}\right)_p$  was also achieved, the approach flow was well modelled.

In the course of acquiring "follow-on" data a velocity error was detected, which affected the February 1984 data. Investigation revealed that extensive use of titanium tetrachloride to produce a visible smoke, during early phases of the study, had coated the velocity sensor (hot-wire anemometer). The resultant change in response of the sensor caused a downward shift in indicated velocity values, subsequent to calibration, which affected the tunnel wind speeds. The sensor, ultrasonically cleaned and recalibrated prior to the start of tests on 7 May 1984 revealed the shift which had occurred.

Tests of the BLES in its present configuration were repeated, prior to accomplishing the "follow-on" tests, over a wide range of wind speeds for comparison to the February 1984 data. The results of that comparison are presented on Figure 2-8. Comparable points from the data were selected and replotted on the graph appearing on Figure 2-9. This graph indicated a 1.5 velocity correction factor for all the original data. That factor has been applied to all the February 1984 data contained in this report. The corrected February 1984 data are valid for the revised wind speeds reported.

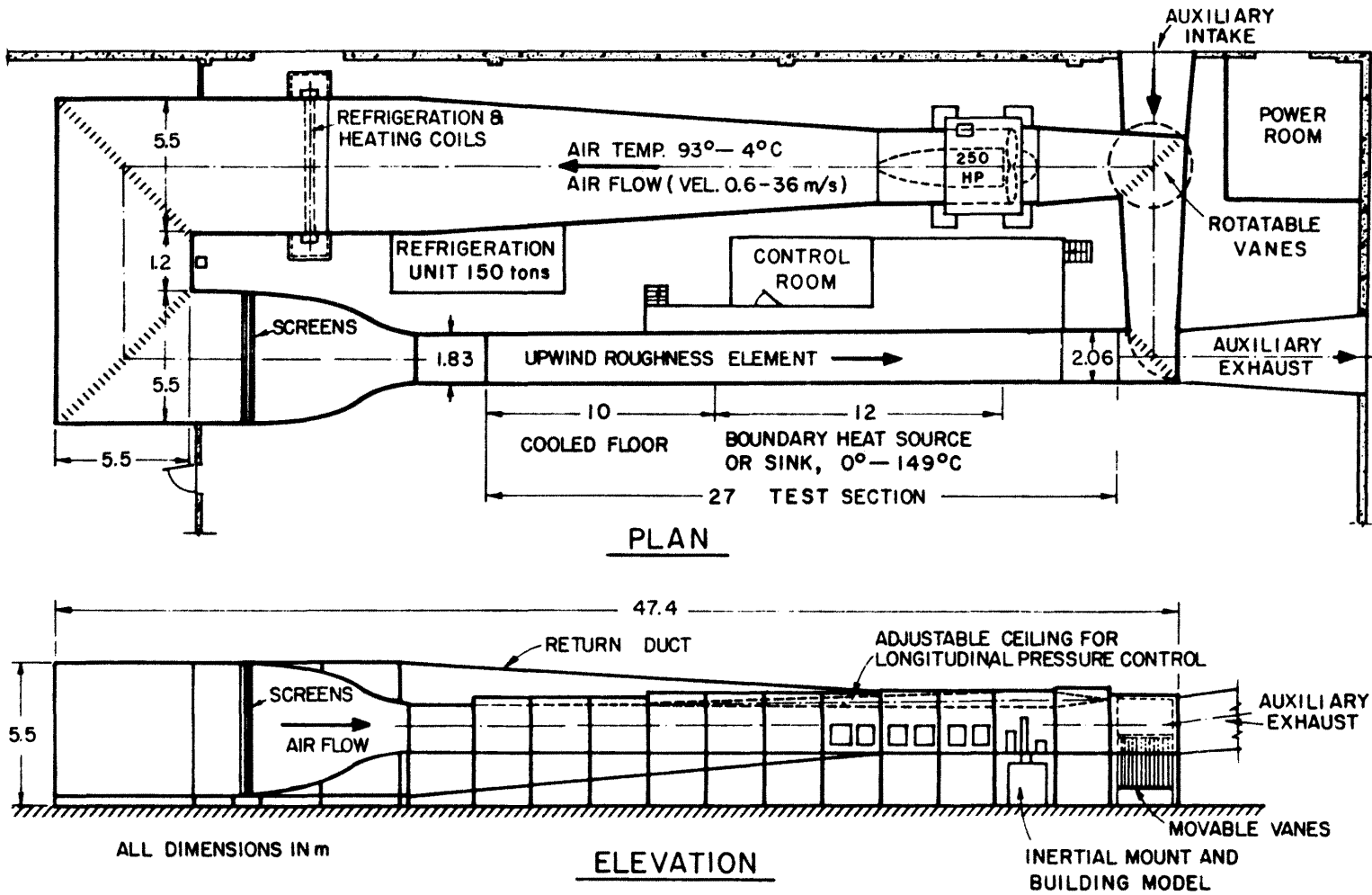
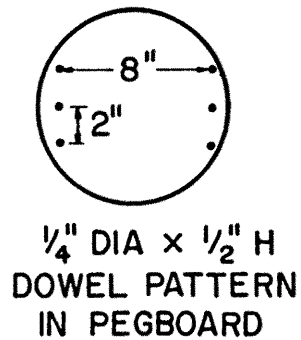
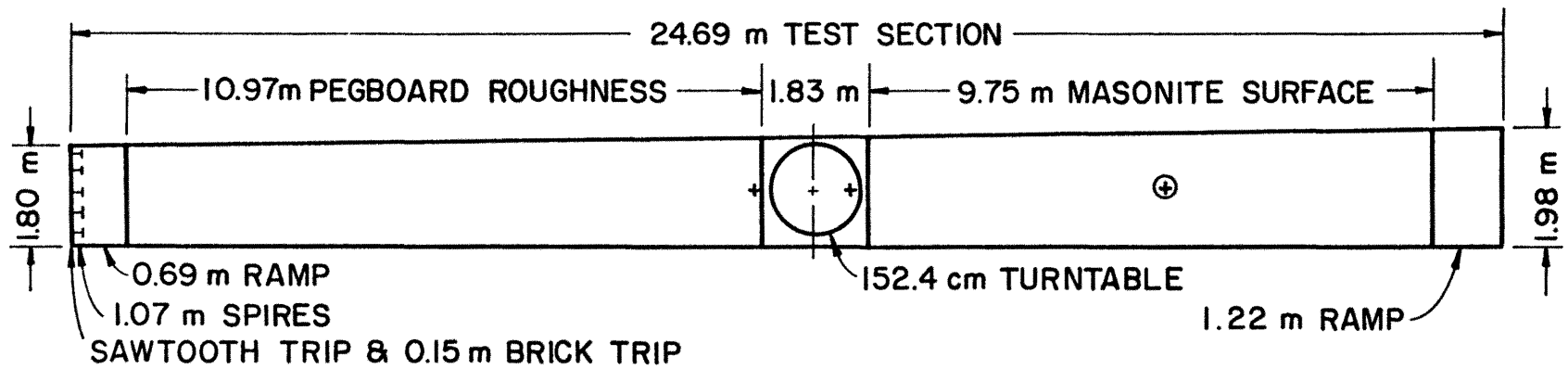


Figure 2-1. Meteorological Wind Tunnel, Fluid Dynamics and Diffusion Laboratory, Colorado State University.



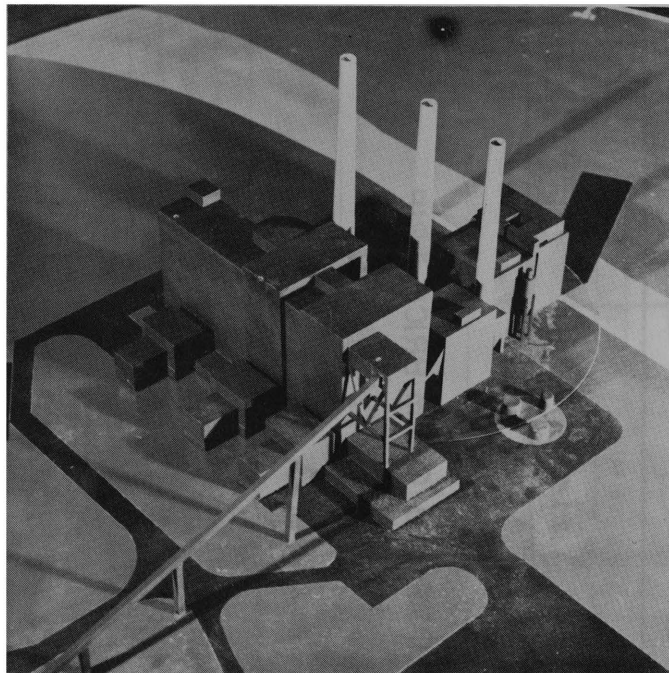
LEGEND:

- DATAMETRICS PROBE AT  
x = 6.1 m & z = 1.2 m
- + VELOCITY PROFILES AT  
x = -1.0, 0.64 & 6.1 m

Figure 2-2. Schematic of MWT Test Section

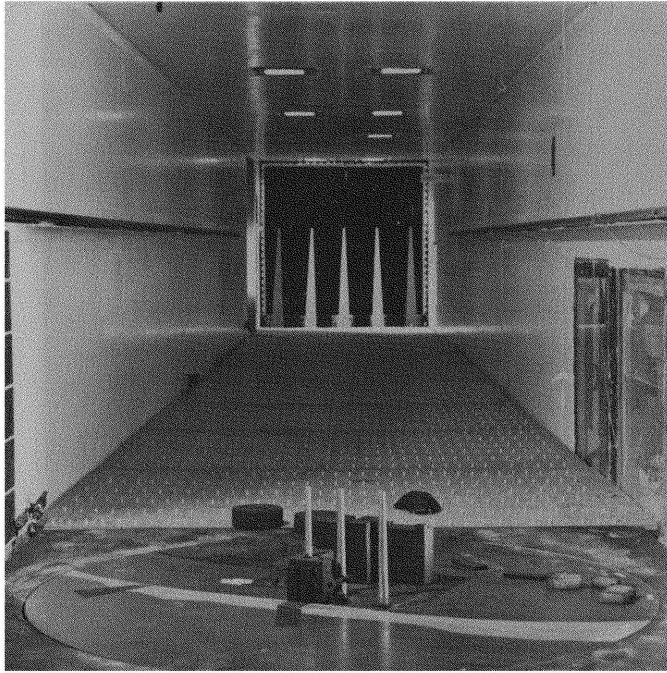


(a)

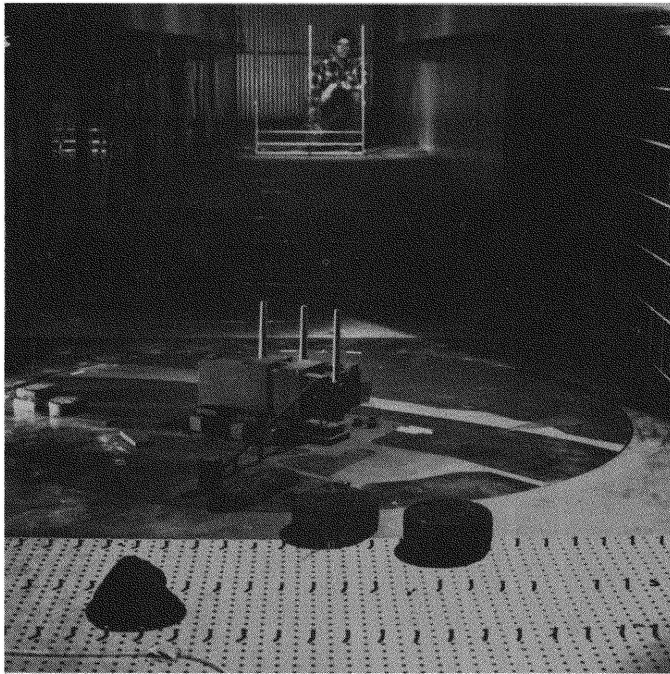


(b)

Figure 2-3. Prototype (a) and Model (b) Photos of the B. L. England Station.



(a)



(b)

Figure 2-4. Upwind (a) and Downwind (b) Views of the BLES Model Installed on MWT Turntable.

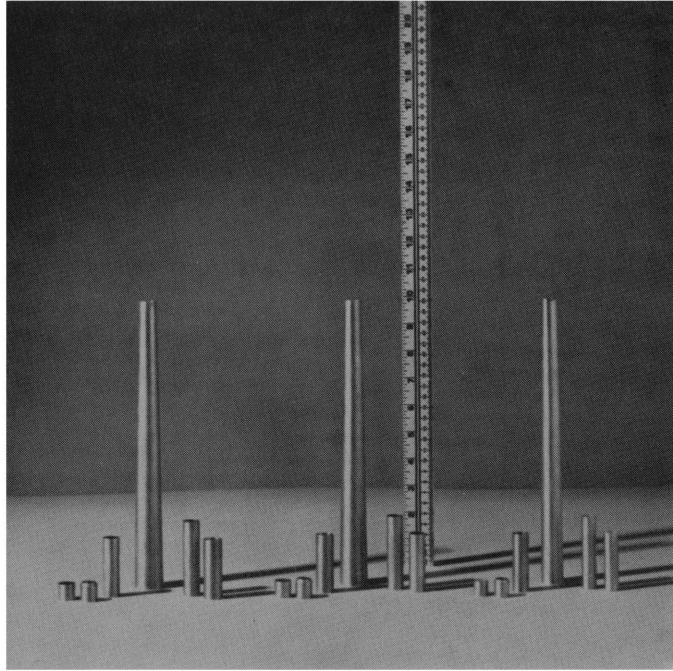


Figure 2-5. Extensions and Nozzles Used to Alter Configuration of Basic Model Stacks.

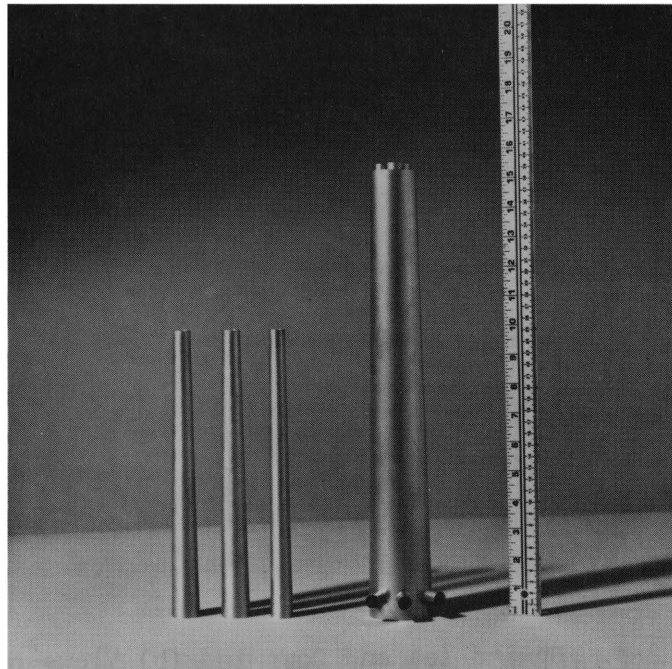


Figure 2-6. Comparison of Existing Stacks with a 385' Three-Flue Chimney.

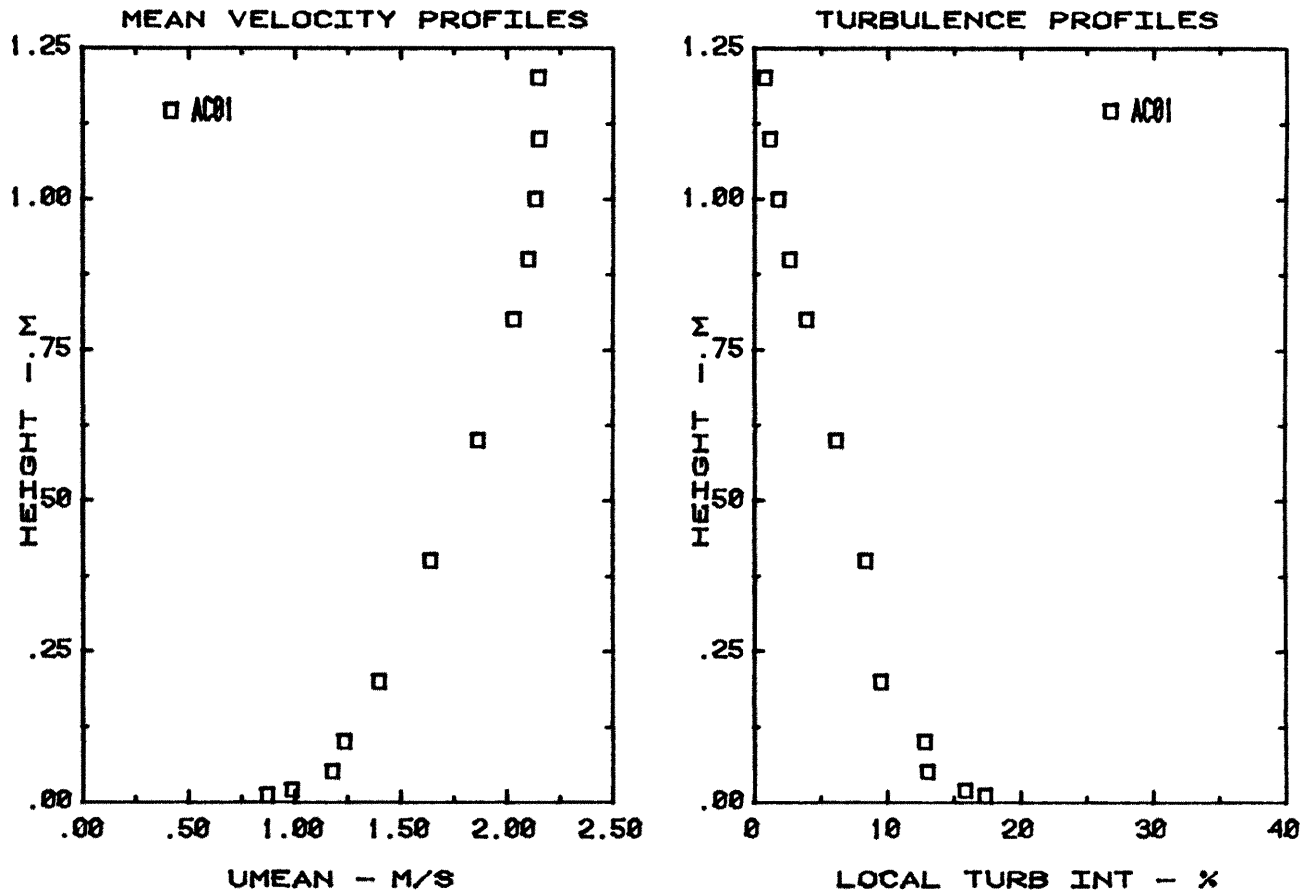


Figure 2-7. Vertical Profiles of Mean Velocity and Turbulence Intensity for a Stack Height Velocity,  $u_s = 1.32$  m/s.

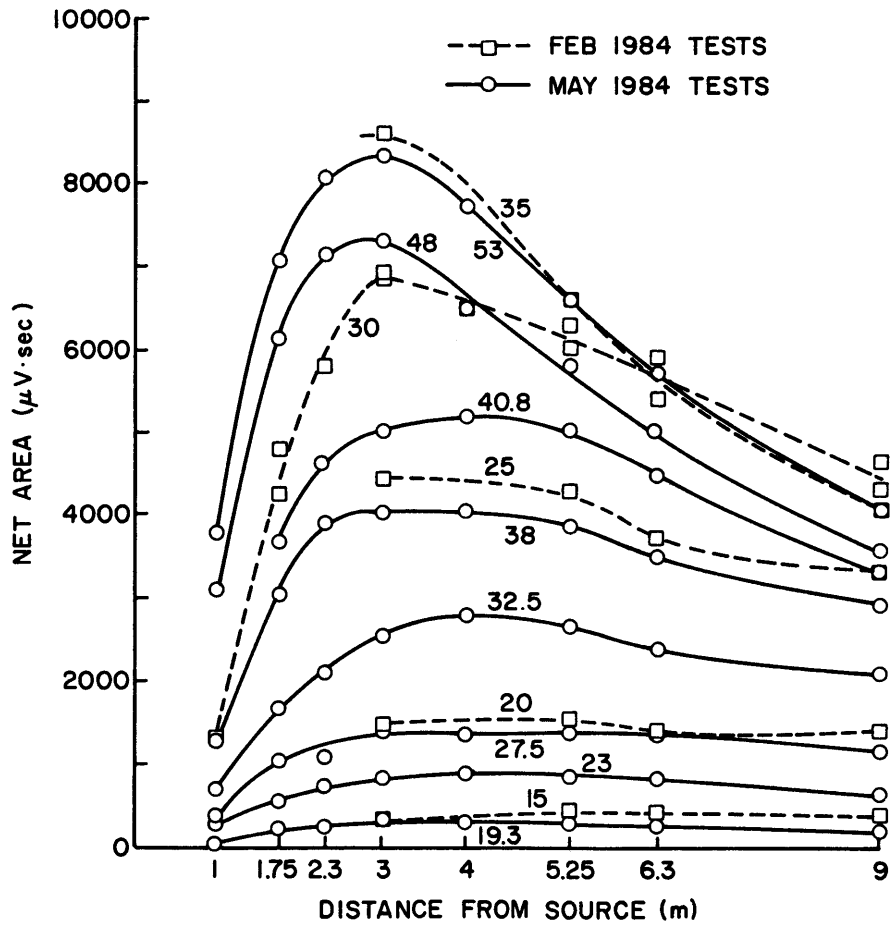


Figure 2-8. Gas Chromatograph Output ( $C_2H_6$  only) for February 1984 and May 1984 Tests at Various Wind Speeds (mph) as a Function of Distance from the Source.

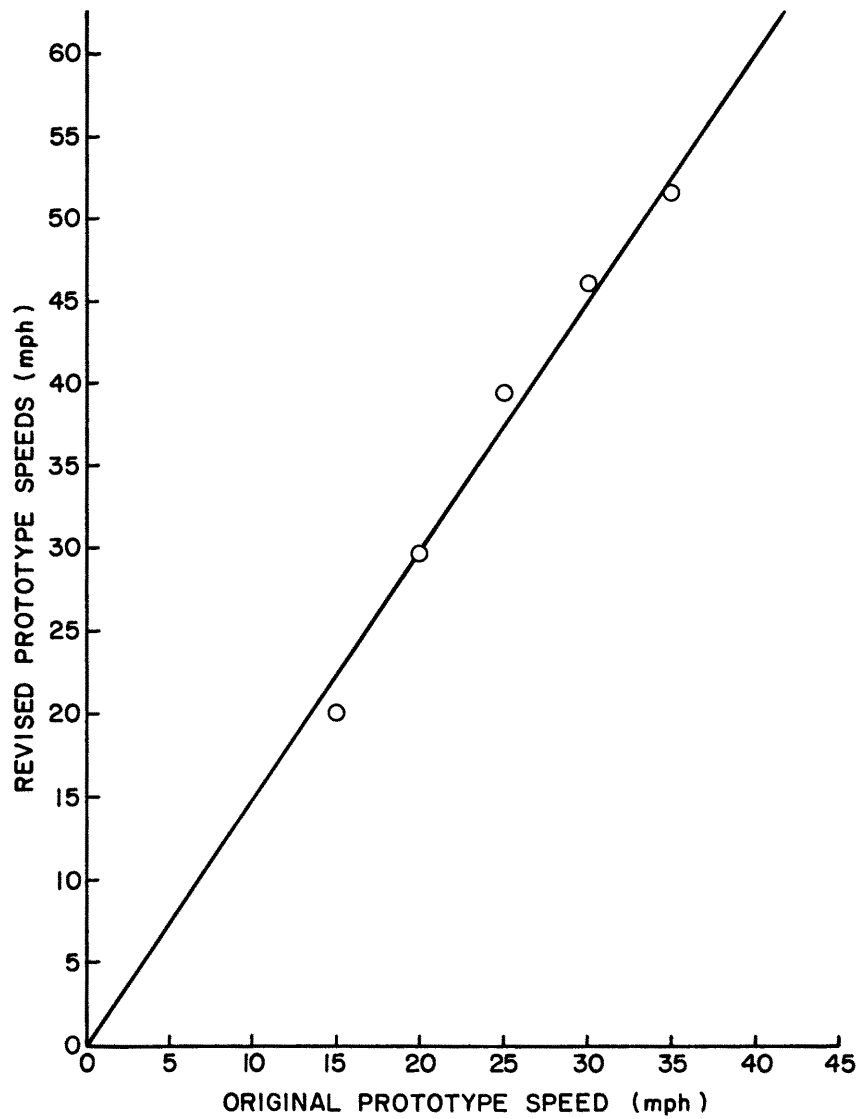


Figure 2-9. Comparison of February 1984 (original) to May 1984 (revised) Prototype Wind Speeds.

### 3.0 SIMILARITY REQUIREMENTS (MODEL/PROTOTYPE SCALING)

#### 3.1 General

Special attention to model and flow considerations are required to assure similitude between model and prototype, in this instance the BLES. Wind tunnel simulation of atmospheric gas diffusion is predicated on the similarity between the wind tunnel and atmospheric flow fields. The criteria for the required similarity have a physical basis in terms of the conservation of mass, momentum and energy. These basic criteria have been discussed in detail by Halitsky (4), Martin (5), Cermak (6), and Lord et al. (7). The model laws may be divided into requirements for geometric, dynamic, kinematic and thermic similarity. In addition, model and prototype similarity of upwind flow characteristics and surface boundary conditions is required.

When interest is focused on the vertical motion of plumes of heated gases emitted from stacks into a thermally neutral atmosphere, the following variables are of primary significance:

$g$  = gravitational acceleration

$\rho_a$  = density of ambient air

$\Delta\gamma = (\rho_a - \rho_s)$

$\Omega$  = local angular velocity component of the earth

$\mu_a$  = dynamic viscosity of ambient air

$u_s$  = velocity of ambient wind at stack height

$V_s$  = exit velocity of stack gas

$B$  = characteristic dimension of building complex

$H$  = stack height

$D$  = stack diameter

$\delta_a$  = thickness of planetary boundary layer

$z_o$  = roughness height for upwind surface

Grouping the independent variables into dimensionless parameters with  $\rho_a$ ,  $u_s$  and  $H$  as reference variables yields the following parameters upon which the dependent quantities of interest must depend:

$$\frac{\delta_a}{H}, \frac{z_o}{H}, \frac{D}{H}, \frac{B}{H}, \frac{u_s}{H\Omega}, \frac{u_s \rho_a B}{\mu_a}, \frac{V_s}{u_s}, \frac{\rho_a u_s^2}{g\Delta\gamma D}, \frac{\Delta\gamma}{\rho g}$$

The boundary-layer-thickness parameter  $\frac{\delta_a}{H}$  was estimated to be nearly equal for model and prototype. Near equality of the surface-roughness parameter  $\frac{z_o}{H}$  for model and prototype was achieved through geometrical scaling of the stacks and upwind roughness. The stack and building geometry parameters  $\frac{D}{H}$  and  $\frac{B}{H}$  were equal for model and prototype.

Dynamic similarity is achieved in a strict sense if the Reynolds number,  $\frac{u_s \rho_a B}{\mu_a}$ , and the Rossby number,  $\frac{u_s}{H\Omega}$ , for the model are equal to their respective counterparts in the atmosphere. The model and prototype Rossby numbers cannot be made equal; however, over the short distances of interest in this study (approximately 3000 m) the Coriolis acceleration has little influence upon the flow. According to standard practice (Cermak, 2), the requirement of equal Rossby numbers was therefore relaxed. The Reynolds number also cannot be made equal for the model and prototype. However, similarity is assured if the model Reynolds number exceeds a minimum value of approximately 11,000.

The velocity ratio  $\frac{V_s}{u_s}$  was maintained equal in model and prototype for the various approach-flow velocities and stack configurations and exit velocities tested. The stack Froude number,  $\frac{u_s^2 \rho_a}{g\Delta\gamma D}$ , was made equivalent in model and prototype by adding helium to the modeled stack gas in order to obtain an appropriately large value of  $\Delta\gamma$ .

In summary, the following criteria were adopted to ensure similarity between the modeled and atmospheric boundary layers:

1.  $Fr_m = Fr_p$  ,  $Fr = \frac{u_s^2 \rho_a}{g \Delta \gamma D}$  ;
2.  $R_m = R_p$  ,  $R = \frac{V_s}{u_s}$  ;
3.  $Re > 11000$  ,  $Re = \frac{u_s \rho_a B}{\mu_a}$  ;
4. Approach flow similarity
5. Geometric similarity

### 3.2 Model Flexibility/Limitations

On a model, such parameters as wind speed, wind direction, flue gas efflux velocity, and flue gas temperature may be separately controlled and their effects isolated. This is not often practicable or even possible for full-scale measurements at the actual prototype site. Geometric changes, such as stack height and location or the use of aerodynamic foils, are easily investigated. Some geometric characteristics of the fluid flow, e.g., cavities, shear boundaries, streamlines, and plume position, can be readily determined by the use of a visible smoke.

The various limitations of wind tunnel modelling are mostly the results of necessary departures from true analog scaling. An obvious example of this is that the wind tunnel itself, i.e., the physical presence of walls and ceiling, is a necessary part of the model but has no real-world analog. A more subtle example is that the spectral distribution of the wind-tunnel turbulence is only an approximation of the appropriately scaled real atmospheric distribution of turbulence frequencies. In the case at hand, the more significant limitations

involve Reynolds number, plume buoyancy, and the directional stability of the ambient flow.

As discussed elsewhere, Reynolds number is neither scaled nor ignored. If the Reynolds number applicable to a certain flow field is sufficiently large, the geometry of the field does not change with further increases of Reynolds number; that is, the geometry of the wake and cavity, and of the streamlines, velocity distribution, and plume dilution, remain constant and independent of Reynolds number. The modelled flow field is then a congruent replica of the prototype flow. The limitations of this "independence" technique arise from the fact that although the tunnel wind speed may be high enough to achieve geometric similarity of the major flow field (the cavity and wake of the plant buildings) it may or may not provide congruent flows around smaller obstructions such as the chimney tops. Also, the appropriately scaled efflux velocity of the flue gas, in this case, yielded a "pipe" Reynolds number in the laminar range whereas the prototype efflux is fully turbulent. The judicious use of artificial distortions is often employed in such cases, and on this particular model the necessary turbulent discharge was developed by "trip" orifices inserted in the model stacks.

It is sometimes necessary to sacrifice equality of some scaling parameters in favor of others of greater importance. In this study, Rossby number equality was of virtually no importance and was readily discounted. The equality of a buoyancy parameter,  $\frac{\Delta\gamma}{\rho g}$ , was also sacrificed in favor of maintaining equality of the Froude number, a very justifiable choice, but one deserving some explanatory comment. In the region near the emitting stacks, the plume trajectory is strongly

influenced by the Froude number and by the velocity ratio,  $\frac{V_s}{u_s}$ ; the ratio  $\frac{\Delta y}{\rho g}$  is of secondary importance. In the far field, the importance of Froude number equality decreases while that of  $\frac{\Delta y}{\rho g}$  increases. The problem under study, being largely a near-field phenomenon, was properly addressed by the requirement of Froude number equality. The relaxation of the  $\frac{\Delta y}{\rho g}$  parameter may have resulted in a small decrease in concentrations measured at the more distant locations, particularly at the 2.7 kilometer distance, and particularly at the lower wind speeds. This distortion is probably of little importance in comparing the relative effects of proposed changes.

The approach flow in the wind tunnel is virtually uni-directional whereas the prototype wind typically displays directional variability. It is difficult and impractical to introduce directional fluctuations in the wind-tunnel approach flow without detriment to its more important features. Directional variability, the  $\sigma\theta$  of the ambient prototype wind, was therefore not modelled in this study. The measured experimental concentrations, reported as predictions of prototype  $\text{SO}_2$  concentrations, should be treated as those which would be obtained at the real site if measurements were made in a very steady wind. Since the worst case conditions at the prototype occur most frequently under conditions of very steady winds, the denial of directional variability considerations in this instance probably results in a more realistic and conservative scaling of this phenomenon than would ordinarily be the case. Furthermore, attempts to account for the effects of a meandering real wind, by employing some functional relationship between model and prototype sampling times, are fruitless unless the variability of the real wind has, in fact, been appropriately modelled in the tunnel.

Estimates of the greater dilution experienced in the presence of a meandering wind, however, may be calculated from a knowledge of the statistical behavior of the real wind.

### 3.3 Model Time Scale

A cursory examination of time scale relationship between model and prototype would yield the following relationship:

$$t_p = t_m \left( \frac{u_m}{u_p} \right) \left( \frac{d_p}{d_m} \right),$$

where  $t$  indicates a time duration,  $u$  a characteristic velocity,  $d$  a characteristic dimension,  $p$  refers to prototype conditions, and  $m$  refers to model conditions. For the experiments reported herein, this would imply a prototype averaging period of approximately  $\frac{1}{2}$  hour. This relationship is valid for a stationary wind--a wind that does not change direction during the averaging time.

Where the wind direction in the prototype varies during an hour period, it has been shown by Kothari (8) and Snyder (9) that the full-scale concentrations can be predicted quite closely by breaking the hour into small increments of 2 to 10 minutes. By applying wind tunnel results for the appropriate wind direction for each time segment and averaging together the results from all time segments, the wind tunnel data agreed well with the full-scale results. The implication is that the appropriate full scale averaging time is about 2-10 minutes.

### 3.4 Scale Up/Scale Down

It is always desirable to work with as large a model as possible, within the constraints of wind tunnel size. Considerations of approach flow similarity, adequate upstream fetch, adequate downstream instrumented distance, and plume width limited the physical size of the model. A scale of 1:300 was selected.

Froude number equality,

$$\frac{u_m^2}{g \gamma_m D_m} = \frac{u_p^2}{g \gamma_p D_p}, \text{ or } \left( \frac{u_m}{u_p} \right)^2 \times \left( \frac{\gamma_p}{\gamma_m} \right) \times \left( \frac{D_p}{D_m} \right) = 1$$

then required that  $\left( \frac{u_m}{u_p} \right)^2 \times \left( \frac{\gamma_p}{\gamma_m} \right) = \frac{1}{300}$ .

The maximum obtainable value of  $\gamma_m$  (without heating the flue gas or chilling the tunnel air) would be .8619 using pure helium, but this was further limited to .8343 by the need to include a sufficient fraction of hydrocarbon tracer gases to permit adequate measurements. Therefore, in investigating the cases involving a 390°F flue gas temperature ( $\gamma_p = .3941$ ), the smallest obtainable value of  $\gamma_p/\gamma_m$  was .4724, requiring that  $\left( \frac{u_m}{u_p} \right)^2 \leq .007056$ , or  $\frac{u_m}{u_p} \leq .08400$ .

The lower limit of  $u_m$ , dictated by the requirement of remaining within the Reynolds number independent range, was determined by

$$\frac{u_m B \rho_a}{\mu_a} \geq 11,000$$

At the local air density and a typical tunnel temperature,  $\mu_a/\rho_a \cong 1.8 \times 10^{-5}$  in mks units. B, a characteristic dimension of the model boiler building, was taken as .21 meters, the geometric mean of its width and height. This yielded the limitation

$$u_m \geq .943 \text{ met/sec}$$

Combining this with  $u_m/u_p \leq .084$  we have

$$u_p \geq 11.22 \text{ met/sec } (\sim 25 \text{ mph})$$

For a 260°F flue gas temperature, we get

$$u_p \geq 9.54 \text{ met/sec } (\sim 21.3 \text{ mph})$$

With the first conditions of interest centering around a 30 mph wind speed, the model parameters were considered to be quite satisfactory.

Froude number equality requires that

$$\left( \frac{u_m}{u_p} \right)^2 \times \left( \frac{\gamma_p}{\gamma_m} \right) \times \left( \frac{D_p}{D_m} \right) = 1$$

The selected 1:300 scale makes  $\frac{D_p}{D_m} = 300$ . Re-arranging,

$$u_m = u_p \left( \frac{\gamma_m/\gamma_p}{300} \right)^{\frac{1}{2}}$$

Introducing the additional requirement that  $\left( \frac{V_s}{u_s} \right)_m = \left( \frac{V_s}{u_s} \right)_p$  and the direct calculations of volume flow,  $Q = V_s A_s$  we have, since

$$V_{s_m} = V_{s_p} \left( \frac{\gamma_m/\gamma_p}{300} \right)^{\frac{1}{2}} \text{ and } \frac{A_{s_m}}{A_{s_p}} = \left( \frac{D_m}{D_p} \right)^2 = \frac{1}{300^2} \text{ the relationship}$$

$$Q_m = Q_p \frac{(\gamma_m/\gamma_p)^{\frac{1}{2}}}{300^{5/2}}$$

These two equations, for  $u_m$  and  $Q_m$ , were used to calculate model velocities and flow rates.

The net result of the preceding relationships was that increases in prototype plume buoyancy (i.e., increases of flue gas temperature) were modelled by reductions in wind tunnel velocity, while momentum ratios were retained by reducing stack exit velocities in proportion to the approach flow velocity reduction.

### 3.5 Similarity Verification

Various tests and observations were made to ensure that the model provided a valid representation of the prototype. Among these were:

- 1) Velocity and turbulence profiles
- 2) Tests of the effect of the boiler building
- 3) Sampling velocity check
- 4) Reynolds number independence tests

- 5) Mass balance
- 6) Plume and streamline visualization (smoke tests)
- 7) Correlation with prototype data

1) Velocity and turbulence profiles of the approach flow verified that the model wind was a satisfactory analog of the prototype, except for wind meander and large scale gustiness, which could not be modelled. The large scale, longer term behavior of the real wind is usually, and more conveniently, treated by statistical methods. Profiles of the wind in the building cavity and wake regions verified that a typical cavity existed and provided velocity data needed for mass balance calculations.

2) Visualization and concentration tests with the boiler building upstream and downstream of the stacks, and with the boiler building removed, confirmed that the problem to be investigated was, as expected, that of a mechanical downwash induced by the presence of the boiler building. This justified the scaling criteria, in which Froude number equality was maintained at the expense of density ratio equality.

3) It is possible that the withdrawal of fluid samples may alter the flow field which those samples are intended to represent. Assurance that this did not occur was obtained by varying the withdrawal velocity and verifying that the sampling rate employed throughout the test series was in a range where the sampling velocity had no measurable effect on the results.

4) Tests were conducted to determine the critical Reynolds number. Reynolds number independence was found to exist for  $Re \geq 11,600$ . Since the 20 mph tests were conducted at Reynolds numbers somewhat below this critical value, less confidence can be assigned to the test data collected at that wind speed.

5) Mass balance computations were performed to relate the total flux of tracer gas in cross-sections of the plume to the total flux of tracer from a particular stack. These tests provide a broad check on the overall combined performance of the instrumentation and on the precision with which calculated model parameters were actually achieved. Vertical and horizontal concentration profiles were obtained in the elevated plume, at four different downstream distances. Point concentrations were multiplied by point wind velocities to obtain point flux figures, which were then integrated over the transverse plume area to obtain total flux. The flux of each of the three tracer gases, at each of the four downstream distances, was compared to the total flux from each stack, as determined by flow instrumentation and source gas concentration. In general, the calculated plume flux was in the range of 1.12 to 1.20 times that of the source flux. This is in good agreement, particularly since the plume was not densely instrumented and assumptions of Gaussian distribution were used when necessary to encompass the whole plume.

6) The exhaust plumes and the streamlines near the building were made visible by the use of smoke. This visualization verified that a turbulent flue discharge had been achieved, and that smoke entrainment in the stack cavities was neither unnaturally absent nor unnaturally great. Visualization of the boiler building cavity and the streamlines around this building revealed that the shear layer created at the leading edge of the roof passed just below the tips of the stacks, about 2 cm on the model, or 6 meters when scaled to the prototype. This suggests that gustiness at the prototype, not experienced at the model, could have a pronounced effect on downstream concentration levels

because of intermittent entrainment of exhaust into the building cavity. Consequently, efforts to relate model and prototype concentrations should treat the real-wind gustiness as a very important consideration, since a gusty 20 mph wind would result in higher recorded downstream concentration levels than those found with a steady-state 20 mph wind.

7) Figure 3-1 shows some of the wind tunnel test results for the existing plant configuration and operating conditions, expressed as predicted SO<sub>2</sub> concentration levels, superimposed on a plot of actual measurements taken at the prototype site. The fact that the model results fall within the range of actual field measurements and grossly approximates the distribution pattern, provides additional confirmation of the validity of the model.

Wind Velocity vs Somers Point SO<sub>2</sub> Levels  
for Wind Direction 194-202 Degrees

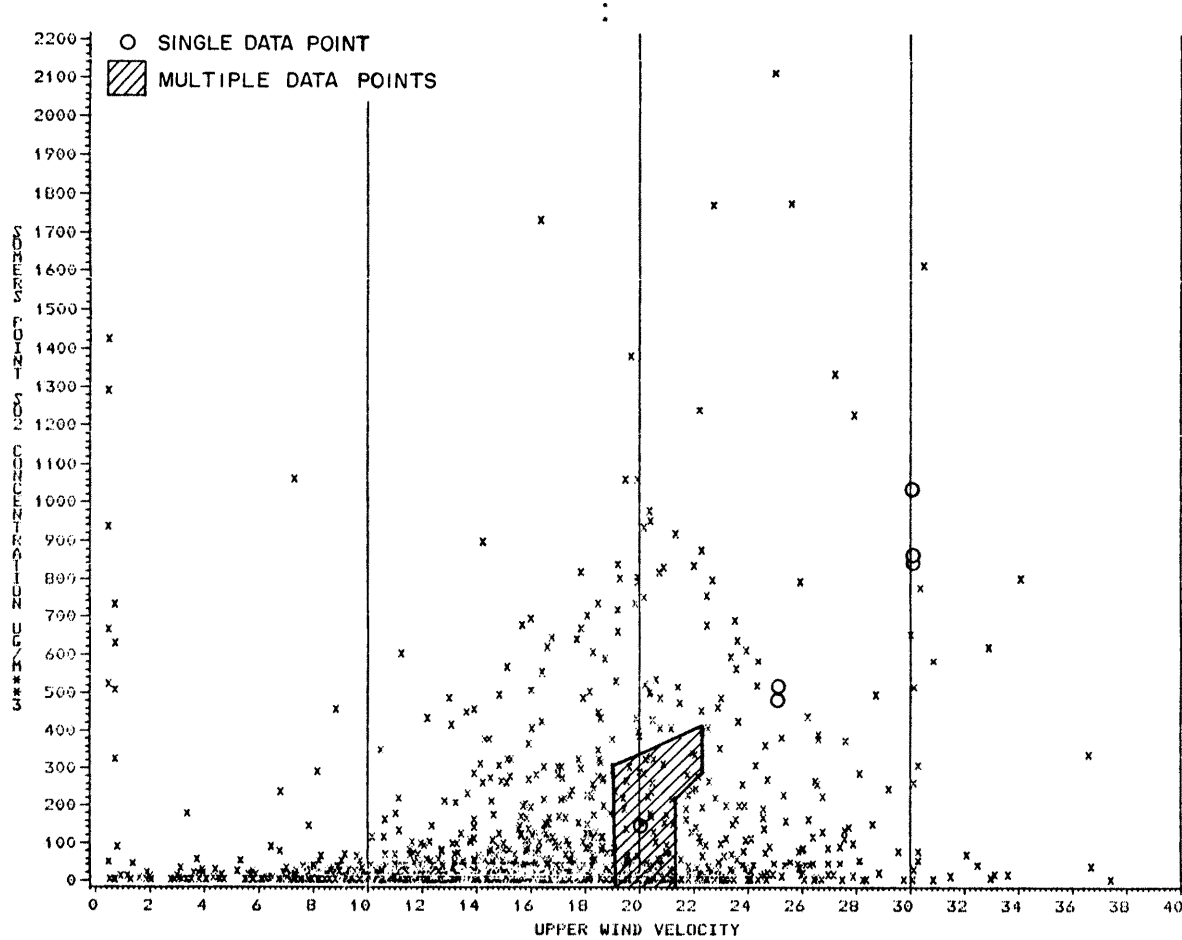


Figure 3-1. Predicted SO<sub>2</sub> Concentrations at Sampling Point #25 Based on Model Studies.

## 4.0 CONCENTRATION MEASUREMENTS

### 4.1 General

Ground-level concentration data were obtained for six different configurations of the BLES chimneys and an equal number of site modifications. The run numbers assigned to wind-tunnel tests, the model parameters, BLES configuration and modelled wind speed are contained in Table 4-1. Model flow rates from the individual stacks were calculated using plant operating conditions for full power loads and minimum power loads, as contained in Table 4-2. Figure 4-1 depicts the location and identification of the 40 position sampling grid at which ground-level concentrations were measured.

The forty sampling points were connected to a fifty-sample collection system (which was located adjacent to the wind tunnel) with one-sixteenth I.D. Tygon tubes. The collection system ("Sampler"), which was designed and fabricated in the CSU Engineering Research Center, basically consists of a circular array of 30-cc syringes, a network of check valves and a manifolded vacuum system, all interconnected, and completing a path from sampling port to gas chromatograph. Sampling time and vacuum pressure of the system are adjustable.

The sampler was calibrated both prior to, and immediately following, the concentration test program to insure proper function of each of the assemblies (tubing, check valve, syringe).

### 4.2 Tracer Gases

During test planning the decision was made to simultaneously sample the concentrations from all three BLES stacks, by using separate hydrocarbon tracers. A further decision was made to simulate a 55°F ambient temperature for all tests.

A nominal 4% Methane, 3% Ethane and 2% Propane tracer in Helium was released through Stacks #1, #2 and #3, respectively, for all studies.

The required buoyant gas mixture, supplied by Scientific Gas Products, Inc., Longmont, Colorado, were analyzed and are certified to be accurate within  $\pm 2\%$ .

#### 4.3 Test Procedure

The test procedure consisted of: 1) setting the proper tunnel wind speed, 2) releasing metered mixtures of source gases from the model stacks, 3) withdrawing samples of air from the tunnel at designated locations, and 4) analyzing the samples with a Flame Ionization Gas Chromatograph (FIGC). Photographs of the sampling system and gas chromatograph are shown in Figure 4-2.

Tunnel speed was determined by integrating the signal from the tunnel-mounted sensor with a digital voltmeter, over a 100 second interval. Speed was adjusted and the integrations repeated until the desired setting was obtained to a  $\pm 2\%$  tolerance.

The tracer gases released to the individual stacks, were routed through ball-type flow meters to control the volume flows. A calibration of the flow-meters, over their operating range with a Helium source, was used to obtain the proper meter settings.

The tracer gas sampling system consists of a series of fifty 30 cc syringes mounted between two circular aluminum plates. A variable-speed motor raises a third plate, which simultaneously lifts all 50 syringe plungers. A set of check valves and tubing are connected such that airflow from each tunnel sampling point passes over the tip of each designated syringe. When the syringe plunger is lifted, a sample from the tunnel is drawn into the syringe container. The sampling procedure

consists of flushing (taking and expending a sample) the syringe several times after which the test sample is taken. The variable draw rate was set to approximately 60 seconds.

The procedure for analyzing air samples from the tunnel is as follows: 1) a 2 cc sample volume drawn from the wind tunnel is introduced into the Flame Ionization Detector (FID), 2) the output from the electrometer (in microvolts) is sent to the Hewlett-Packard 3380 Integrator, 3) the output signal is analyzed by the HP 3380 to obtain the proportional amount of hydrocarbons present in the sample, 4) the record is integrated, and the methane, ethane, or propane concentration, as appropriate, is determined, 5) a summary of the integrator analysis (gas retention time and integrated area ( $\mu\text{v}\cdot\text{s}$ ) is printed out on the integrator at the wind tunnel, 6) the integrated (raw) values for each tracer are entered into a computer along with pertinent run parameters, and 7) the computer program converts the raw data into a full-scale  $\text{SO}_2$  concentration, and the results are printed out in the report format contained in Appendix A.

The computer also printed the  $\text{SO}_2$  concentrations onto a page arranged in the format of Figure 4-1 to facilitate plotting of the isopleths which are contained in Appendix B.

#### 4.4 Sample Concentration Calculation

The data provided in the computer printouts, and used in the data analysis were calculated from the equation:

$$\text{SO}_2 \left( \frac{\text{gm}}{\text{m}^3} \right) = \frac{(\text{RAW-BG})\mu\text{v}\cdot\text{s}}{\text{S.S. (ppm)}} \times \frac{\text{CAL.FAC} \left( \frac{\text{PPM}}{\mu\text{v}\cdot\text{s}} \right)}{(\text{S.F.})^2} \times \frac{u_m (\text{m/s})}{Q_m (\text{m}^3/\text{s})} \times \frac{Q_p (\text{gm/sec})}{u_p (\text{m/sec})}$$

where:

- (RAW-BG) - refers to integrator values of a tracer sample minus a background reading measured in microvolt·seconds,
- SS - refers to source strength of the tracer in ppm,
- CAL.FAC. - is a daily calibration of the GC which provides a base line to compensate for changes in operation and also compensates for the use of tracers with varying molecular weights,
- (S.F.)<sup>2</sup> - a square of the model scaling factor,
- $u_m$  - stack height velocity of the wind-tunnel test,
- $Q_m$  - volume flow of the tracer through a model stack,
- $Q_p$  - effluent output from the prototype stack, and
- $u_p$  - stack height velocity of the prototype.

The foregoing calculations, made for each stack output, were further summarized by the computer to provide a total SO<sub>2</sub> output in grams per cubic meter, for each point analyzed on the sampling grid.

The GC-integrator data was entered into the Cyber 206 computer for reduction.

#### 4.5 Data Analysis

Data from the 161 separate concentration tests, which is contained in the separately bound Appendix A, was tabulated and graphed for the different wind speeds and configurations investigated. Particular emphasis was directed to the studies which documented the effects of flue gas reheat, stack extensions, and added air.

Tables 4-3a through 4-3e contain a tabulation of sulfur dioxide concentrations for equivalent wind speeds of 20, 25, 30, 37.5 and 45 mph at full power operating conditions for selected tests. These

concentration results were compared in each instance with the data from the basic, or existing configuration. Tables 4-4a through 4-4e contain comparable data for a minimum power load.

The figures contained within Chapter 4.0 provide a graphic presentation of selected data to supplement the tables. Each set of figures contains plots of maximum SO<sub>2</sub> concentrations at various distances along the plume centerline, or across the plume at 9.0 m (2.7 km prototype), for different wind speeds.

- o The effects of reheat at full and minimum power load are illustrated in the graphs contained in Figures 4-3 and 4-4.

- o The effects of the 50-ft extensions and extensions with reheat are graphed on Figures 4-5 and 4-6.

- o The effects of adding varying amounts of air to the flue gas are depicted on Figures 4-7 and 4-8.

- o Figures 4-9a through 4-9d provide a comparison of SO<sub>2</sub> concentrations over a range of wind speeds for existing plant conditions.

- o Figures 4-10a and 4-10b compare the effects of wind speed upon concentration levels at, or near the Somers Point monitor.

Additional tables and/or figures may be prepared to study the effects of wind direction, or other chimney/plant configuration changes, from the Appendix A data.

Isopleth concentrations in  $\mu\text{g}/\text{m}^3$ , were plotted for all test runs containing sufficient data points and are separately bound in Appendix B.

Table 4-1. Run Numbers and Model Parameters Used on BLES Wind Tunnel Tests.

Run No.	Power Load	Stack Ht. (cm)	Stack Temp (°F)	Wind Dir.	Tunnel Speed (m/s)	Vol. Flow (m <sup>3</sup> /s x 10 <sup>-6</sup> )			Remarks	
						Stack #1	Stack #2	Stack #3	Config.	Wind (mph)
1	MIN	25.4	260	198	1.98	129.0	134.7	129.4	Basic	45
2	MIN	30.48	260	198	1.98	129.0	134.7	129.4	50' extensions	45
3	MIN	~25.6	260	198	1.98	129.0	134.7	129.4	Nozzles	45
4	MIN	~30.7	260	198	1.98	129.0	134.7	129.4	50' ext. & nozzles	45
5	MIN	25.4	260	198	1.98	129.0	134.7	129.4	125' x 275' canopy	45
6	MIN	25.4	260	198	1.98	129.0	134.7	129.4	50' x 275' canopy	45
7	MIN	25.4	260	198	1.98	129.0	134.7	129.4	60' x 300' wall	45
8	FULL	25.4	260	198	1.98	294.8	314.0	296.6	Basic	45
9	FULL	30.48	260	198	1.98	294.8	314.0	296.6	50' extensions	45
10	FULL	~25.6	260	198	1.98	294.8	314.0	296.6	Nozzles	45
11	FULL	~30.7	260	198	1.98	294.8	314.0	296.6	50' ext. & nozzles	45
12	FULL	25.4	260	198	1.98	294.8	314.0	296.6	125' x 275' canopy	45
13	FULL	25.4	260	198	1.98	294.8	314.0	296.6	50' x 275' canopy	45
14	FULL	25.4	260	198	1.98	294.8	314.0	296.6	60' x 300' wall	45

Table 4-1. continued.

Run No.	Power Load	Stack Ht. (cm)	Stack Temp (°F)	Wind Dir.	Tunnel Speed (m/s)	Vol. Flow ( $\text{m}^3/\text{s} \times 10^{-6}$ )			Remarks	
						Stack #1	Stack #2	Stack #3	Config.	Wind (mph)
15	MIN	25.4	390	198	1.55	119.0	124.4	119.4	Basic	45
16	MIN	30.48	390	198	1.55	119.0	124.4	119.4	50' extensions	45
17	MIN	25.4	390	198	1.55	119.0	124.4	119.4	125' x 275' canopy	45
18	MIN	25.4	390	198	1.55	119.0	124.4	119.4	50' x 275' canopy	45
19	MIN	25.4	390	198	1.55	119.0	124.4	119.4	60' x 300' wall	45
20	FULL	25.4	390	198	1.55	272.1	289.8	273.8	Basic	45
21	FULL	30.48	390	198	1.55	272.1	289.8	273.8	50' extensions	45
22	FULL	25.4	390	198	1.55	272.1	289.8	273.8	125' x 275' canopy	45
23	FULL	25.4	390	198	1.55	272.1	289.8	273.8	50' x 275' canopy	45
24	FULL	25.4	390	198	1.55	272.1	289.8	273.8	60' x 300' wall	45
27	MIN	39.12	260	198	1.98	129.0	134.7	129.4	385' comb. stack	45
28	FULL	39.12	260	198	1.98	294.8	314.0	296.6	385' comb. stack	45
29	MIN	43.18	260	198	1.98	129.0	134.7	129.4	425' comb. stack	45
30	FULL	43.18	260	198	1.98	294.8	314.0	296.6	425' comb. stack	45

Table 4-1. continued.

Run No.	Power Load	Stack Ht. (cm)	Stack Temp (°F)	Wind Dir.	Tunnel Speed (m/s)	Vol. Flow (m <sup>3</sup> /s x 10 <sup>-6</sup> )			Remarks	
						Stack #1	Stack #2	Stack #3	Config.	Wind (mph)
51R	FULL	25.4	260	198	1.65	294.8	314.0	296.6	Basic	37.5
52	FULL	25.4	260	198	1.32	294.8	314.0	296.6	Basic	30
53	FULL	25.4	260	198	0.99	294.8	314.0	296.6	Basic	22.5
54	FULL	25.4	260	198	2.31	294.8	314.0	296.6	Basic	52.5
55	MIN	25.4	260	198	2.31	129.0	134.7	129.4	Basic	52.5
56	MIN	25.4	260	198	1.65	129.0	134.7	129.4	Basic	37.5
57	MIN	25.4	260	198	1.32	129.0	134.7	129.4	Basic	30
58	MIN	25.4	260	198	0.99	129.0	134.7	129.4	Basic	22.5
59	FULL	25.4	390	198	0.77	272.1	289.8	273.8	Basic	22.5
60	FULL	30.48	390	198	0.77	272.1	289.8	273.8	50' extensions	22.5
61	FULL	25.4	390	198	1.03	272.1	289.8	273.8	Basic	30
62R	FULL	30.48	390	198	1.03	272.1	289.8	273.8	50' extensions	30
63	FULL	25.4	390	198	1.29	272.1	289.8	273.8	Basic	37.5
64	FULL	30.48	390	198	1.29	272.1	289.8	273.8	50' extensions	37.5

Table 4-1. continued.

Run No.	Power Load	Stack Ht. (cm)	Stack Temp (°F)	Wind Dir.	Tunnel Speed (m/s)	Vol. Flow (m <sup>3</sup> /s x 10 <sup>-6</sup> )			Remarks	
						Stack #1	Stack #2	Stack #3	Config.	Wind (mph)
65	FULL	25.4	390	198	1.80	272.1	289.8	273.8	Basic	52.5
66	FULL	30.48	390	198	1.80	272.1	289.8	273.8	50' extensions	52.5
67	FULL	30.48	390	190	1.29	272.1	289.8	273.8	50' extensions	37.5
68	FULL	30.48	390	205	1.29	272.1	289.8	273.8	50' extensions	37.5
69	FULL	30.48	390	275	1.29	272.1	289.8	273.8	50' extensions	37.5
70	FULL	30.48	390	295	1.29	272.1	289.8	273.8	50' extensions	37.5
71	FULL	30.48	390	320	1.29	272.1	289.8	273.8	50' extensions	37.5
72	FULL	25.4	390	320	1.29	272.1	289.8	273.8	Basic	37.5
73	FULL	25.4	390	295	1.29	272.1	289.8	273.8	Basic	37.5
74	FULL	25.4	390	275	1.29	272.1	289.8	273.8	Basic	37.5
75	FULL	25.4	390	205	1.29	272.1	289.8	273.8	Basic	37.5
76	FULL	25.4	390	190	1.29	272.1	289.8	273.8	Basic	37.5

Table 4-1. continued.

Run No.	Power Load	Stack Ht. (cm)	Stack Temp (°F)	Wind Dir.	Tunnel Speed (m/s)	Vol. Flow (m <sup>3</sup> /s x 10 <sup>-6</sup> )			Remarks	
						Stack #1	Stack #2	Stack #3	Config.	Wind (mph)
77	MIN	25.4	260	190	1.65	129.0	134.7	129.4	Basic	37.5
78	MIN	25.4	260	205	1.65	129.0	134.7	129.4	Basic	37.5
79	MIN	25.4	260	275	1.65	129.0	134.7	129.4	Basic	37.5
80	MIN	25.4	260	295	1.65	129.0	134.7	129.4	Basic	37.5
81	MIN	25.4	260	320	1.65	129.0	134.7	129.4	Basic	37.5
82	FULL	25.4	260	320	1.65	294.8	314.0	296.6	Basic	37.5
83	FULL	25.4	260	295	1.65	294.8	314.0	296.6	Basic	37.5
84	FULL	25.4	260	275	1.65	294.8	314.0	296.6	Basic	37.5
85	FULL	25.4	260	205	1.65	294.8	314.0	296.6	Basic	37.5
86	FULL	25.4	260	190	1.65	294.8	314.0	296.6	Basic	37.5
87	FULL	25.4	290	198	1.20	281.0	299.3	282.7	Basic	30
88	FULL	25.4	290	198	1.80	281.0	299.3	282.7	Basic	45
89	FULL	25.4	390	045	1.55	272.1	289.8	273.8	Basic	45
90	FULL	30.48	390	045	1.55	272.1	289.8	273.8	50' extensions	45

Table 4-1. continued.

Run No.	Power Load	Stack Ht. (cm)	Stack Temp (°F)	Wind Dir.	Tunnel Speed (m/s)	Vol. Flow (m <sup>3</sup> /s x 10 <sup>-6</sup> )			Remarks	
						Stack #1	Stack #2	Stack #3	Config.	Wind (mph)
101	FULL	25.4	260	315	1.98	294.8	314.0	296.6	Stacks align wind	45
102	FULL	25.4	260	045	1.98	294.8	314.0	314.0	Stacks upwind	45
103	FULL	25.4	260	198	1.98	294.8	314.0	296.6	Without buildings	45
104	FULL	25.4	260	198	1.98	294.8	314.0	296.6	50' treeline	45
105	FULL	25.4	260	198	1.98	294.8	314.0	296.6	100' vertical vanes	45
106	FULL	43.18	260	198	1.98	294.8	314.0	296.6	425' comb. stack	45
107	FULL	25.4	260	198	1.32	294.8	314.0	296.6	Basic	30
108	FULL	30.48	260	198	1.32	294.8	314.0	296.6	50' extensions	30
109	FULL	25.4	260	198	1.32	294.8	314.0	296.6	125' x 275' canopy	30

Table 4-1. continued.

Run No.	Power Load	Stack Ht. (cm)	Stack Temp (°F)	Wind Dir.	Tunnel Speed (m/s)	Vol. Flow (m <sup>3</sup> /s x 10 <sup>-6</sup> )			Remarks	
						Stack #1	Stack #2	Stack #3	Config.	Wind (mph)
211	FULL	25.4	260	174	0.884	295.4	314.6	298.5	Basic	20
212	FULL	25.4	260	198	0.884	295.4	314.6	298.5	Basic	20
212R	FULL	25.4	260	198	0.884	295.4	314.6	298.5	Basic	20
213	FULL	25.4	260	232	0.884	295.4	314.6	298.5	Basic	20
214	MIN	25.4	260	198	0.884	129.6	134.7	129.6	Basic	20
215	MIN	25.4	260	232	0.884	129.6	134.7	129.6	Basic	20
221	FULL	25.4	390	198	0.751	292.4	305.1	280.1	Basic	20
222	FULL	25.4	390	232	0.751	292.4	305.1	280.1	Basic	20
223	MIN	25.4	390	232	0.751	130.0	135.2	130.0	Basic	20
224	MIN	25.4	390	317	0.751	130.0	135.2	130.0	Basic	20
225	MIN	25.4	390	198	0.751	130.0	135.2	130.0	Basic	20
226	MIN	25.4	390	198	0.939	130.0	135.2	130.0	Basic	25
227	MIN	25.4	390	198	1.127	130.0	135.2	130.0	Basic	30
227R	MIN	25.4	390	198	1.127	130.0	135.2	130.0	Basic	30

Table 4-1. continued.

Run No.	Power Load	Stack Ht. (cm)	Stack Temp (°F)	Wind Dir.	Tunnel Speed (m/s)	Vol. Flow (m <sup>3</sup> /s x 10 <sup>-6</sup> )			Remarks	
						Stack #1	Stack #2	Stack #3	Config.	Wind (mph)
231	FULL	25.4	340	198	0.790	289.4	302.0	277.3	Basic	20
232	FULL	25.4	340	198	0.987	289.4	302.0	277.3	Basic	25
233	FULL	25.4	340	198	1.185	289.4	302.0	277.3	Basic	30
234	MIN	25.4	340	198	0.790	128.7	133.8	128.7	Basic	20
235	MIN	25.4	340	198	0.987	128.7	133.8	128.7	Basic	25
236	MIN	25.4	340	198	1.185	128.7	133.8	128.7	Basic	30
236R	MIN	25.4	340	198	1.185	128.7	133.8	128.7	Basic	30
241	FULL	25.4	297.7	198	0.833	327.3	345.4	330.2	Basic + 100,000 air	20
242	FULL	25.4	297.7	198	1.041	327.3	345.4	330.2	Basic + 100,000 air	25
243	FULL	25.4	297.7	198	1.249	327.3	345.4	330.2	Basic + 100,000 air	30
243R	FULL	25.4	297.7	198	1.249	327.3	345.4	330.2	Basic + 100,000 air	30
244	MIN	25.4	285.7	198	0.847	174.0	178.9	174.0	Basic + 100,000 air	20
244R	MIN	25.4	285.7	198	0.847	174.0	178.9	174.0	Basic + 100,000 air	20
245	MIN	25.4	285.7	198	1.059	174.0	178.9	174.0	Basic + 100,000 air	25

Table 4-1. continued.

Run No.	Power Load	Stack Ht. (cm)	Stack Temp (°F)	Wind Dir.	Tunnel Speed (m/s)	Vol. Flow (m <sup>3</sup> /s x 10 <sup>-6</sup> )			Remarks	
						Stack #1	Stack #2	Stack #3	Config.	Wind (mph)
246	MIN	25.4	285.7	198	1.271	174.0	178.9	174.0	Basic + 100,000 air	30
251	FULL	25.4	305.1	198	0.825	372.3	390.2	375.2	Basic + 200,000 air	20
252	FULL	25.4	305.1	198	1.031	372.3	390.2	375.2	Basic + 200,000 air	25
253	FULL	25.4	305.1	198	1.237	372.3	390.2	375.2	Basic + 200,000 air	30
253R	FULL	25.4	305.1	198	1.237	372.3	390.2	375.2	Basic + 200,000 air	30
254	MIN	25.4	274.8	198	0.862	151.7	156.7	151.7	Basic + 50,000 air	20
255	MIN	25.4	274.8	198	1.077	151.7	156.7	151.7	Basic + 50,000 air	25
256	MIN	25.4	274.8	198	1.293	151.7	156.7	151.7	Basic + 50,000 air	30
261	FULL	25.4	288	198	0.845	282.4	300.7	285.3	Basic	20
262	FULL	25.4	288	198	1.056	282.4	300.7	285.3	Basic	25
262R	FULL	25.4	288	198	1.056	282.4	300.7	285.3	Basic	25
262RR	FULL	25.4	288	198	1.056	282.4	300.7	285.3	Basic	25
263	FULL	25.4	288	198	1.267	282.4	300.7	285.3	Basic	30
263R	FULL	25.4	288	198	1.267	282.4	300.7	285.3	Basic	30

Table 4-1. continued.

Run No.	Power Load	Stack Ht. (cm)	Stack Temp (°F)	Wind Dir.	Tunnel Speed (m/s)	Vol. Flow (m <sup>3</sup> /s x 10 <sup>-6</sup> )			Remarks	
						Stack #1	Stack #2	Stack #3	Config.	Wind (mph)
264	MIN	25.4	260	198	0.883	129.5	134.7	129.5	Basic	20
265	MIN	25.4	260	198	1.104	129.5	134.7	129.5	Basic	25
266	MIN	25.4	260	198	1.325	129.5	134.7	129.5	Basic	30
266R	MIN	25.4	260	198	1.325	129.5	134.7	129.5	Basic	30
267	FULL	30.48	288	198	0.845	282.4	300.7	285.3	50' extensions	20
268	FULL	30.48	288	198	1.056	282.4	300.7	285.3	50' extensions	25
269	FULL	30.48	288	198	1.267	282.4	300.7	285.3	50' extensions	30
301	MIN	25.4	260	174	1.104	129.6	134.7	129.6	Basic	25
302	FULL	25.4	260	174	1.104	295.4	314.6	298.5	Basic	25
303	FULL	25.4	390	174	0.939	292.4	305.1	280.1	Basic	25
304	MIN	25.4	260	198	1.104	129.6	134.7	129.6	Basic	25
305	FULL	25.4	260	198	1.104	295.4	314.6	298.5	Basic	25
306	FULL	25.4	390	198	0.939	292.4	305.1	280.1	Basic	25

Table 4-1. continued.

Run No.	Power Load	Stack Ht. (cm)	Stack Temp (°F)	Wind Dir.	Tunnel Speed (m/s)	Vol. Flow (m <sup>3</sup> /s x 10 <sup>-6</sup> )			Remarks	
						Stack #1	Stack #2	Stack #3	Config.	Wind (mph)
307	MIN	25.4	260	232	1.104	129.6	134.7	129.6	Basic	25
308	FULL	25.4	260	232	1.104	295.4	314.6	298.5	Basic	25
309	FULL	25.4	390	232	0.939	292.4	305.1	280.1	Basic	25
310	MIN	25.4	260	317	1.104	129.6	134.7	129.6	Basic	25
311	FULL	25.4	260	317	1.104	295.4	314.6	298.5	Basic	25
312	FULL	25.4	390	317	0.939	292.4	305.1	280.1	Basic	25
313	FULL	30.48	390	174	0.939	292.4	305.1	280.1	50' extensions	25
313R	FULL	30.48	390	174	0.939	292.4	305.1	280.1	50' extensions	25
314	FULL	30.48	390	198	0.939	292.4	305.1	280.1	50' extensions	25
315	FULL	30.48	390	232	0.939	292.4	305.1	280.1	50' extensions	25
316	FULL	30.48	390	317	0.939	292.4	305.1	280.1	50' extensions	25
317	MIN	25.4	260	198	1.325	129.6	134.7	129.6	Basic	30
318	FULL	25.4	260	198	1.325	295.4	314.6	298.5	Basic	30
318R	FULL	25.4	260	198	1.325	295.4	314.6	298.5	Basic	30

Table 4-1. continued.

Run No.	Power Load	Stack Ht. (cm)	Stack Temp (°F)	Wind Dir.	Tunnel Speed (m/s)	Vol. Flow (m <sup>3</sup> /s x 10 <sup>-6</sup> )			Remarks	
						Stack #1	Stack #2	Stack #3	Config.	Wind (mph)
319	FULL	25.4	390	198	1.127	292.4	305.1	280.1	Basic	30
320	MIN	30.48	260	198	1.325	129.6	134.7	129.6	50' extensions	30
321	FULL	30.48	260	198	1.325	295.4	314.6	298.5	50' extensions	30
322	MIN	30.48	390	198	1.127	130.0	135.2	130.0	50' extensions	30
323	FULL	30.48	390	198	1.127	292.4	305.1	280.1	50' extensions	30
324	MIN	25.4	260	198	1.325	129.6	134.7	129.6	50' x 275' canopy	30
325	FULL	25.4	260	198	1.325	295.4	314.6	298.5	50' x 275' canopy	30
326	MIN	39.12	260	198	1.325	129.6	134.7	129.6	385' comb. stack	30
327	FULL	39.12	260	198	1.325	295.4	314.6	298.5	385' comb. stack	30
328	MIN	43.18	260	198	1.325	129.6	134.7	129.6	425' comb. stack	30
329	FULL	43.18	260	198	1.325	295.4	314.6	298.5	425' comb. stack	30
330	FULL	30.48	390	198	0.751	292.4	305.1	280.1	50' extensions	20
330R	FULL	30.48	390	198	0.751	292.4	305.1	280.1	50' extensions	20

Table 4-2. Prototype Operating Conditions Used in Model Calculations.

B. L. ENGLAND STATION - ATLANTIC ELECTRIC

FULL LOAD STUDY CRITERIA

<u>Unit</u>	<u>MW</u>	<u>Fuel</u>	<u>ACFM</u>	<u>Exit Gas Temp °F</u>	<u>3 M /sec</u>	<u>Stack Diam-M</u>	<u>Exit Gas Velocity M/S</u>	<u>Stack Height-M</u>	<u>Stack SO<sub>2</sub> Emission Gr/sec</u>	<u>Stack SO<sub>2</sub> Conc.3 Gr./M</u>
1	127	coal	570,000	270	269.0	3.66	25.6	76.2	850	3.16
2	160	coal	607,000	285	286.5	4.02	22.5	76.2	1050	3.67
3	160	oil	576,000	310	271.9	3.96	22.0	76.2	220	0.81

45

LOW LOAD STUDY CRITERIA

1	60	coal	250,000	260	118.0	3.66	11.2	76.2	400	3.39
2	60	coal	260,000	260	122.7	4.02	9.7	76.2	400	3.26
3	40	oil	250,000	260	118.0	3.96	9.6	76.2	55	0.47

Table 4-3a. Tabulation of SO<sub>2</sub> Concentrations (µg/m<sup>3</sup>) and Percentage Change from Existing Configuration for a 8.94 m/s (20 mph) Wind Speed and Full Power Load.

Run & Config.	Sum of Maximum at 1.75, 3.0, 5.25 & 9.0 m	% Chg	Maximum Reading & Point	% Chg	Somers Point Equiv.	% Chg
212R - Basic 260°F	480	-	185 (25)	-	185 (25)	-
261 - Basic 288°F	522	-	156 (38)	-	146 (25)	-
231 - 340°F Reheat	212	-59	80 (25)	-49	80 (25)	-45
221 - 390°F Reheat	161	-69	67 (26)	-57	67 (26)	-54
267 - 50' ext. 288°F	180	-66	74 (25)	-53	74 (25)	-49
330R - 50' ext. 390°F	67	-87	38 (25)	-76	38 (25)	-74
241 - 100,000 air	287	-45	103 (25)	-34	103 (25)	-29
251 - 200,000 air	146	-72	50 (38)	-68	46 (25)	-68

Table 4-3b. Tabulation of SO<sub>2</sub> Concentrations (µg/m<sup>3</sup>) and Percentage Change from Existing Configuration for a 11.18 m/s (25 mph) Wind Speed and Full Power Load.

Run & Config.	Sum of Maximum at 1.75, 3.0, 5.25 & 9.0 m	% Chg	Maximum Reading & Point	% Chg	Somers Point Equiv.	% Chg
305 - Basic 260°F	1787	-	557 (39)	-	529 (24)	-
262 - Basic 288°F	1626	-	508 (38)	-	450 (24)	-
232 - 340°F Reheat	752	-54	237 (38)	-53	232 (24)	-48
306 - 390°F Reheat	788	-52	269 (39)	-47	253 (25)	-44
268 - 50' ext 288°F	380	-77	165 (24)	-68	165 (24)	-63
314 - 50' ext 390°F	176	-89	95 (25)	-81	95 (25)	-79
242 - 100,000 air	1344	-17	398 (36)	-22	314 (25)	-30
252 - 200,000 air	592	-64	176 (36)	-65	173 (24)	-62

Table 4-3c. Tabulation of SO<sub>2</sub> Concentrations (µg/m<sup>3</sup>) and Percentage Change from Existing Configuration for a 13.41 m/s (30 mph) Wind Speed and Full Power Load.

Run & Config.	Sum of Maximum at 1.75, 3.0, 5.25 & 9.0 m	% Chg	Maximum Reading & Point	% Chg	Somers Point Equiv.	% Chg
318 - Basic 260°F	3650	-	1160 (36)	-	854 (24)	-
263 - Basic 288°F	3414	-	1050 (17)	-	860 (24)	-
233 - 340°F Reheat	2266	-34	691 (18)	-34	617 (25)	-28
319 - 390°F Reheat	2095	-39	652 (36)	-38	524 (24)	-39
321 - 50' ext. 260°F	1763	-52	676 (24)	-42	676 (24)	-21
269 - 50' ext. 288°F	1532	-55	571 (24)	-46	571 (24)	-34
323 - 50' ext. 390°F	515	-85	247 (24)	-76	247 (24)	-71
243R - 100,000 air	2437	-29	774 (18)	-26	634 (25)	-26
253 - 200,000 air	1691	-50	547 (36)	-48	440 (24)	-49
325 - 50' canopy	3377	-1	1030 (18)	-2	874 (24)	+2
327 - 385' stack	322	-91	150 (24)	-86	150 (24)	-83
329 - 425' stack	280	-92	139 (24)	-87	139 (24)	-84

Table 4-3d. Tabulation of SO<sub>2</sub> Concentrations (µg/m<sup>3</sup>) and Percentage Change from Existing Configuration for a 16.76 m/s (37.5 mph) Wind Speed and Full Power Load.

Run & Config.	Sum of Maximum at 3.0, 5.25 & 9.0 m	% Chg	Maximum Reading & Point	% Chg	Somers Point Equiv.	% Chg
51R - 37.5 mph	6050	-	2180 (18)	-	1750 (24)	-
8R - 45 mph	9580	+58	3740 (11)	+72	2520 (25)	+44
52 - 30 mph	2303	-62	817 (24)	-63	817 (24)	-53
53 - 22.5 mph	739	-88	335 (24)	-85	335 (24)	-81
54 - 52.5 mph	10550	+74	4410 (11)	102	2490 (24)	+42
82 - 320°	972	-84	434 (24)	-80	434 (24)	-75
83 - 295°	318	-95	230 (24)	-89	230 (24)	-87
84 - 275°	4080	-33	1520 (17)	-30	1260 (24)	-28
85 - 205°	4550	-25	1700 (18)	-22	1410 (25)	-19
86 - 190°	3920	-35	1450 (17)	-33	1320 (25)	-25

Table 4-3e. Tabulation of SO<sub>2</sub> Concentrations (µg/m<sup>3</sup>) and Percentage Change from Existing Configuration for a 20.12 m/s (45 mph) Wind Speed and Full Power Load.

Run & Config.	Sum of Maximum at 1.75, 3.0, 5.25 & 9.0 m	% Chg	Maximum Reading & Point	% Chg	Somers Point Equiv.	% Chg
8R - Basic	11690	-	3740 (11)	-	2520 (25)	-
9 - 50' Ext.	5095	-56	1860 (18)	-50	1690 (25)	-33
10R - Nozzles	10640	-09	3300 (36)	-12	2410 (25)	-4
11 - Ext. & Nozzles	5145	-56	1880 (18)	-50	1750 (24)	-31
12 - 125' Canopy	8880	-24	2850 (18)	-24	2230 (25)	-12
13 - 50' Canopy	7930	-32	2500 (36)	-33	1920 (25)	-24
14 - 60' Wall	10010	-14	3000 (11)	-20	2290 (25)	-9
20 - 390° Reheat	4126	-65	1230 (39)	-67	1120 (25)	-56
21 - Ext. & Reheat	1556	-87	641 (24)	-83	641 (24)	-75
28 - 385' Stack	2986	-74	1430 (24)	-62	1430 (24)	-43
30 - 425' Stack	1122	-90	537 (24)	-86	537 (24)	-79
88 - 290° Reheat	9410	-20	3740 (11)	0	2340 (25)	-7
103 - w/o Buildings	2778	-76	1300 (25)	-65	1300 (25)	-48

Table 4-4a. Tabulation of SO<sub>2</sub> Concentrations (µg/m<sup>3</sup>) and Percentage Change from Existing Configuration for a 8.94 m/s (20 mph) Wind Speed and Minimum Power Road.

Run & Config.	Sum of Maximum at 1.75, 3.0, 5.25 & 9.0 m	% Chg	Maximum Reading & Point	% Chg	Somers Point Equiv.	% Chg
214 - Basic 260°F	2052	-	563 (11)	-	489 (25)	-
264 - Basic 260°F	1642	-	464 (38)	-	457 (24)	-
234 - 340°F Reheat	882	-46	253 (36)	-45	208 (24)	-54
225 - 390°F Reheat	587	-64	200 (24)	-57	200 (24)	-56
254 - 50,000 air	643	-61	193 (24)	-58	193 (24)	-58
244R - 100,000 air	443	-73	148 (24)	-68	148 (24)	-68

Table 4-4b. Tabulation of SO<sub>2</sub> Concentrations (µg/m<sup>3</sup>) and Percentage Change from Existing Configuration for a 11.18 m/s (25 mph) Wind Speed and Minimum Power Load.

Run & Config.	Sum of Maximum at 1.75, 3.0, 5.25 & 9.0 m	% Chg	Maximum Reading & Point	% Chg	Somers Point Equiv.	% Chg
265 - Basic 260°F	6860	-	2150 (33)	-	1180 (24)	-
304 - Basic 260°F	6035	-	1970 (11)	-	885 (24)	-
235 - 340°F Reheat	2781	-54	802 (38)	-59	621 (24)	-30
226 - 390°F Reheat	2255	-63	636 (18)	-68	524 (25)	-41
255 - 50,000 air	3267	-46	925 (11)	-53	656 (24)	-26
245 - 100,000 air	2024	-66	589 (35)	-70	501 (24)	-43

Table 4-4c. Tabulation of SO<sub>2</sub> Concentrations (µg/m<sup>3</sup>) and Percentage Change from Existing Configuration for a 13.41 m/s (30 mph) Wind Speed and Minimum Power Load.

Run & Config.	Sum of Maximum at 1.75, 3.0, 5.25 & 9.0 m	% Chg	Maximum Reading & Point	% Chg	Somers Point Equiv.	% Chg
266 - Basic 260°F	10,090	-	3430 (33)	-	1300 (24)	-
317 - Basic 260°F	10,560	-	3510 (33)	-	1470 (25)	-
236R - 340°F Reheat	8090	-23	2490 (33)	-29	1290 (25)	-12
227R - 390°F Reheat	6440	-39	1930 (33)	-45	1070 (25)	-27
320 - 50' ext. 260°F	4998	-53	1610 (11)	-54	989 (25)	-33
322 - 50' ext. 390°F	1871	-82	553 (36)	-84	465 (25)	-68
256 - 50,000 air	6860	-35	2170 (11)	-38	1040 (24)	-29
246 - 100,000 air	5330	-50	1650 (11)	-53	910 (24)	-38
324 - 50' canopy	10,910	+3	3610 (4)	+3	1510 (24)	+3
326 - 385' stack	1707	-84	637 (24)	-82	637 (24)	-57
328 - 425' stack	1084	-90	452 (23)	-87	452 (23)	-69

Table 4-4d. Tabulation of SO<sub>2</sub> Concentrations (µg/m<sup>3</sup>) and Percentage Change from Existing Configuration for a 16.76 m/s (37.5 mph) Wind Speed and Minimum Power Load.

Run & Config.	Sum of Maximum at 3.0, 5.25 & 9.0 m	% Chg	Maximum Reading & Point	% Chg	Somers Point Equiv.	% Chg
56 - 37.5 mph	8580	-	4350 (11)	-	1550 (24)	-
1 - 45 mph	8470	-1	4430 (11)	+2	1480 (24)	-5
55 - 52.5 mph	7720	-10	4080 (4)	-6	1270 (25)	-18
57 - 30 mph	5190	-40	2130 (11)	-51	1240 (25)	-20
58 - 22.5 mph	1565	-82	614 (11)	-86	471 (25)	-70
77 - 190°	9200	+7	4410 (11)	+1	1840 (25)	+19
78 - 205°	8050	-6	3850 (11)	-11	1540 (25)	-1
79 - 275°	8700	+1	3860 (11)	-11	1810 (24)	-17
80 - 295°	6090	-29	2520 (11)	-42	1440 (25)	-7
81 - 320°	2590	-70	971 (18)	-78	792 (24)	-49

Table 4-4e. Tabulation of SO<sub>2</sub> Concentrations (µg/m<sup>3</sup>) and Percentage Change from Existing Configuration for a 20.12 m/s (45 mph) Wind Speed and Minimum Power Load.

Run & Config.	Sum of Maximum at 1.75, 3.0, 5.25 & 9.0 m	% Chg	Maximum Reading & Point	% Chg	Somers Point Equiv.	% Chg
1 - Basic	14180	-	5710 (4)	-	1480 (24)	-
2 - 50' Ext.	8220	-42	2670 (11)	-53	1400 (24)	-5
3 - Nozzles	14070	-1	5300 (4)	-7	1620 (25)	-9
4 - Ext. & Nozzles	7300	-49	2320 (11)	-59	1420 (24)	-4
5 - Large Canopy	14230	+0	5140 (4)	-10	1630 (25)	+10
6 - Small Canopy	15350	+8	5650 (4)	-1	1750 (25)	+18
7 - 60' Wall	14790	+4	5690 (4)	+0	1590 (25)	+7
15 - 390° Reheat	10900	-23	4200 (4)	-26	1270 (25)	-14
16 - Ext. & Reheat	4196	-70	1380 (35)	-76	834 (25)	-44
27 - 385' Stack	2408	-83	856 (16)	-85	803 (24)	-46
29 - 425' Stack	1586	-89	641 (23)	-89	641 (23)	-57

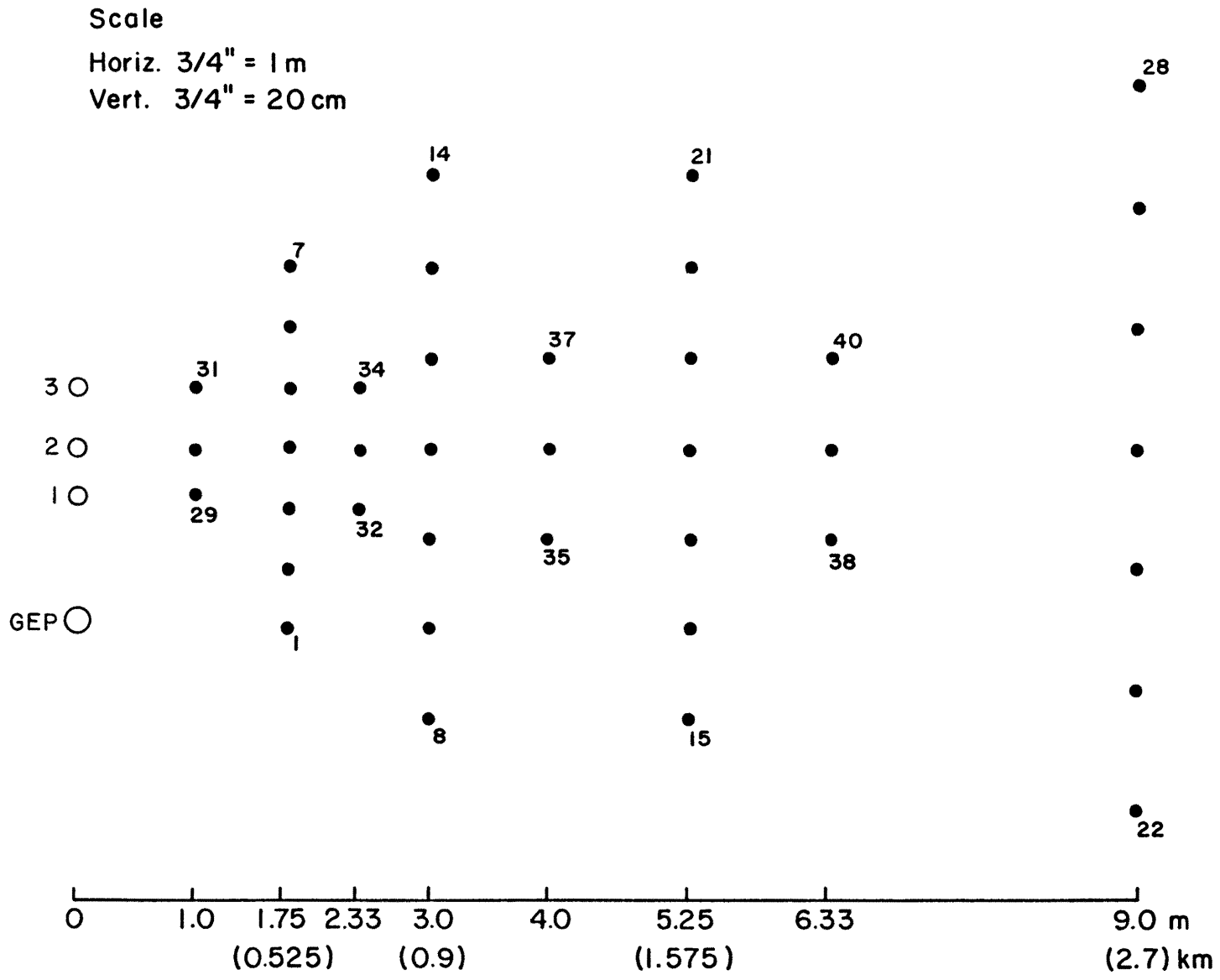
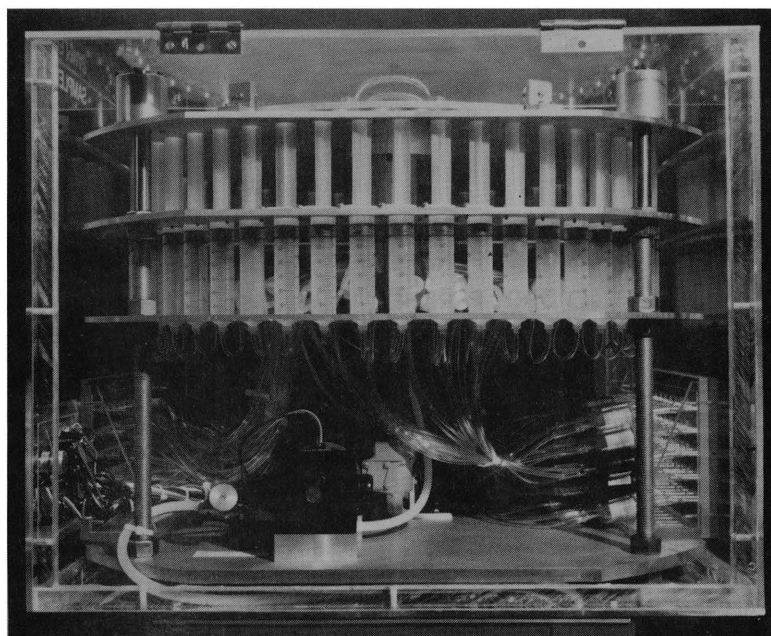
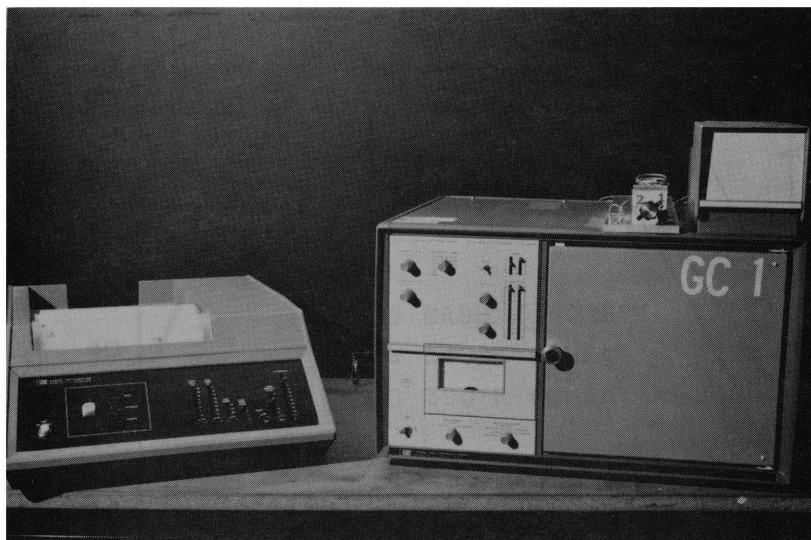


Figure 4-1. Location/Identification of Ground-level Sampling Grid Used in BLES Diffusion Study.



(a)



(b)

Figure 4-2. Photographs of (a) the Gas Sampling System, and (b) the HP Integrator and Chromatograph.

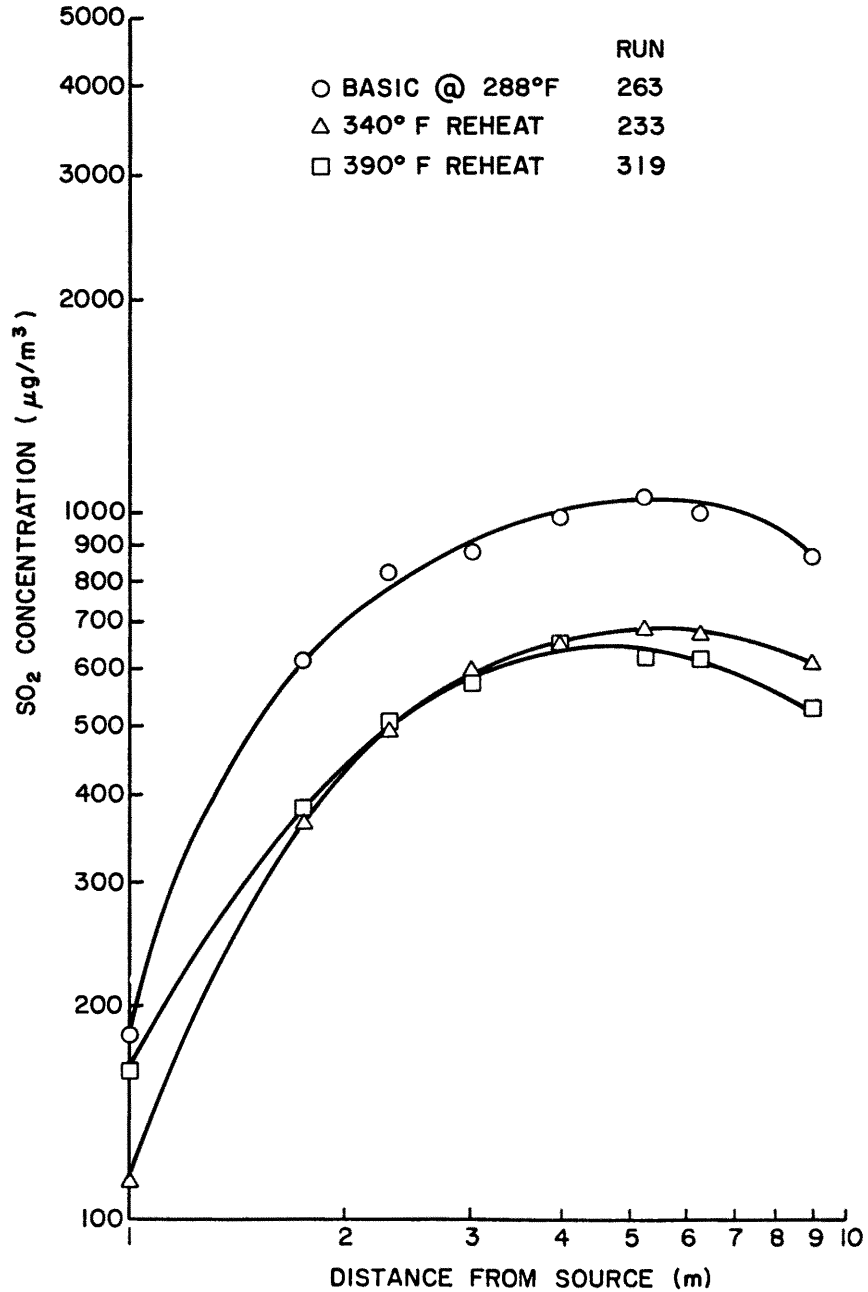


Figure 4-3a. Effect of Reheat on Ground-level  $\text{SO}_2$  Concentrations Along Plume Centerline for a 30 mph/198° Wind and Full Power Load.

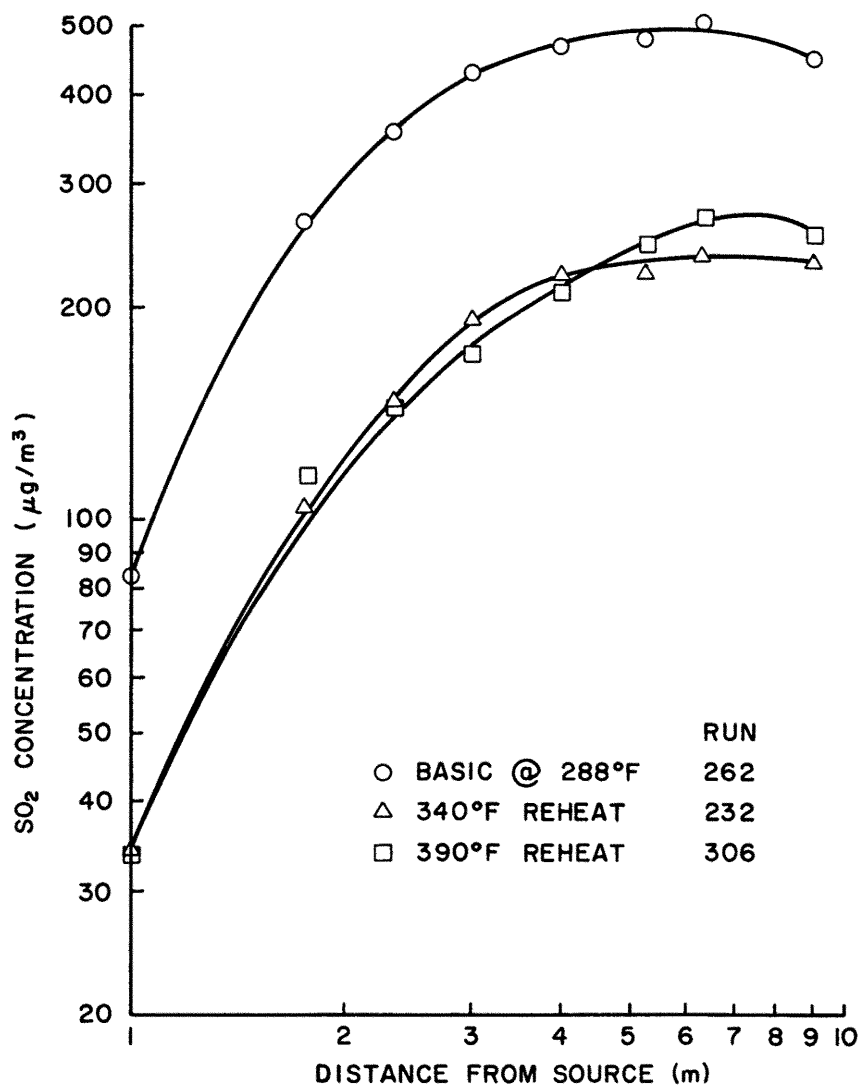


Figure 4-3b. Effect of Reheat on Ground-level  $\text{SO}_2$  Concentrations Along Plume Centerline for a 25 mph/198° Wind and Full Power Load.

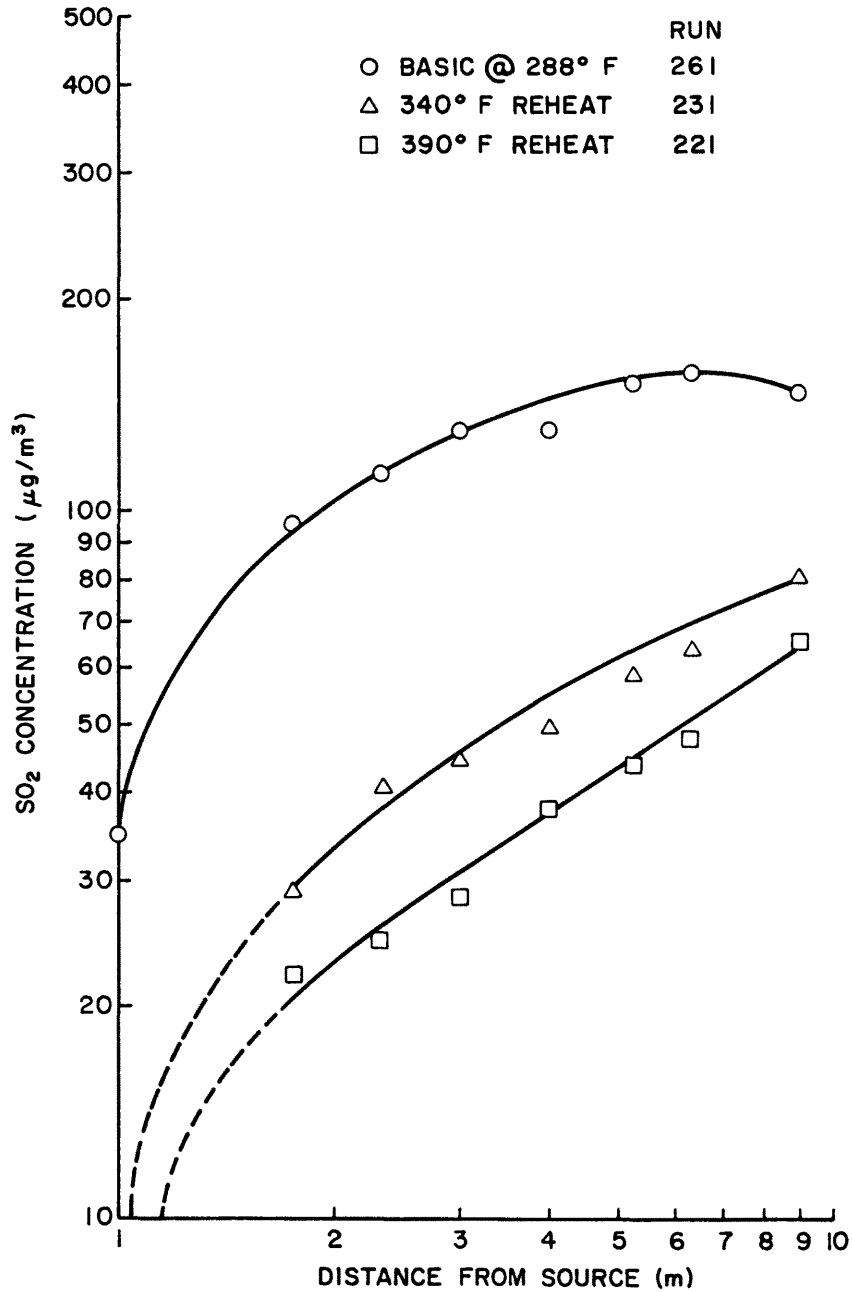


Figure 4-3c. Effect of Reheat on Ground-level  $\text{SO}_2$  Concentrations Along Plume Centerline for a 20 mph/198° Wind and Full Power Load.

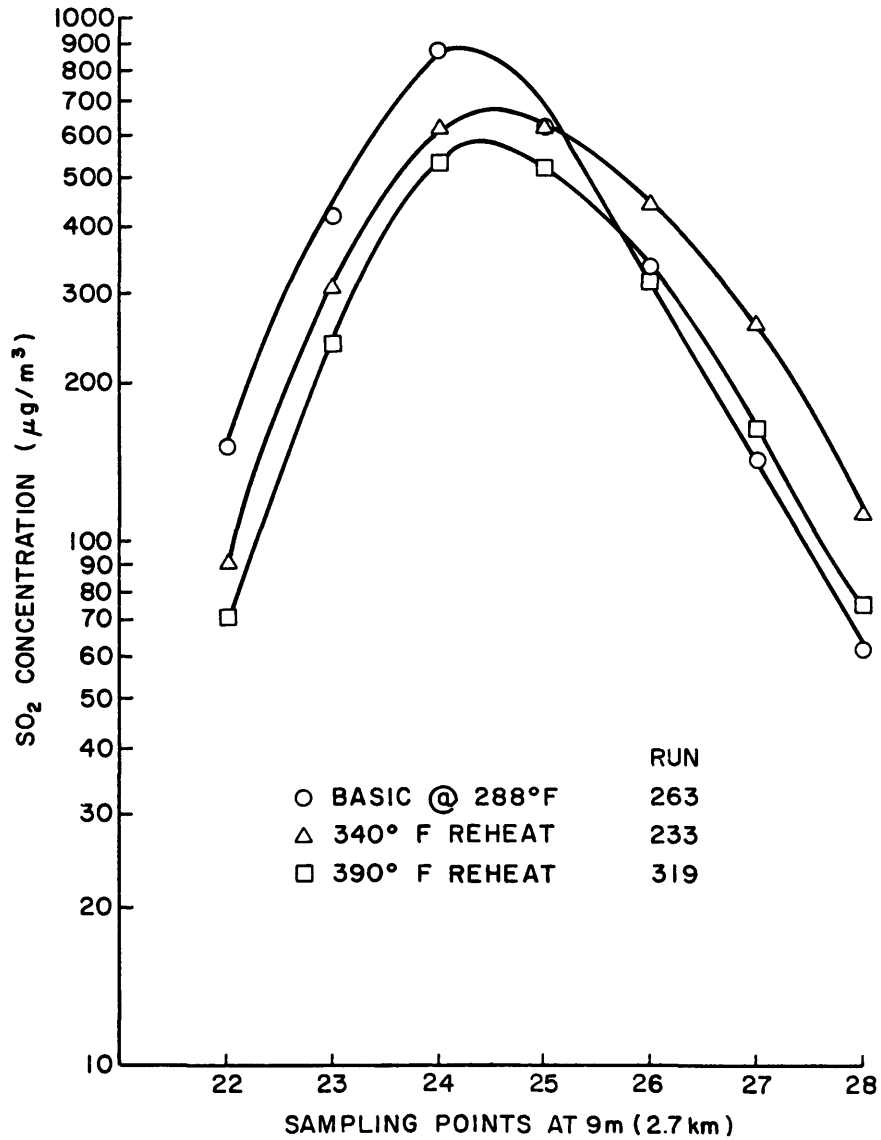


Figure 4-3d. Effect of Reheat on Ground-level  $\text{SO}_2$  Concentrations at 2.7 km for a 30 mph/198° Wind and Full Power Load.

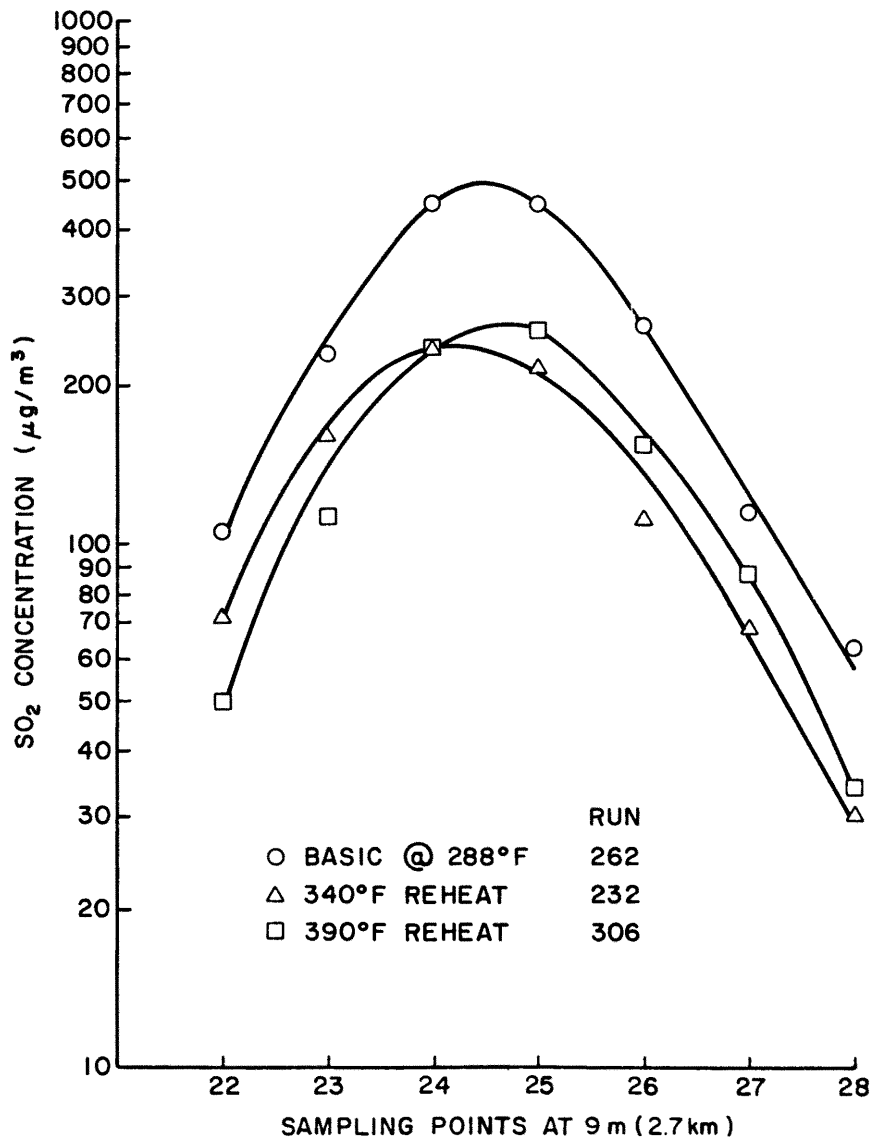


Figure 4-3e. Effect of Reheat on Ground-level SO<sub>2</sub> Concentrations at 2.7 km for a 25 mph/198° Wind and Full Power Load.

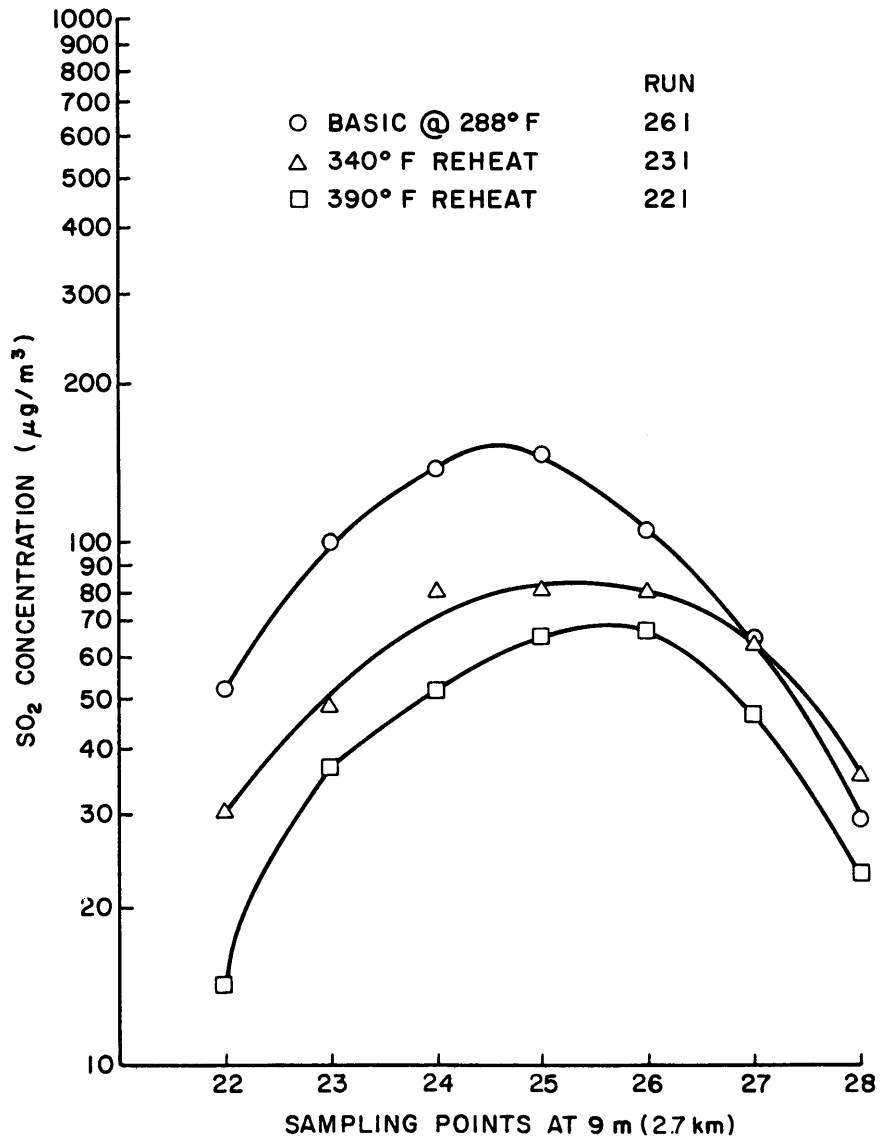


Figure 4-3f. Effect of Reheat on Ground-level SO<sub>2</sub> Concentrations at 2.7 km for a 20 mph/198° Wind and Full Power Load.

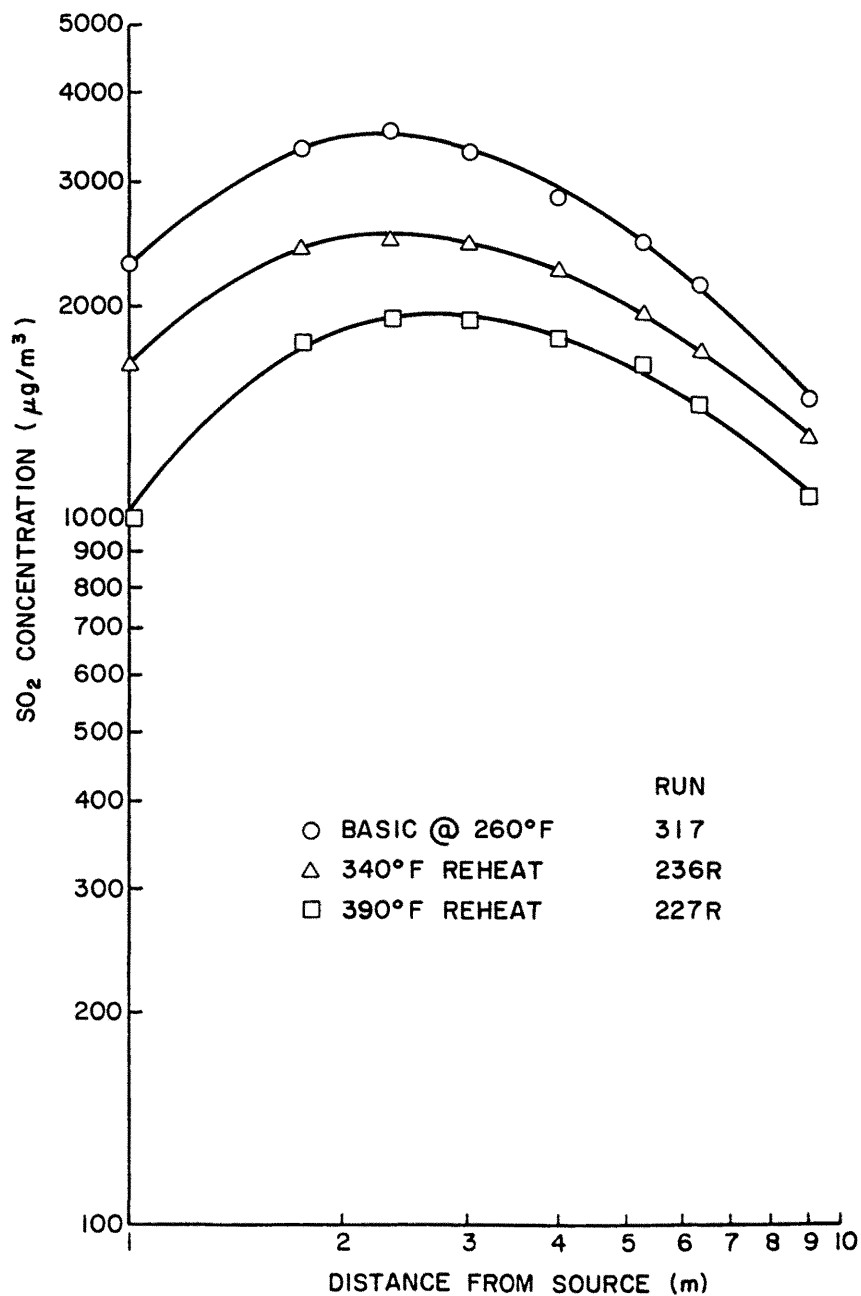


Figure 4-4a. Effect of Reheat on Ground-level  $\text{SO}_2$  Concentration Along Plume Centerline for a 30 mph/198° Wind and Minimum Power Load.

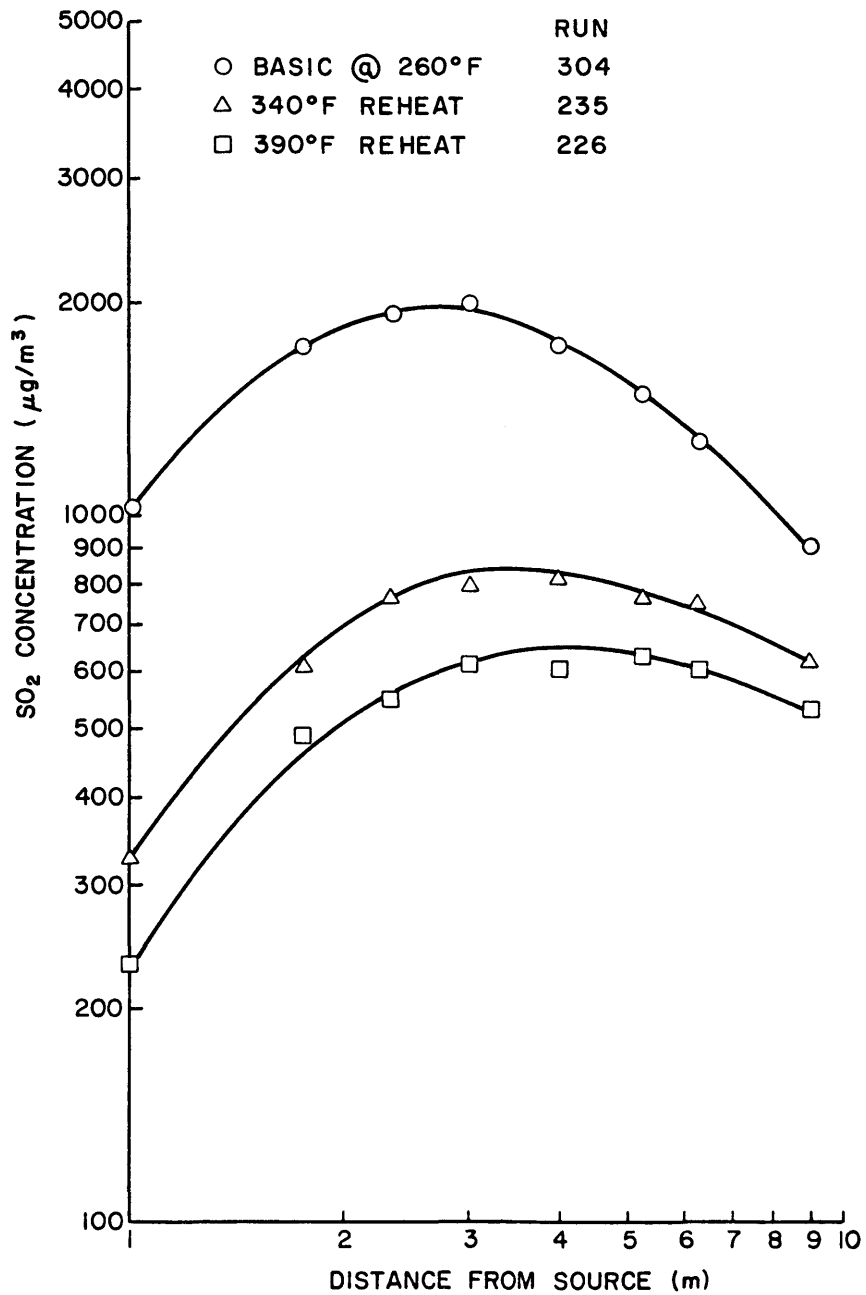


Figure 4-4b. Effect of Reheat on Ground-level  $\text{SO}_2$  Concentrations Along Plume Centerline for a 25 mph/198° Wind and Minimum Power Load.

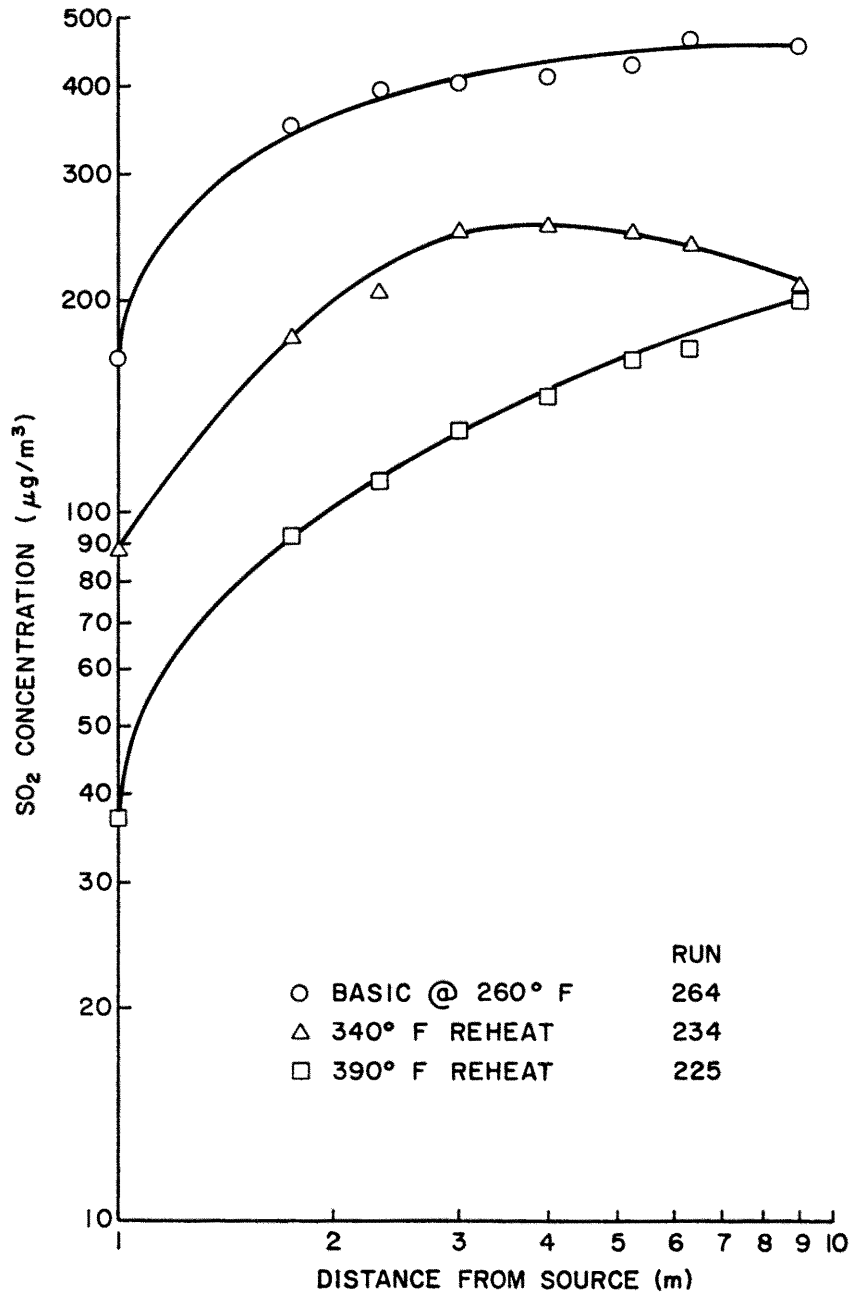


Figure 4-4c. Effect of Reheat on Ground-level  $\text{SO}_2$  Concentrations Along Plume Centerline for a 20 mph/198° Wind and Minimum Power Load.

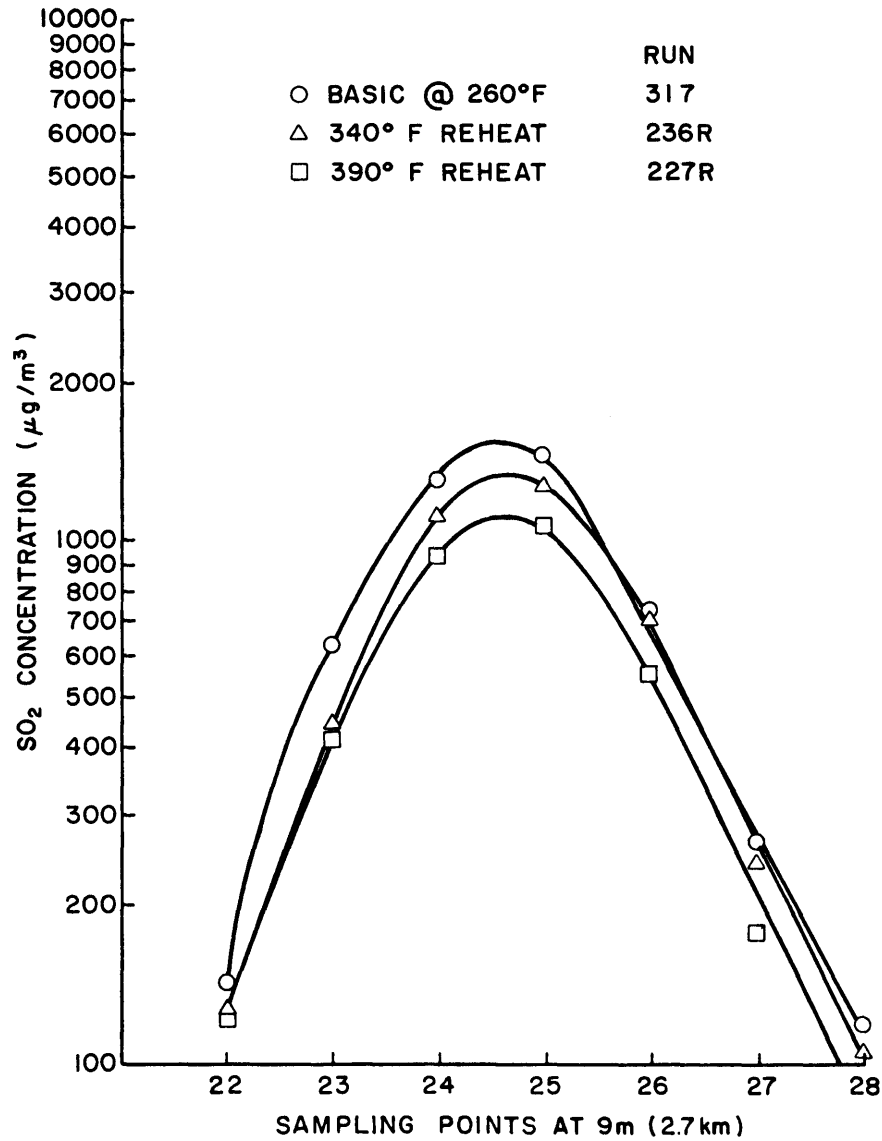


Figure 4-4d. Effect of Reheat on Ground-level SO<sub>2</sub> Concentrations at 2.7 km for a 30 mph/198° Wind and Minimum Power Load.

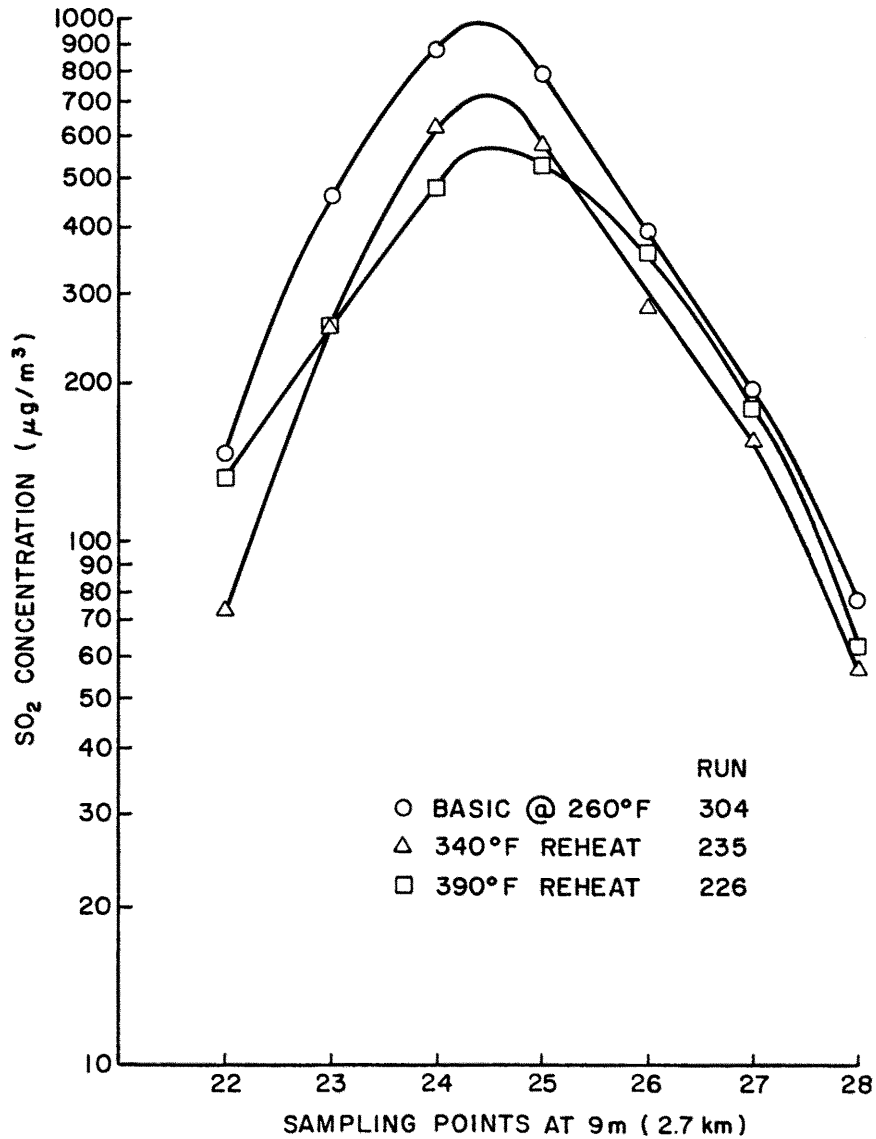


Figure 4-4e. Effect of Reheat on Ground-level SO<sub>2</sub> Concentrations at 2.7 km for a 25 mph/198° Wind and Minimum Power Load.

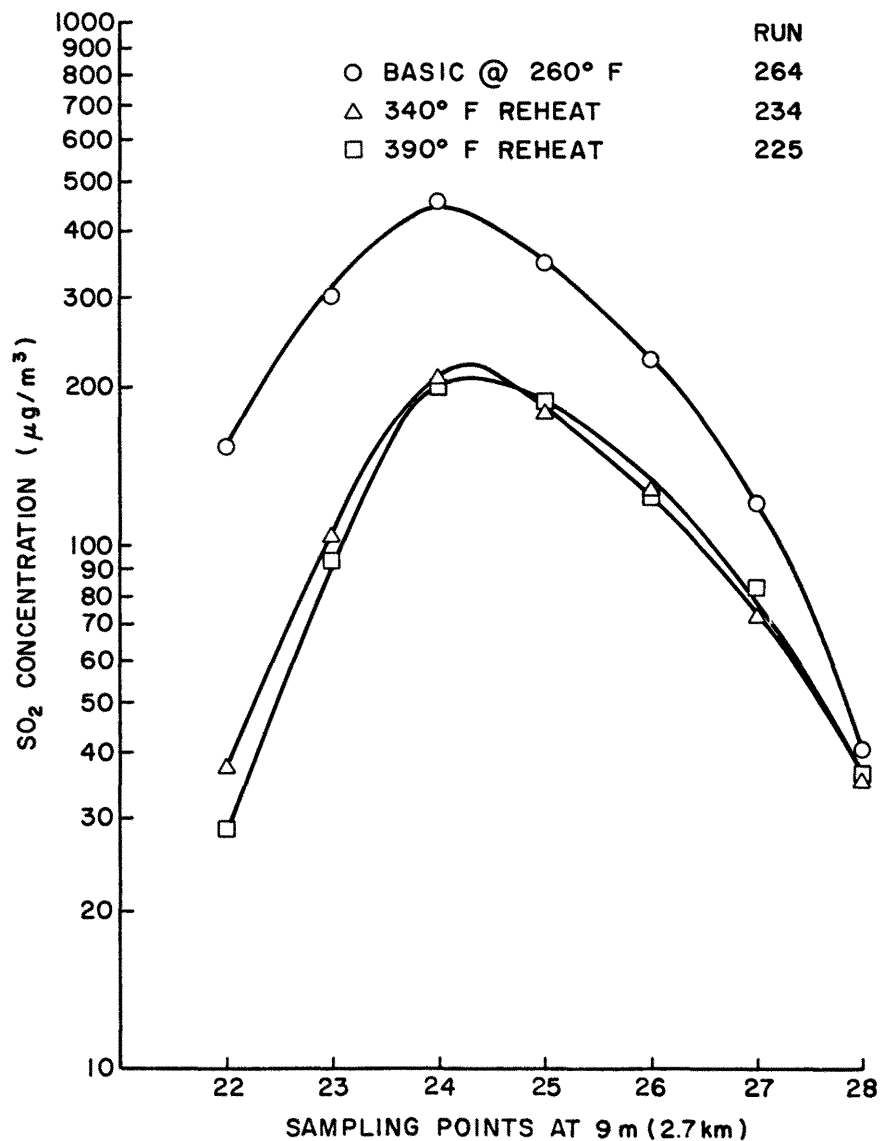


Figure 4-4f. Effect of Reheat on Ground-level  $\text{SO}_2$  Concentrations at 2.7 km for a 20 mph/198° Wind and Minimum Power Load.

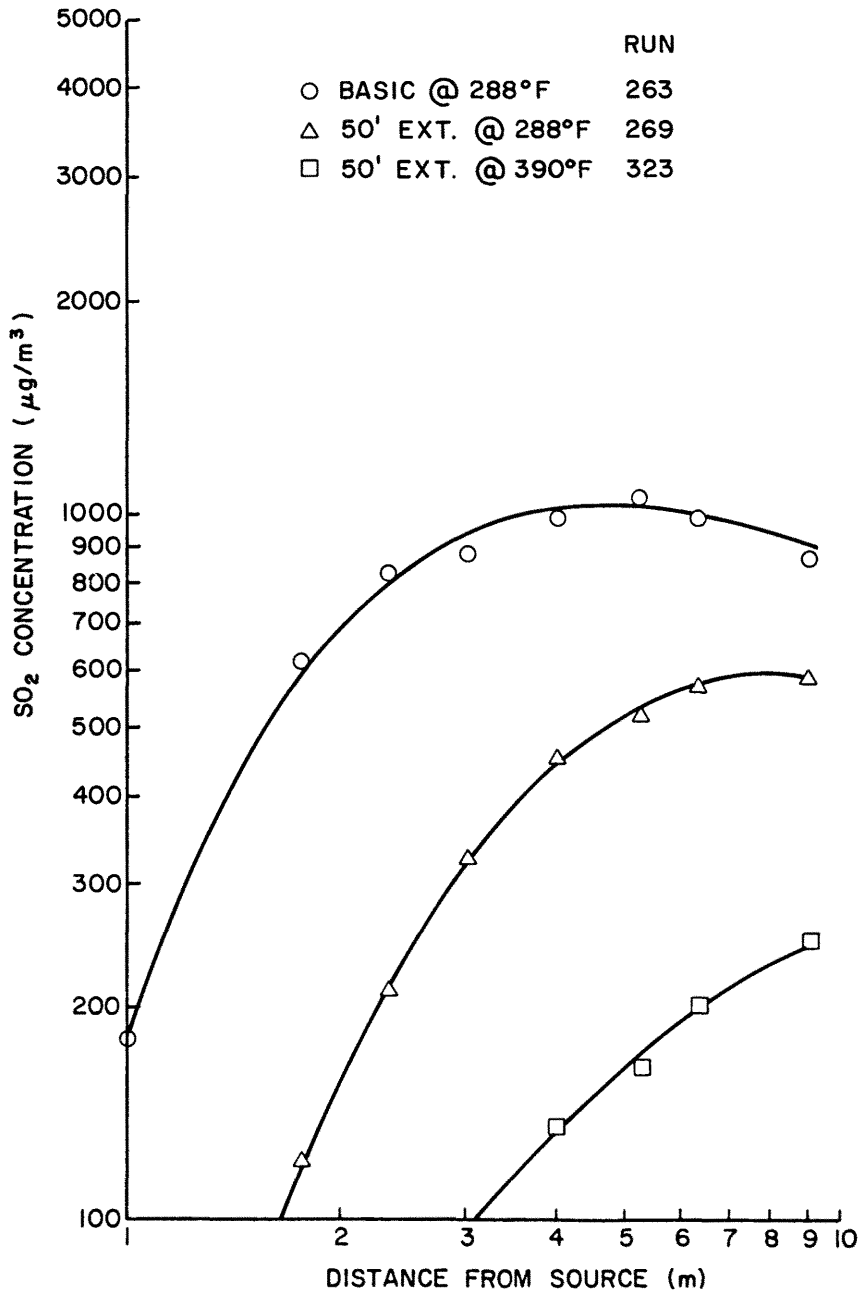


Figure 4-5a. Effect of 50' Extensions on Ground-level SO<sub>2</sub> Concentrations Along Plume Centerline for a 30 mph/198° Wind and Full Power Load.

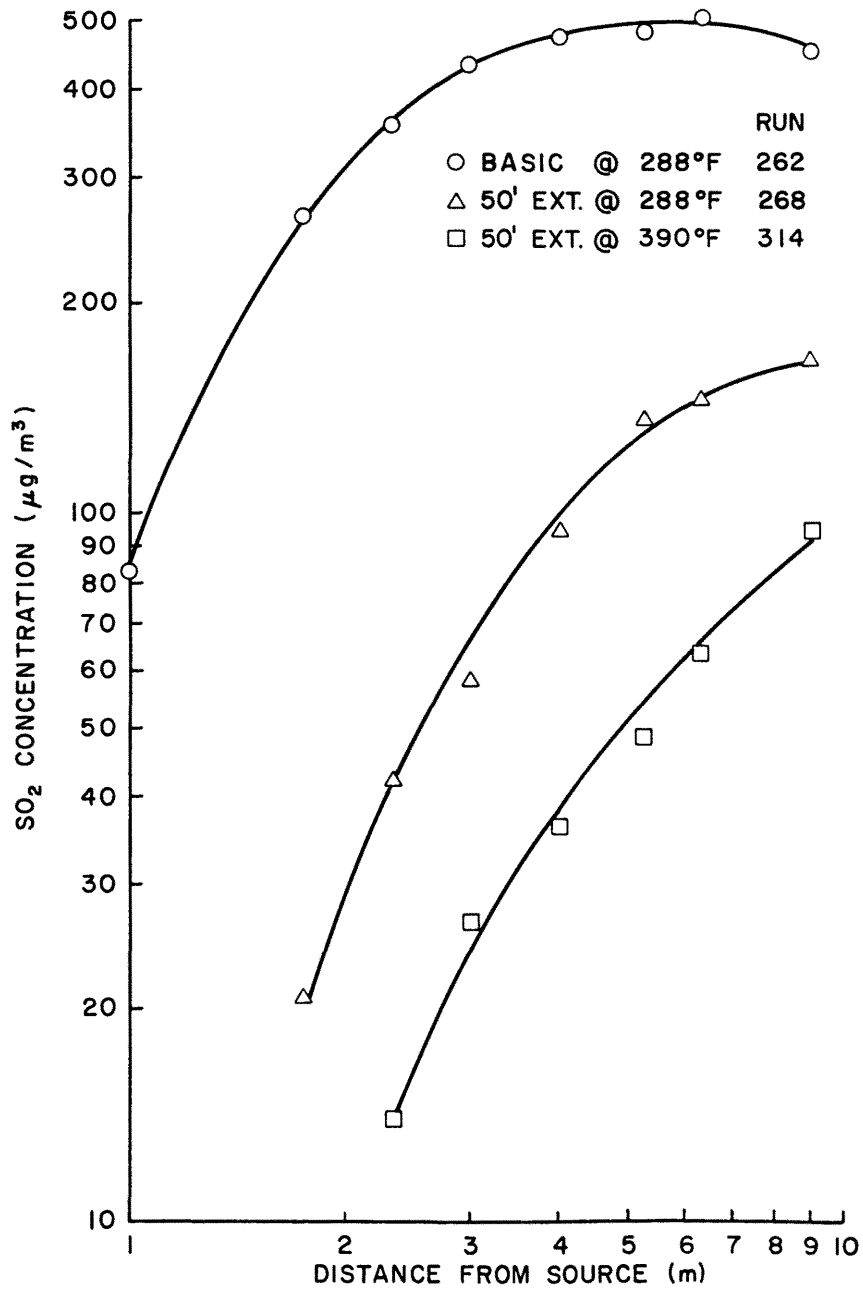


Figure 4-5b. Effect of 50' Extensions on Ground-level SO<sub>2</sub> Concentrations Along Plume Centerline for a 25 mph/198° Wind and Full Power Load.

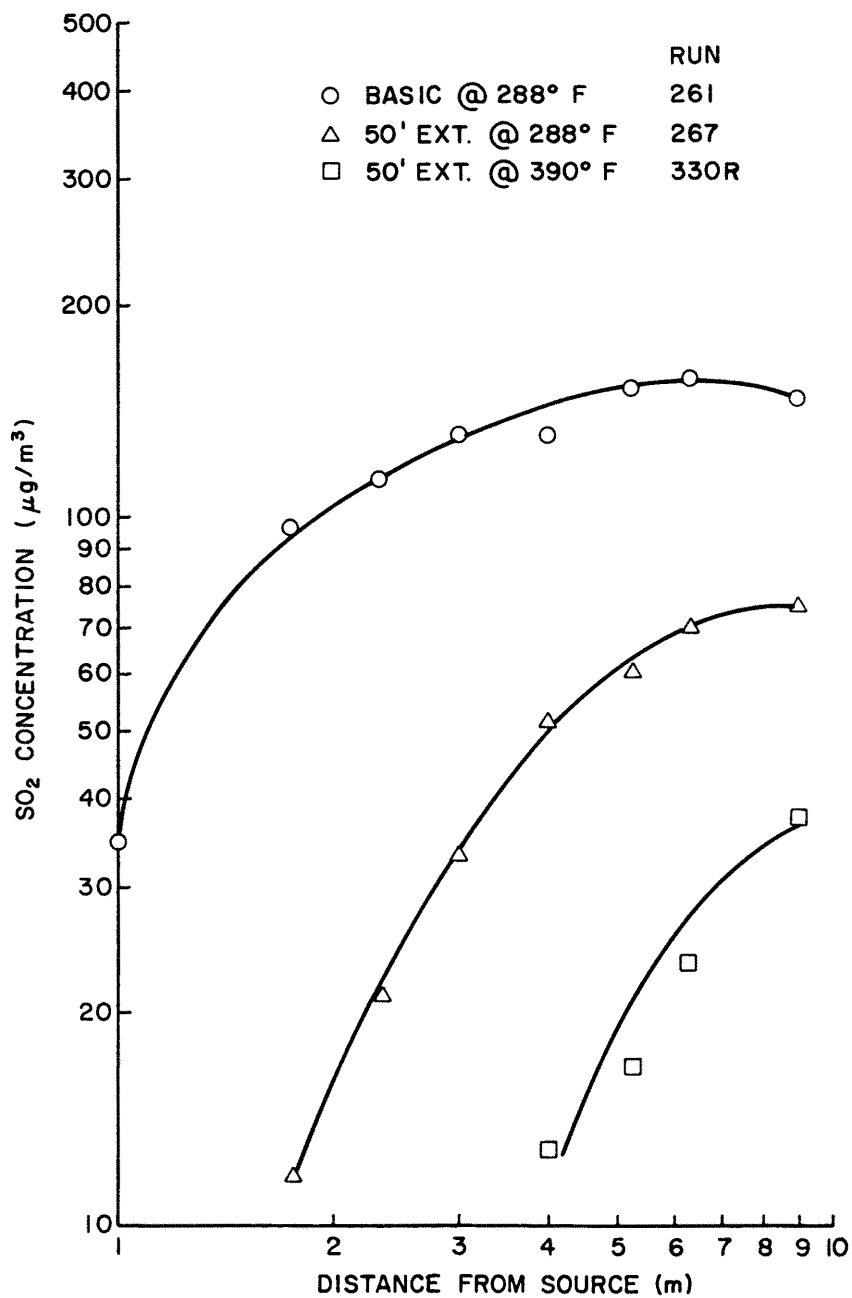


Figure 4-5c. Effect of 50' Extensions on Ground-level  $\text{SO}_2$  Concentrations Along Plume Centerline for a 20 mph/198° Wind and Full Power Load.

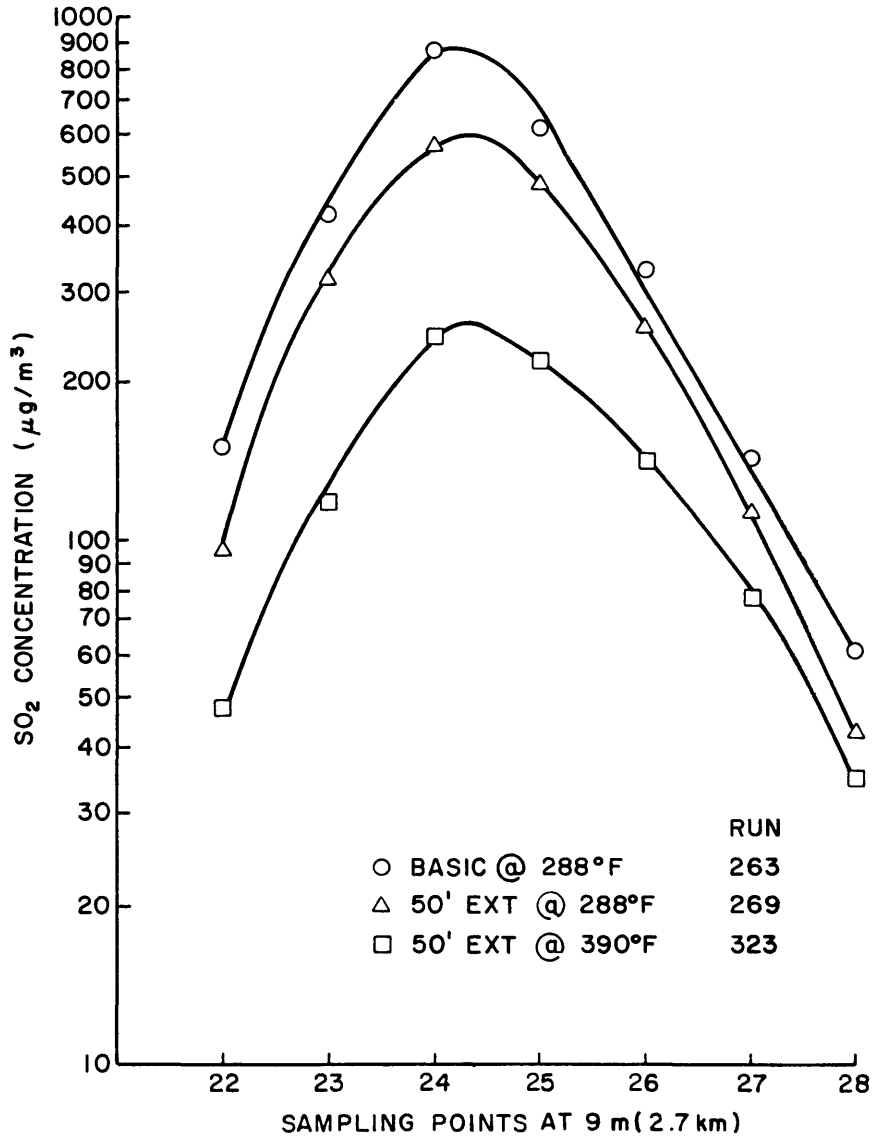


Figure 4-5d. Effect of 50' Extensions on Ground-level SO<sub>2</sub> Concentrations at 2.7 km for a 30 mph/198° Wind and Full Power Load.

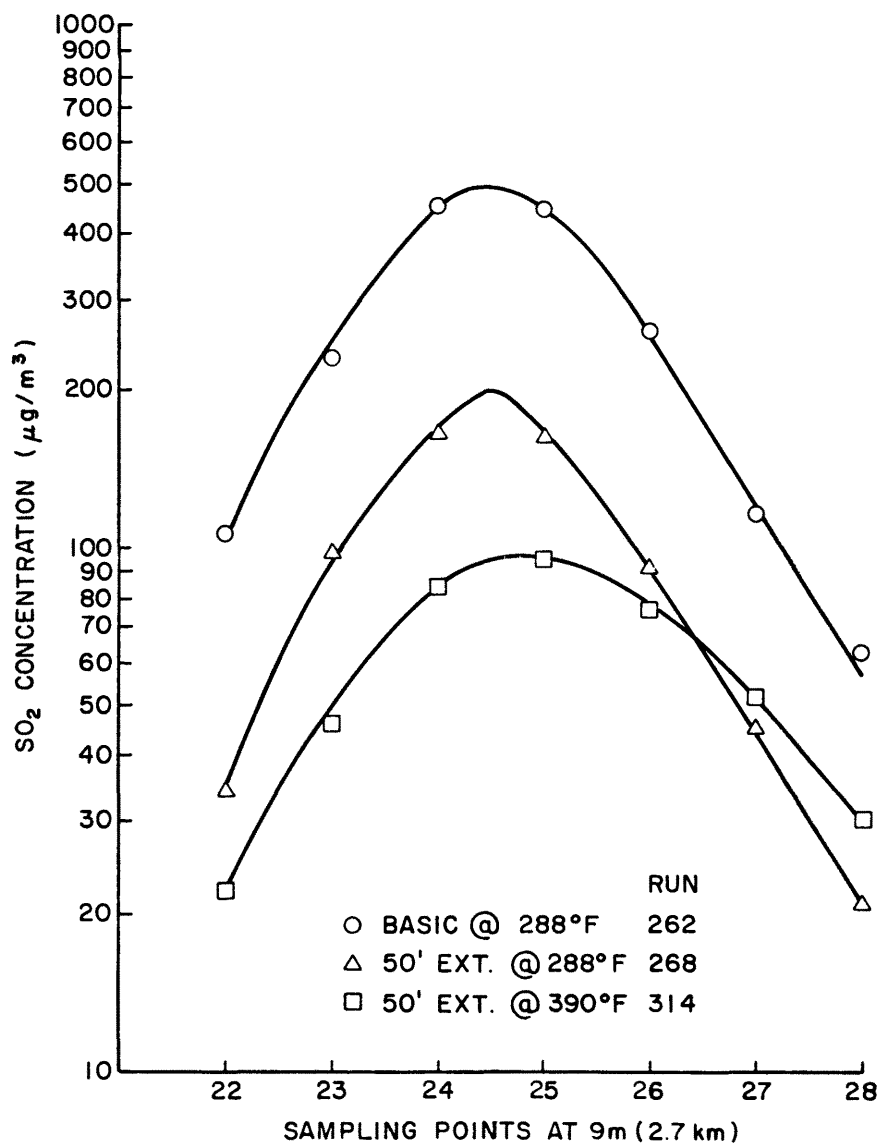


Figure 4-5e. Effect of 50' Extensions on Ground-level SO<sub>2</sub> Concentrations at 2.7 km for a 25 mph/198° Wind and Full Power Load.

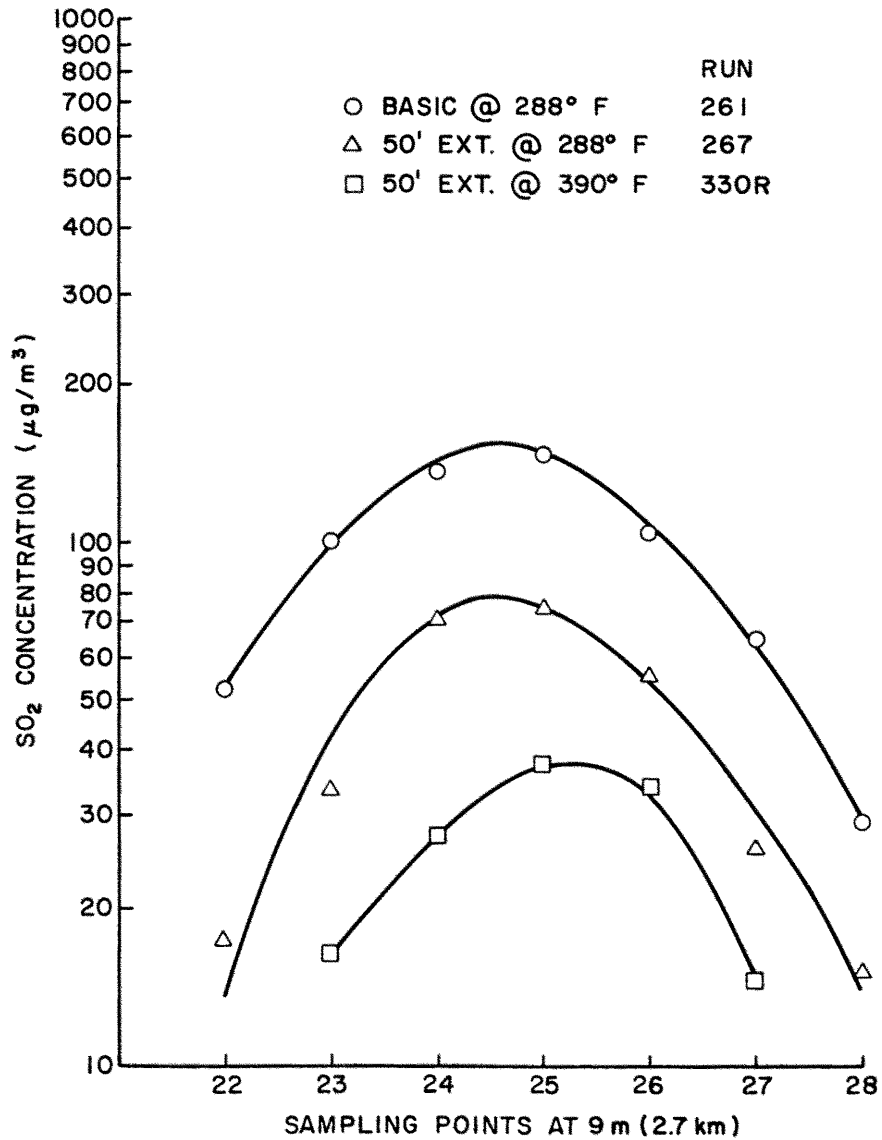


Figure 4-5f. Effect of 50' Extensions on Ground-level  $\text{SO}_2$  Concentrations at 2.7 km for a 20 mph/198° Wind and Full Power Load.

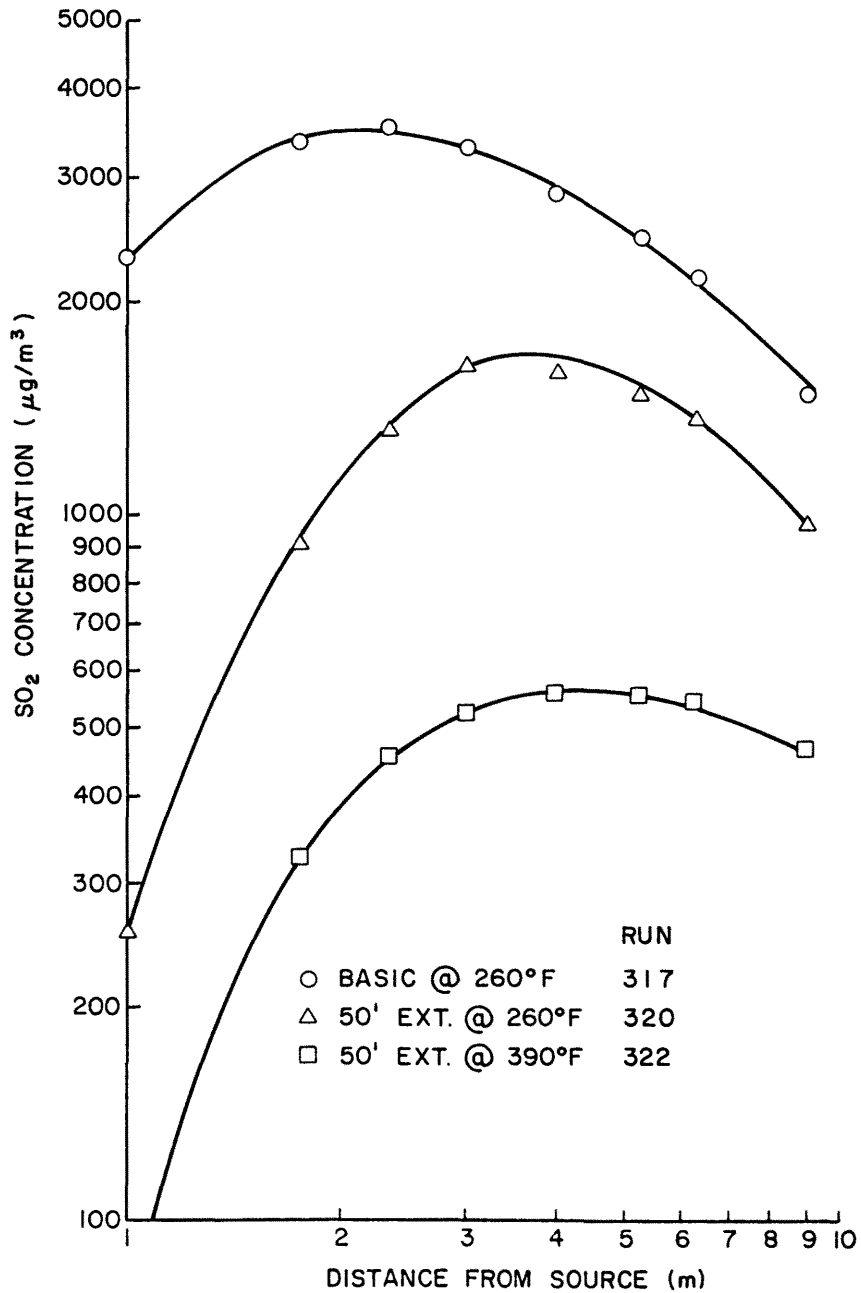


Figure 4-6a. Effect of 50' Extensions on Ground-level SO<sub>2</sub> Concentrations Along Plume Centerline for a 30 mph/198° Wind and Minimum Power Load.

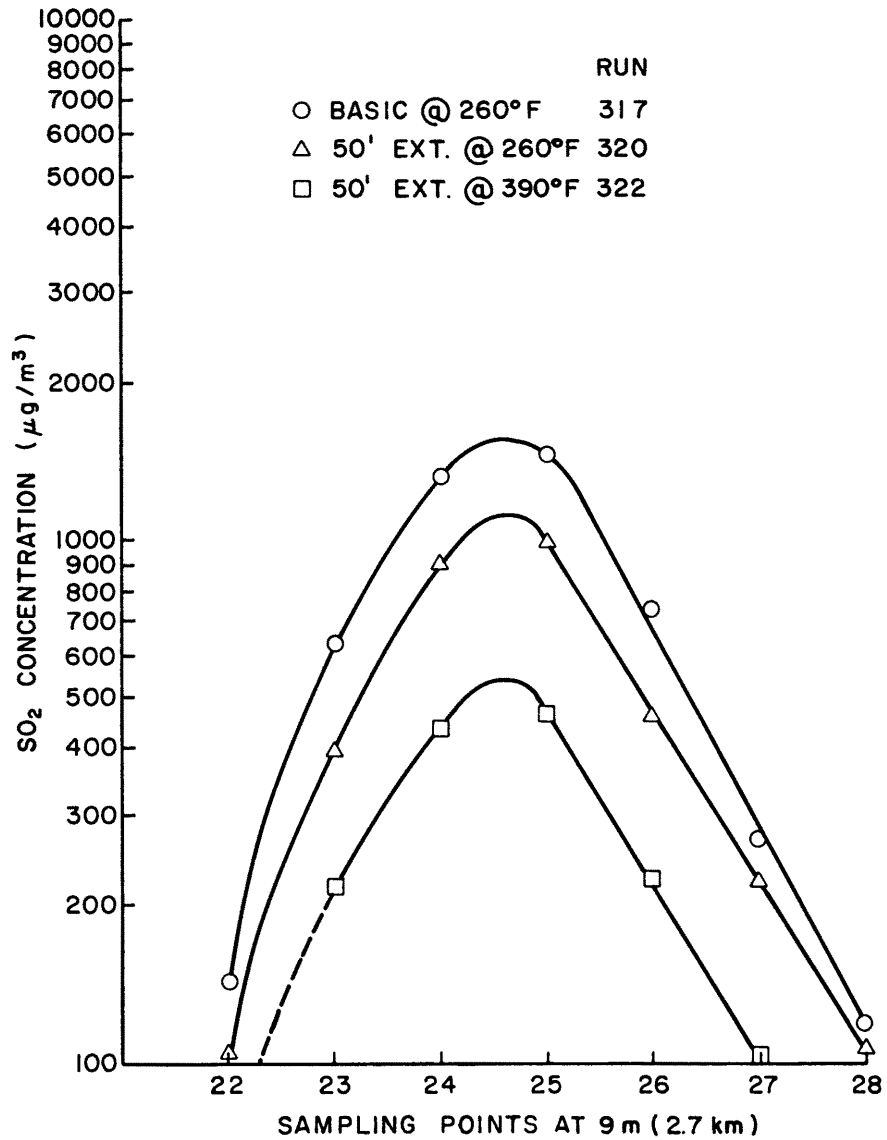


Figure 4-6b. Effect of 50' Extensions on Ground-level SO<sub>2</sub> Concentrations at 2.7 km for a 30 mph/198° Wind and Minimum Power Load.

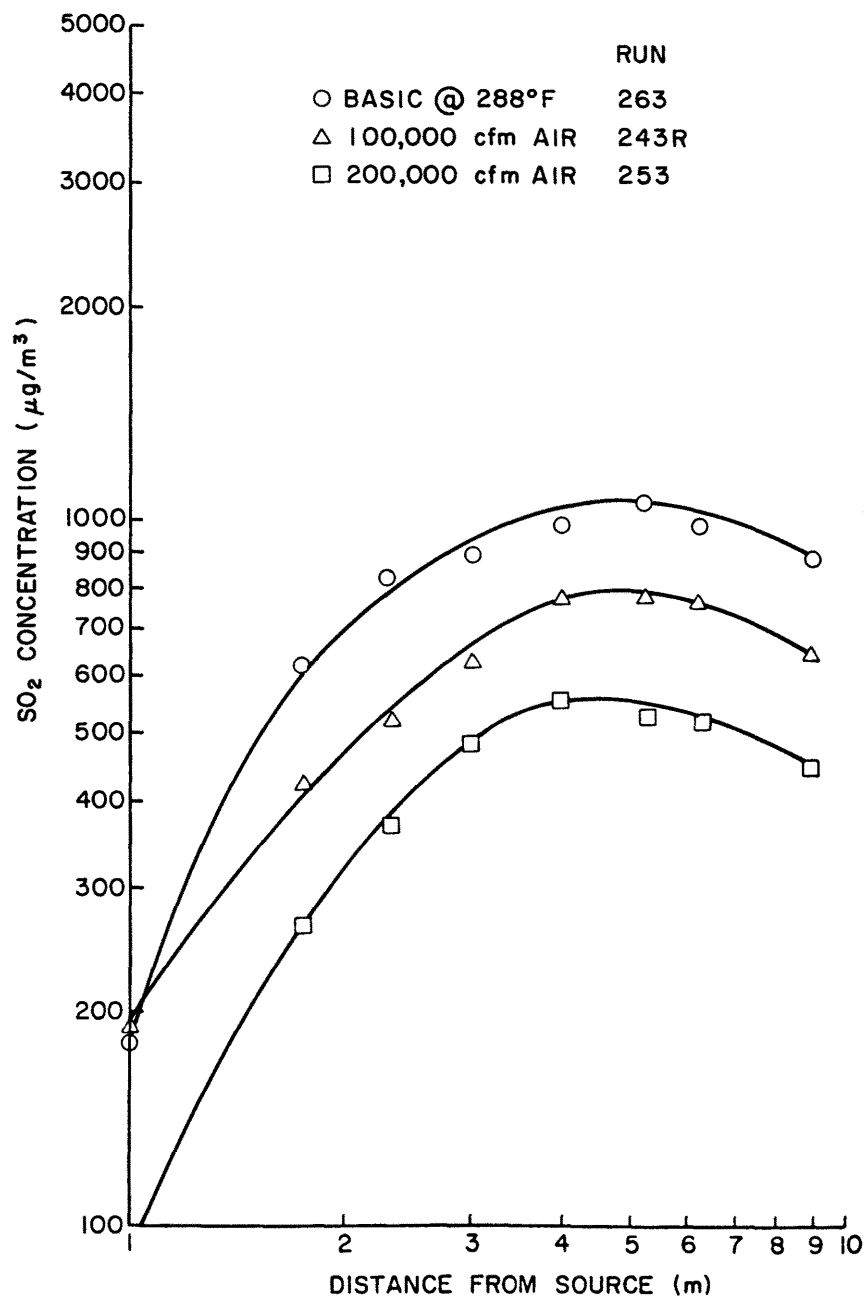


Figure 4-7a. Effect of Added Air on Ground-level SO<sub>2</sub> Concentrations Along Plume Centerline for a 30 mph/198° Wind and Full Power Load.

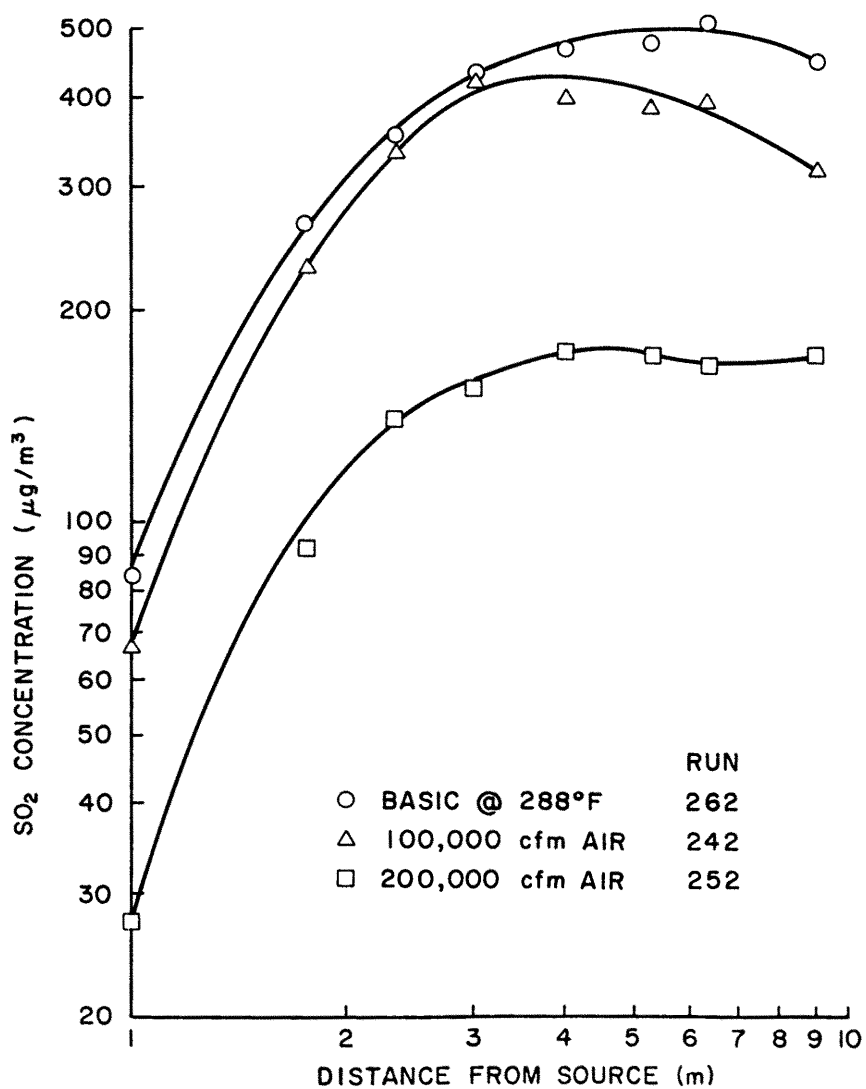


Figure 4-7b. Effect of Added Air on Ground-level SO<sub>2</sub> Concentrations Along Plume Centerline for a 25 mph/198° Wind and Full Power Load.

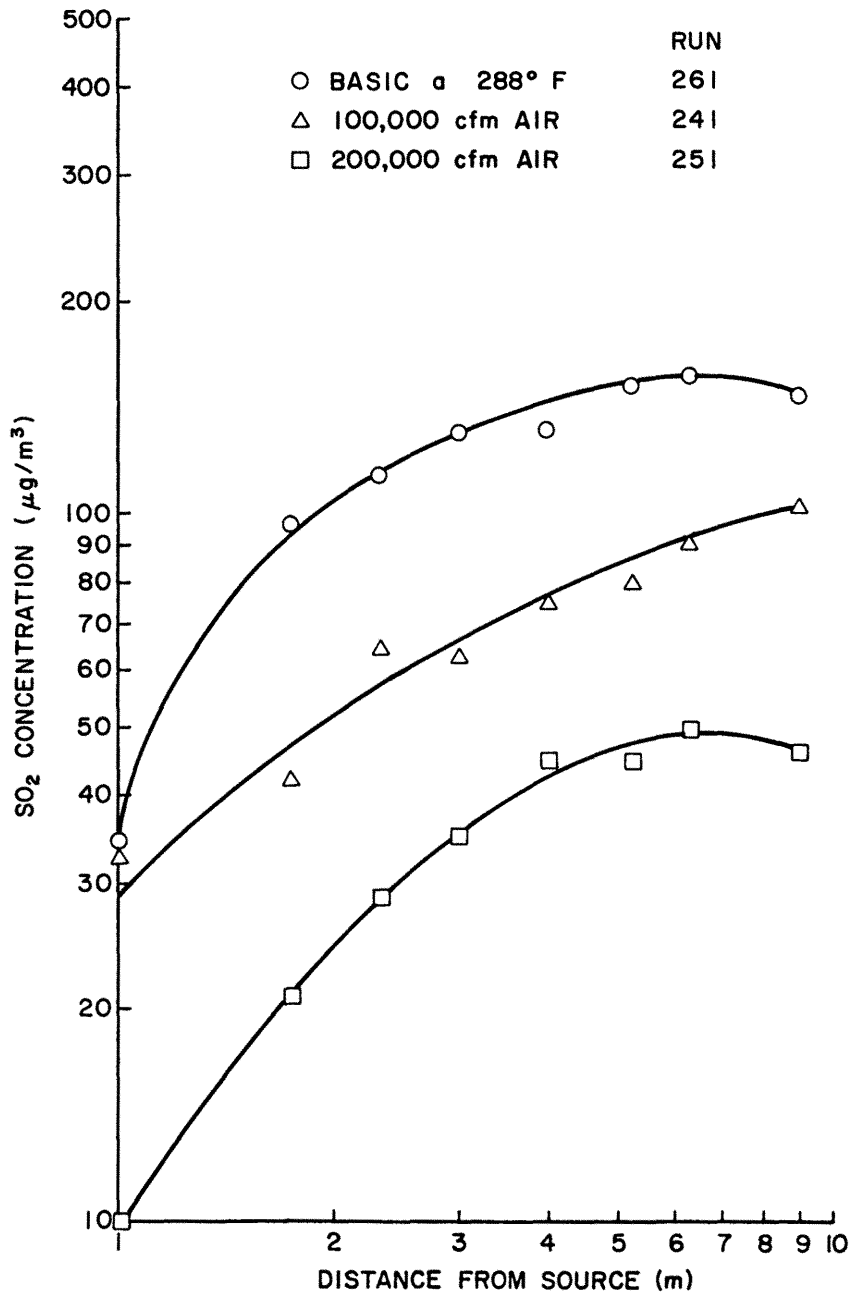


Figure 4-7c. Effect of Added Air on Ground-level SO<sub>2</sub> Concentrations Along Plume Centerline for a 20 mph/198° Wind and Full Power Load.

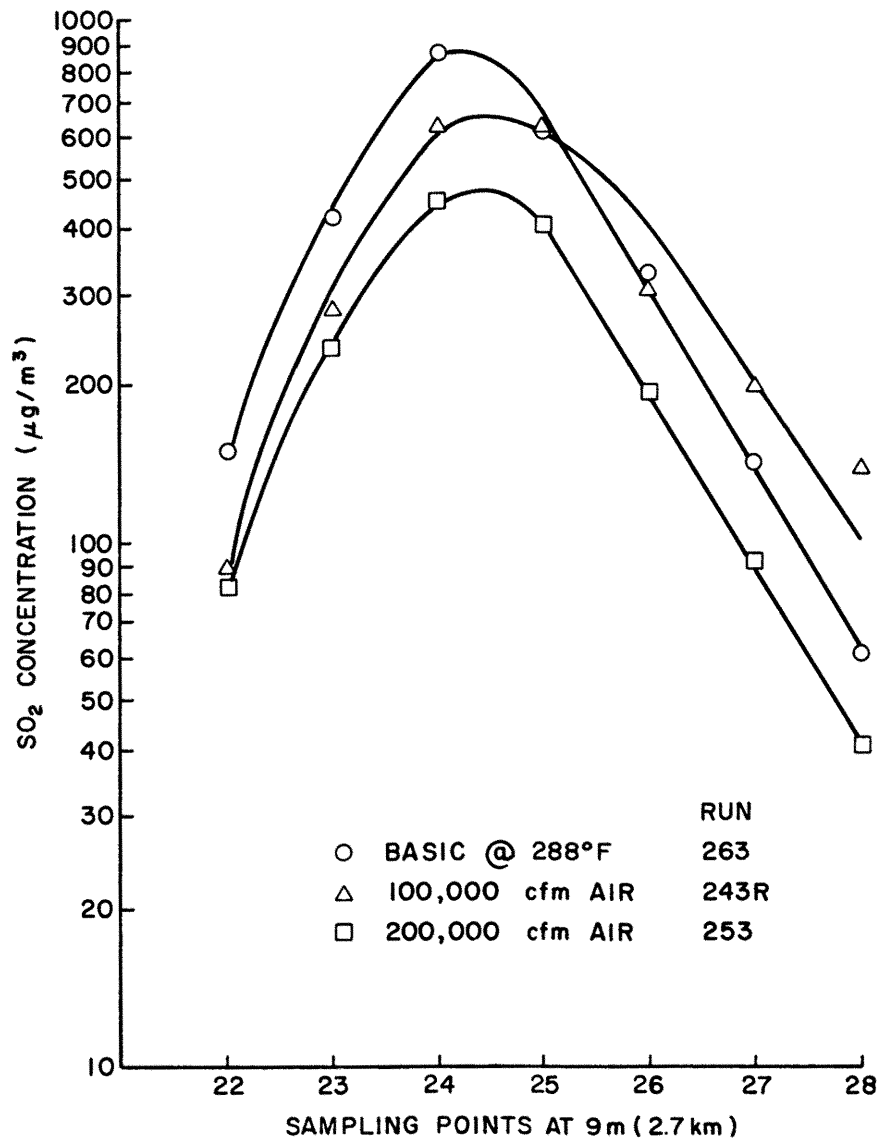


Figure 4-7d. Effect of Added Air on Ground-level  $\text{SO}_2$  Concentrations at 2.7 km for a 30 mph/198° Wind and Full Power Load.

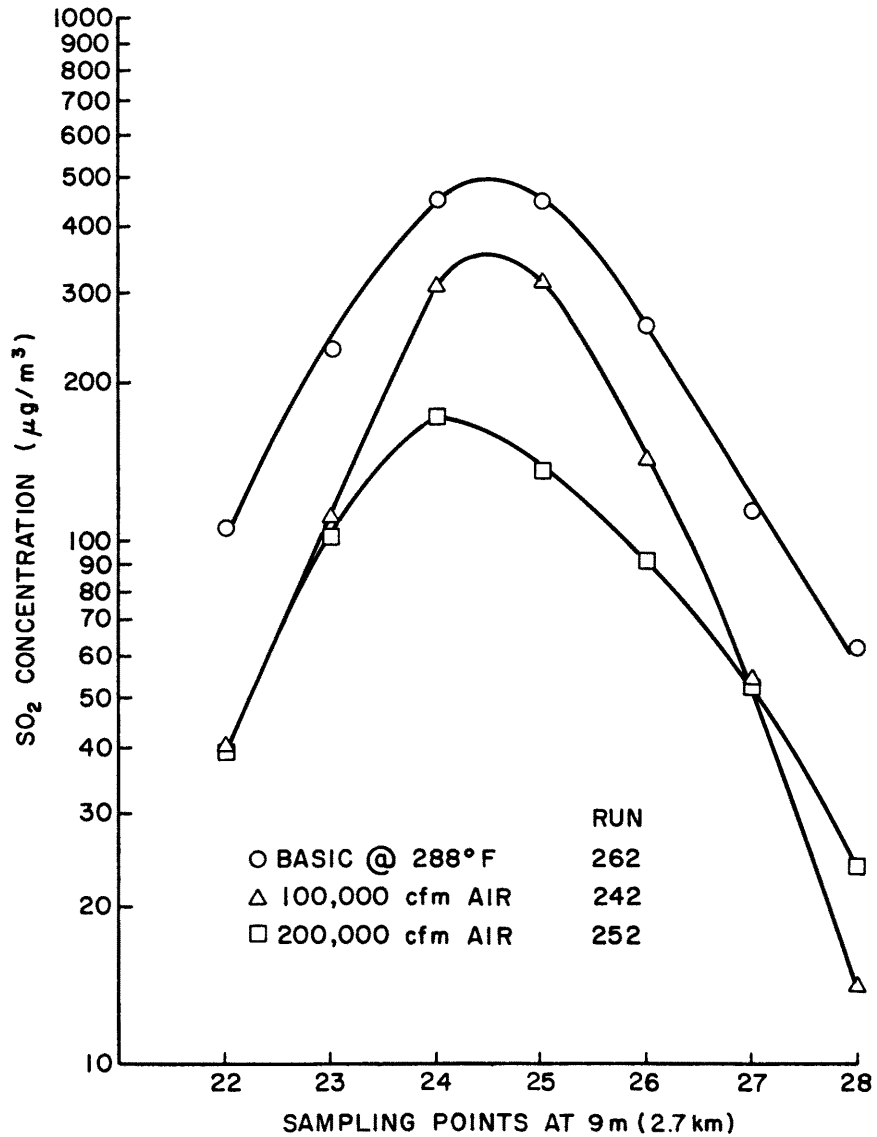


Figure 4-7e. Effect of Added Air on Ground-level SO<sub>2</sub> Concentrations at 2.7 km for a 25 mph/198° Wind and Full Power Load.

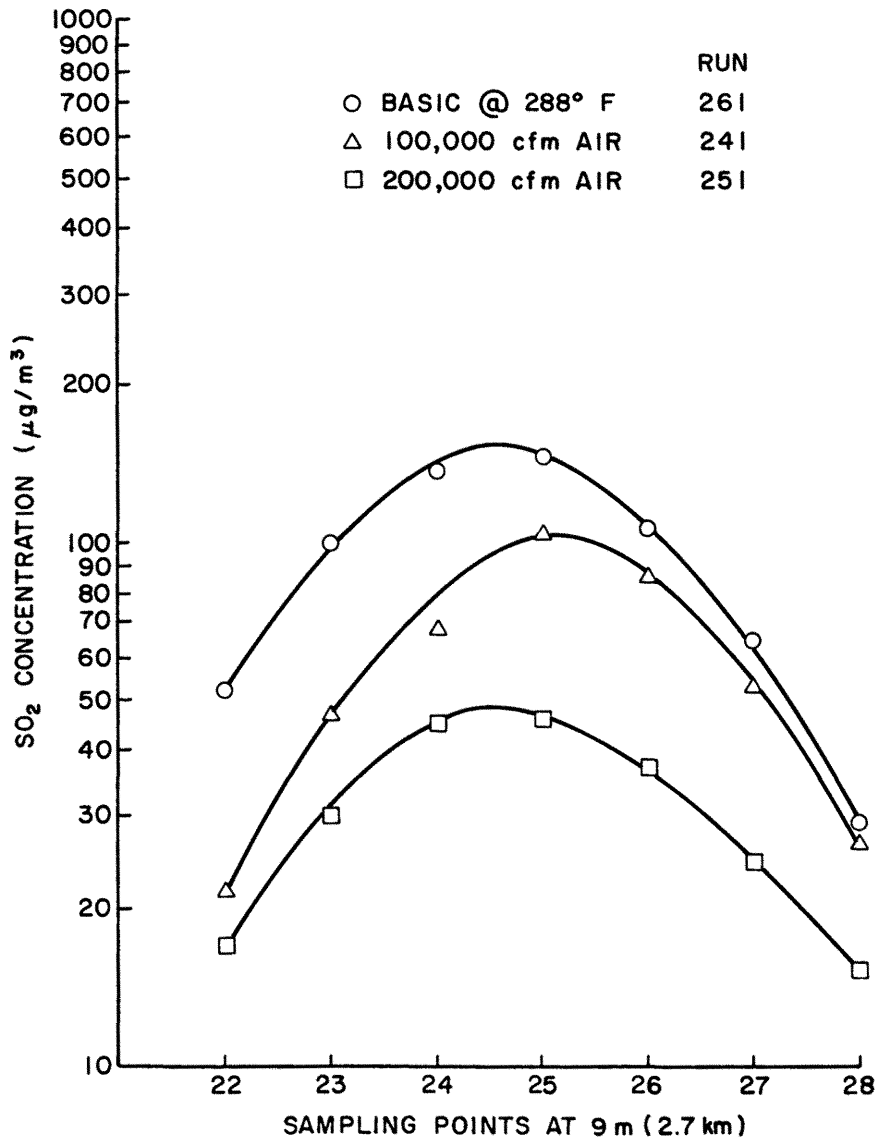


Figure 4-7f. Effect of Added Air on Ground-level  $\text{SO}_2$  Concentrations at 2.7 km for a 20 mph/198° Wind and Full Power Load.

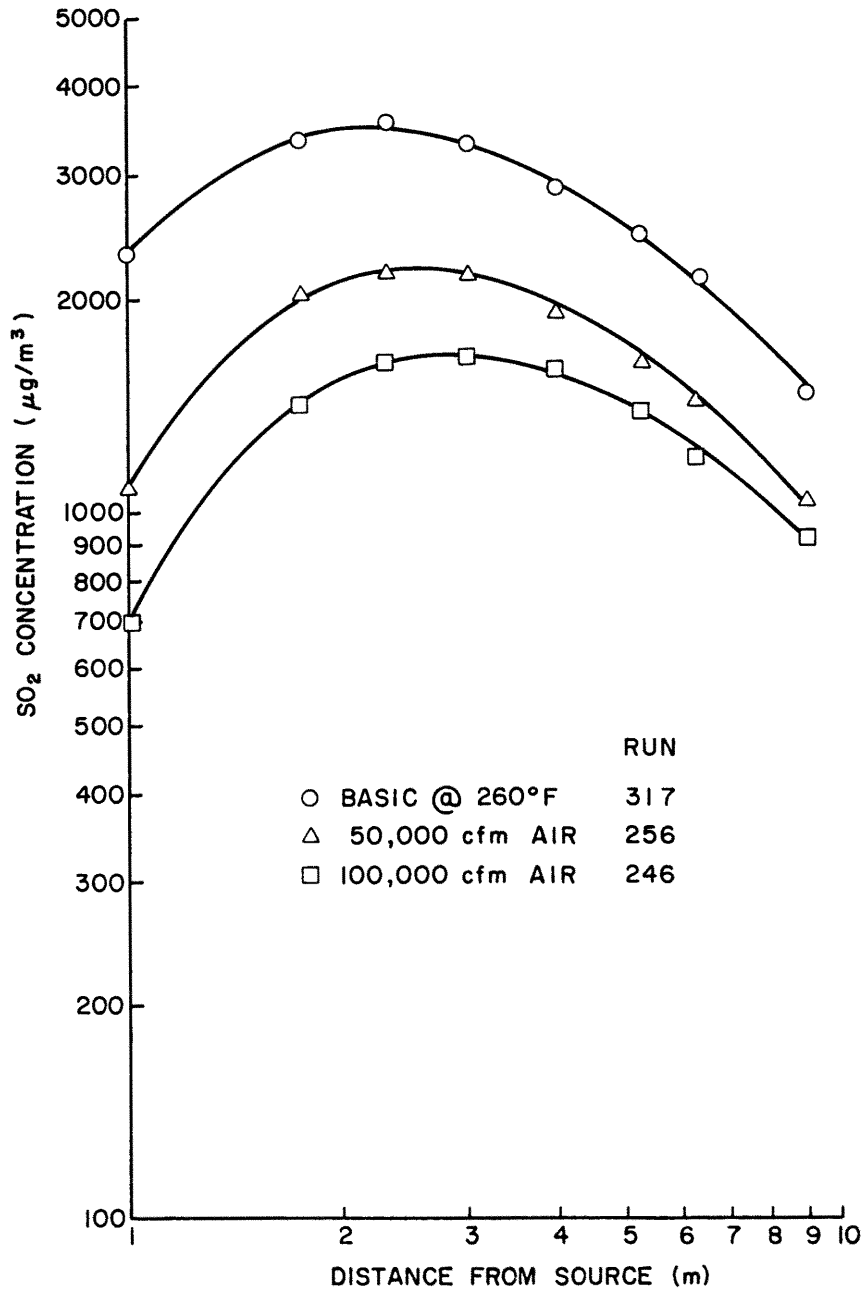


Figure 4-8a. Effect of Added Air on Ground-level  $\text{SO}_2$  Concentrations Along Plume Centerline for a 30 mph/198° Wind and Minimum Power Load.

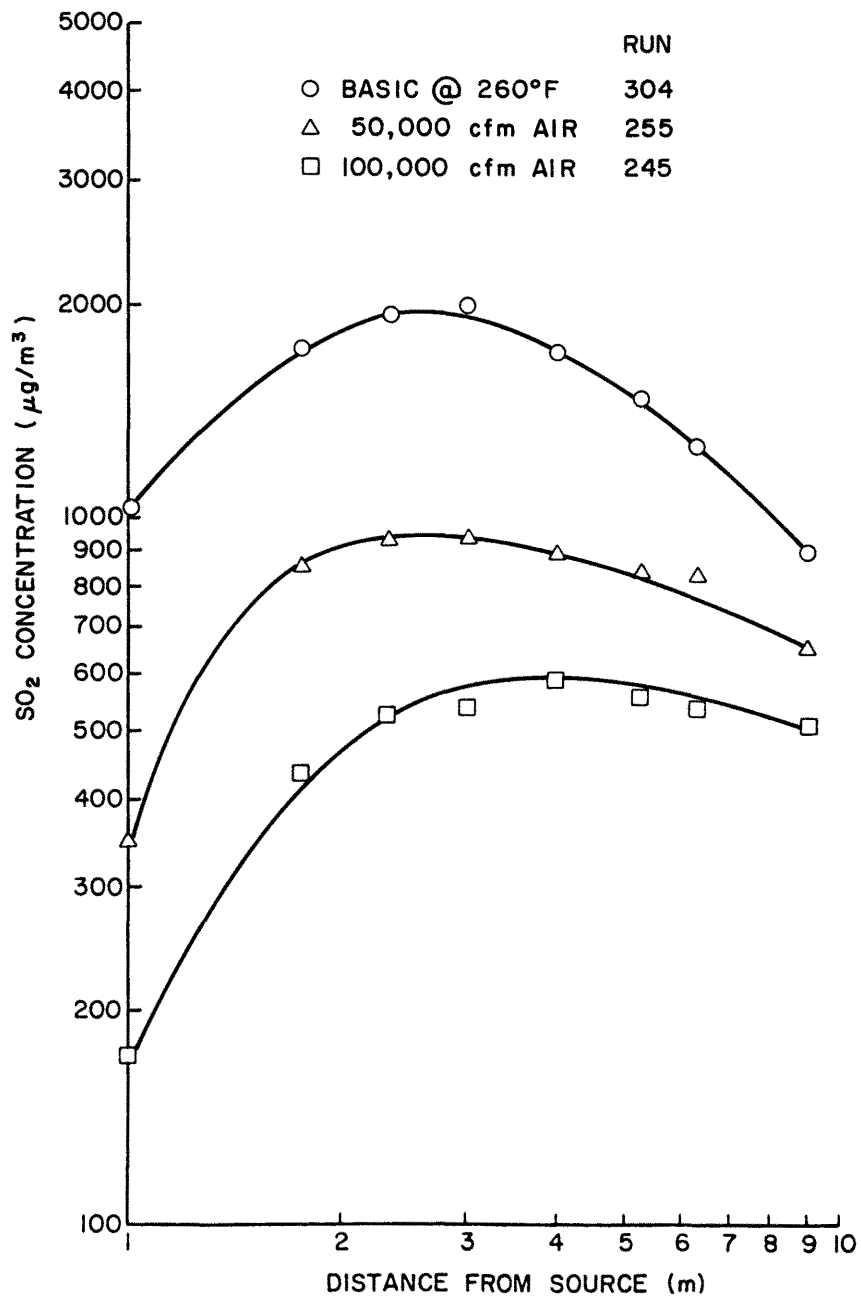


Figure 4-8b. Effect of Added Air on Ground-level  $\text{SO}_2$  Concentrations Along Plume Centerline for a 25 mph/198° Wind and Minimum Power Load.

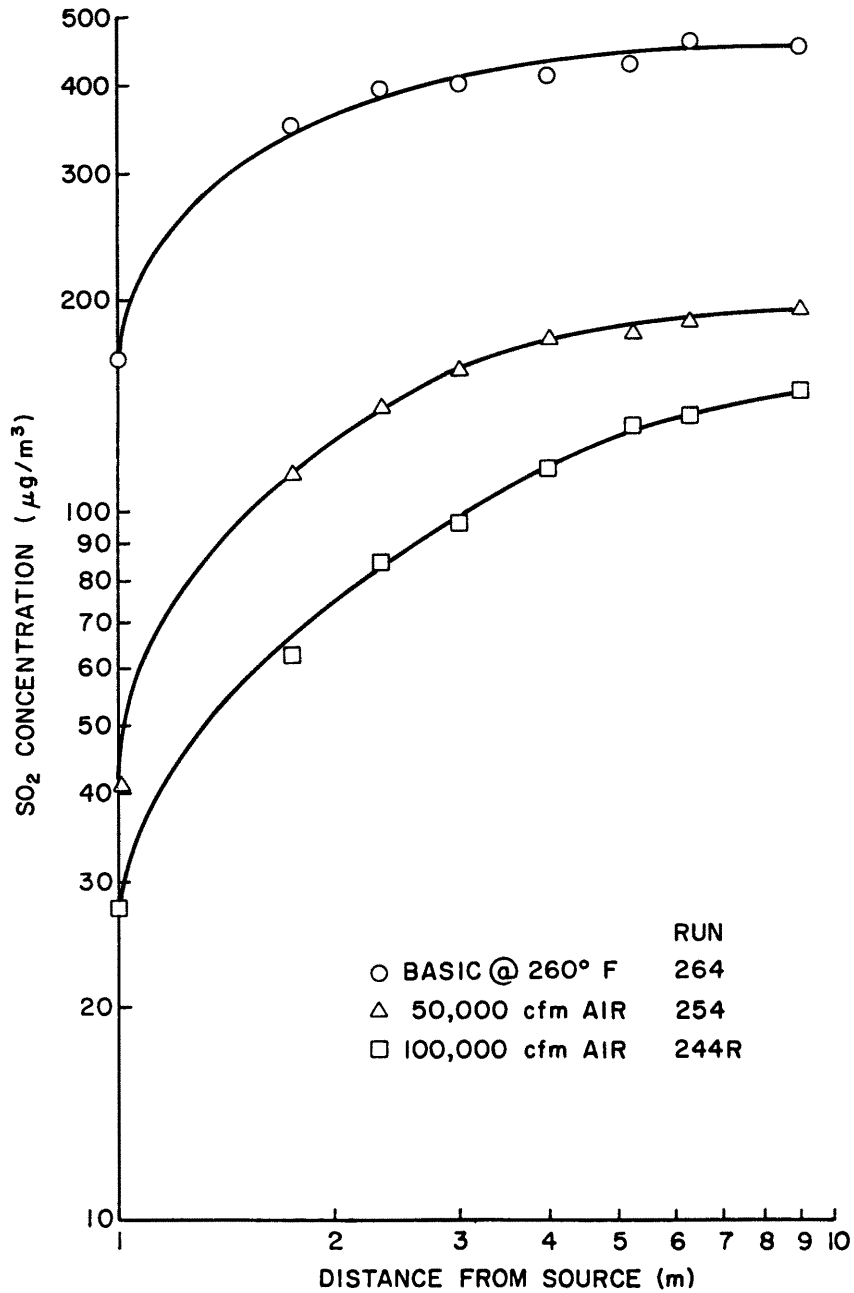


Figure 4-8c. Effect of Added Air on Ground-level  $\text{SO}_2$  Concentrations Along Plume Centerline for a 20 mph/198° Wind and Minimum Power Load.

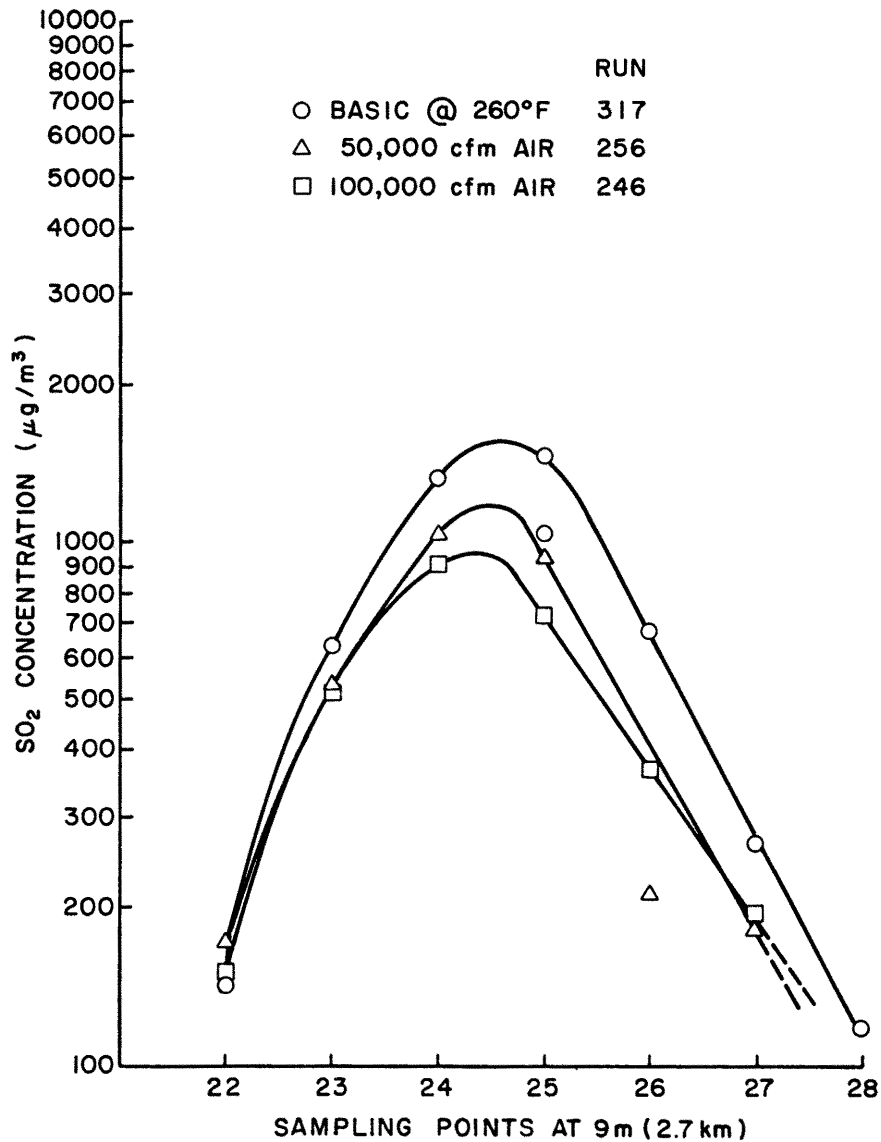


Figure 4-8d. Effect of Added Air on Ground-level  $\text{SO}_2$  Concentrations at 2.7 km for a 30 mph/198° Wind and Minimum Power Load.

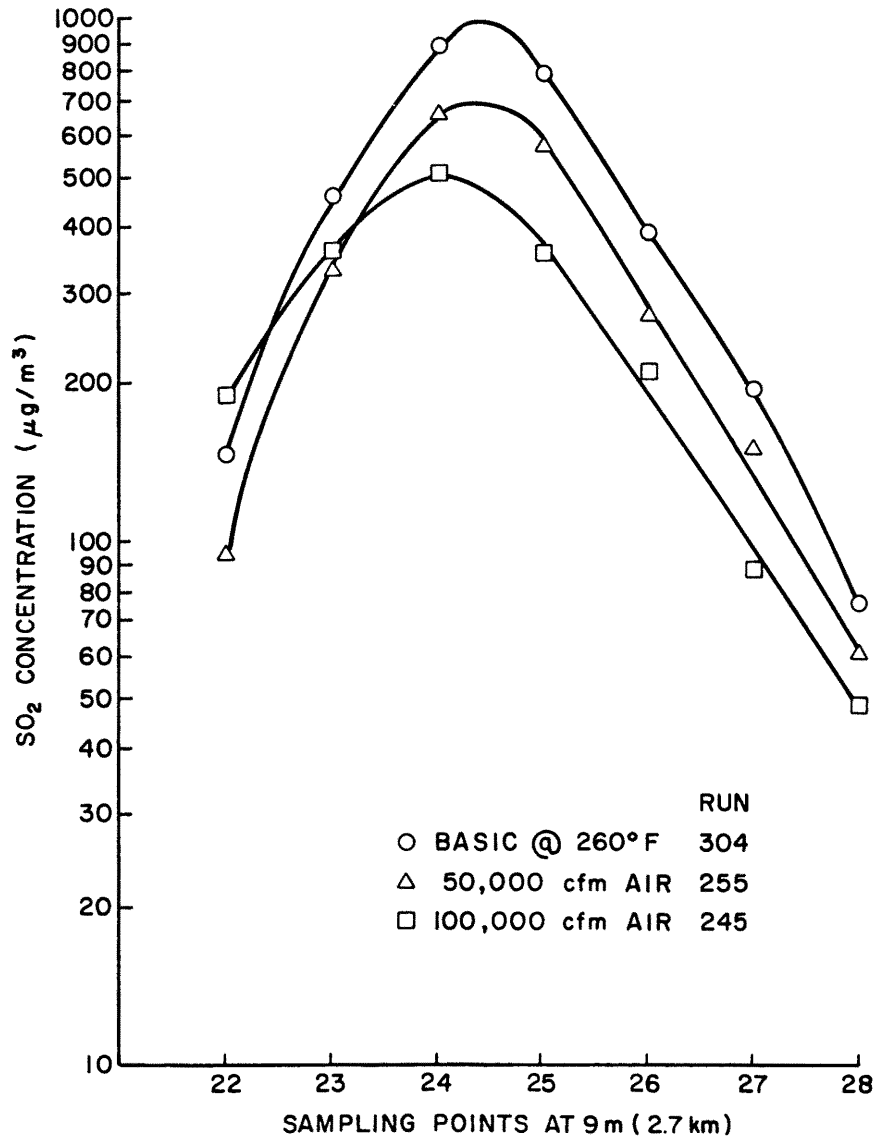


Figure 4-8e. Effect of Added Air on Ground-level SO<sub>2</sub> Concentrations at 2.7 km for a 25 mph/198° Wind and Minimum Power Load.

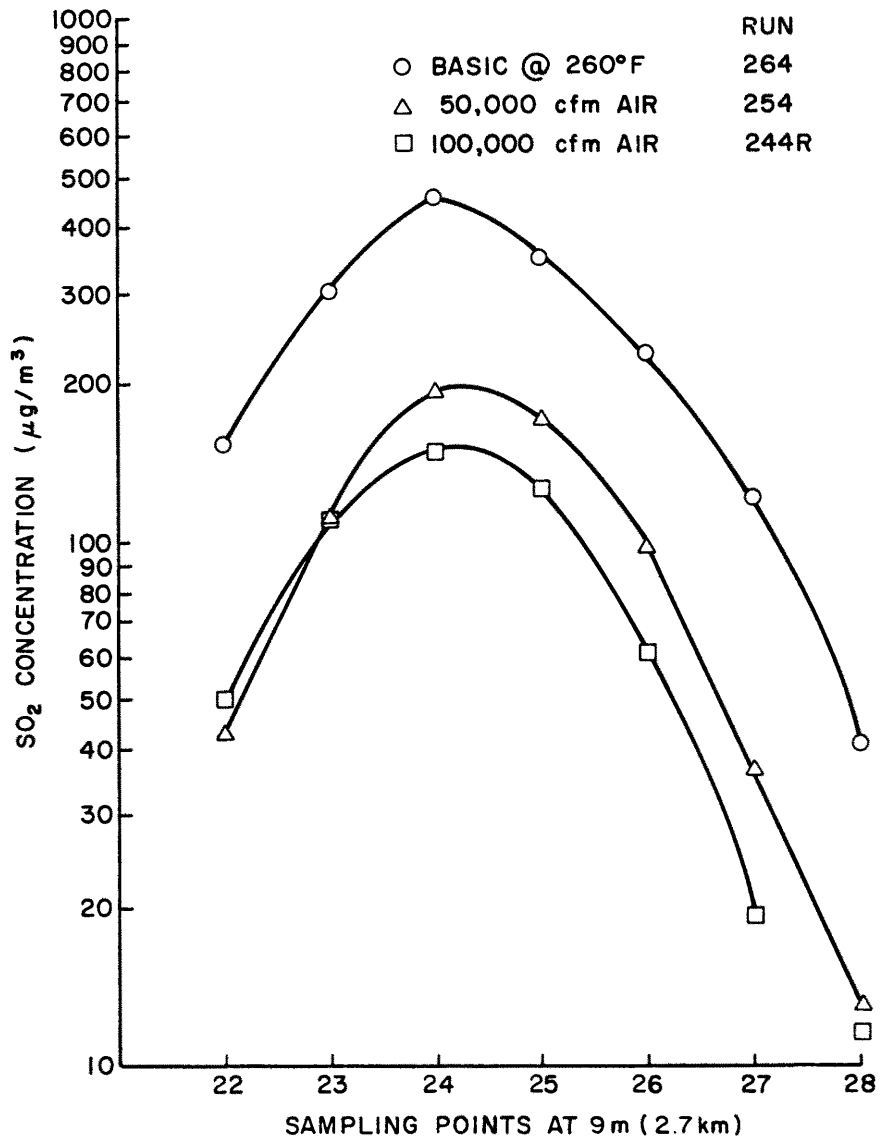


Figure 4-8f. Effect of Added Air on Ground-level SO<sub>2</sub> Concentrations at 2.7 km for a 20 mph/198° Wind and Minimum Power Load.

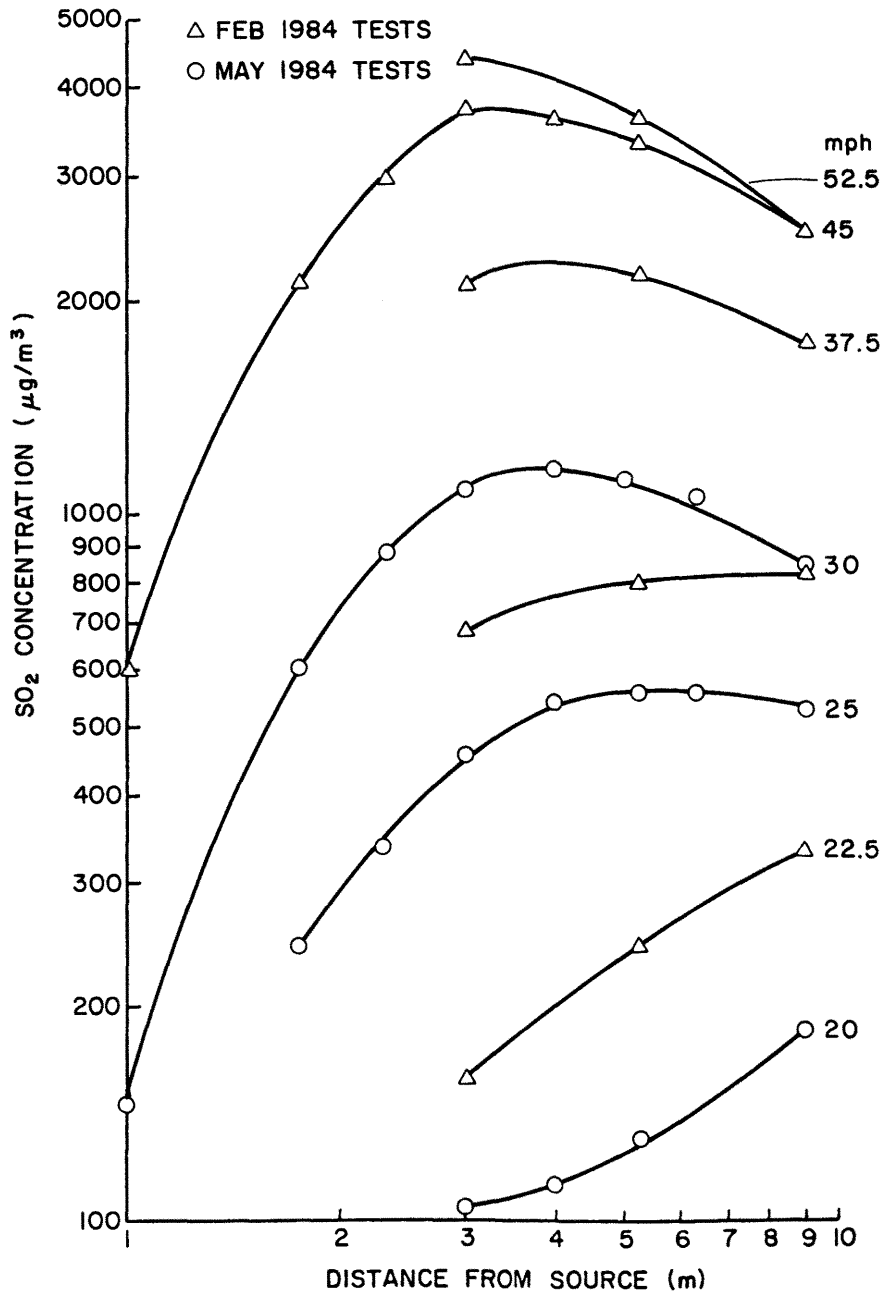


Figure 4-9a. Effect of Wind Speed on Ground-level SO<sub>2</sub> Concentrations Along Plume Centerline with Full Power Load for Existing BLES Configuration.

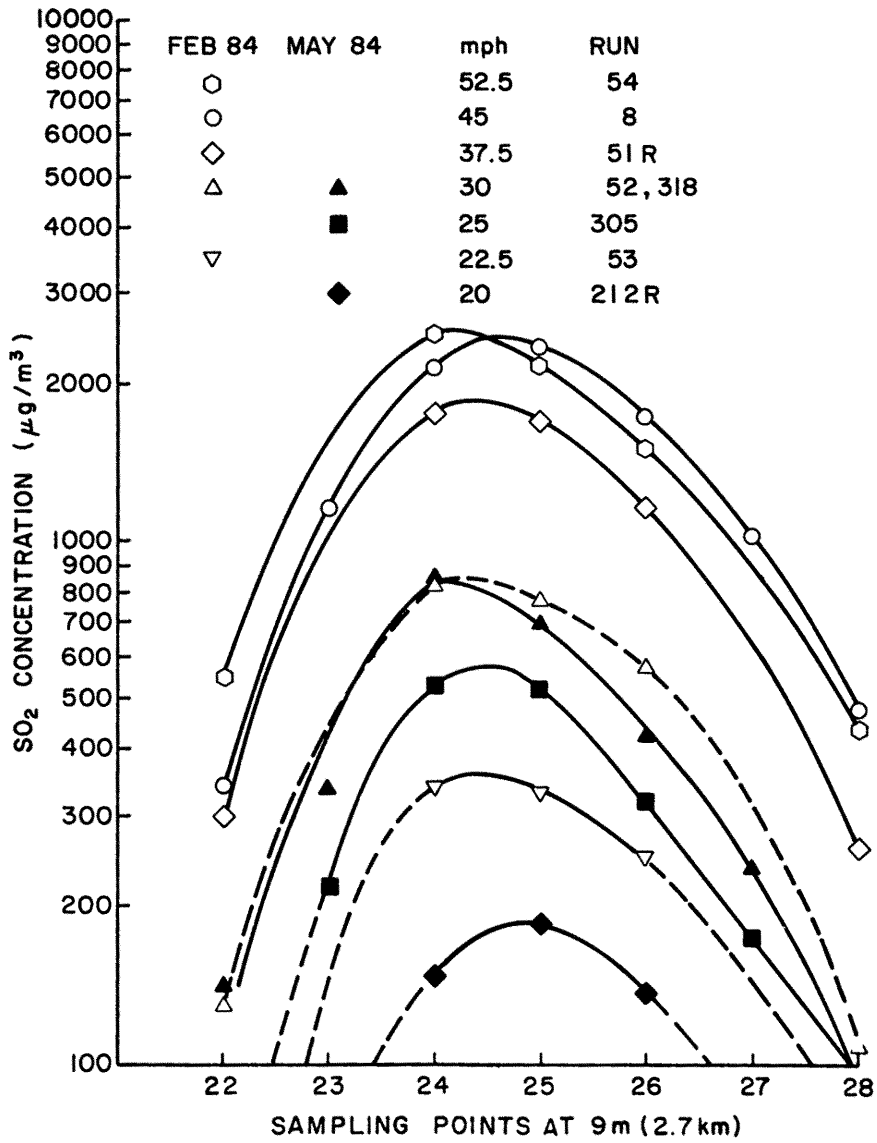


Figure 4-9b. Effect of Wind Speed on Ground-level SO<sub>2</sub> Concentrations at 2.7 km with Full Power Load for Existing BLES Configuration.

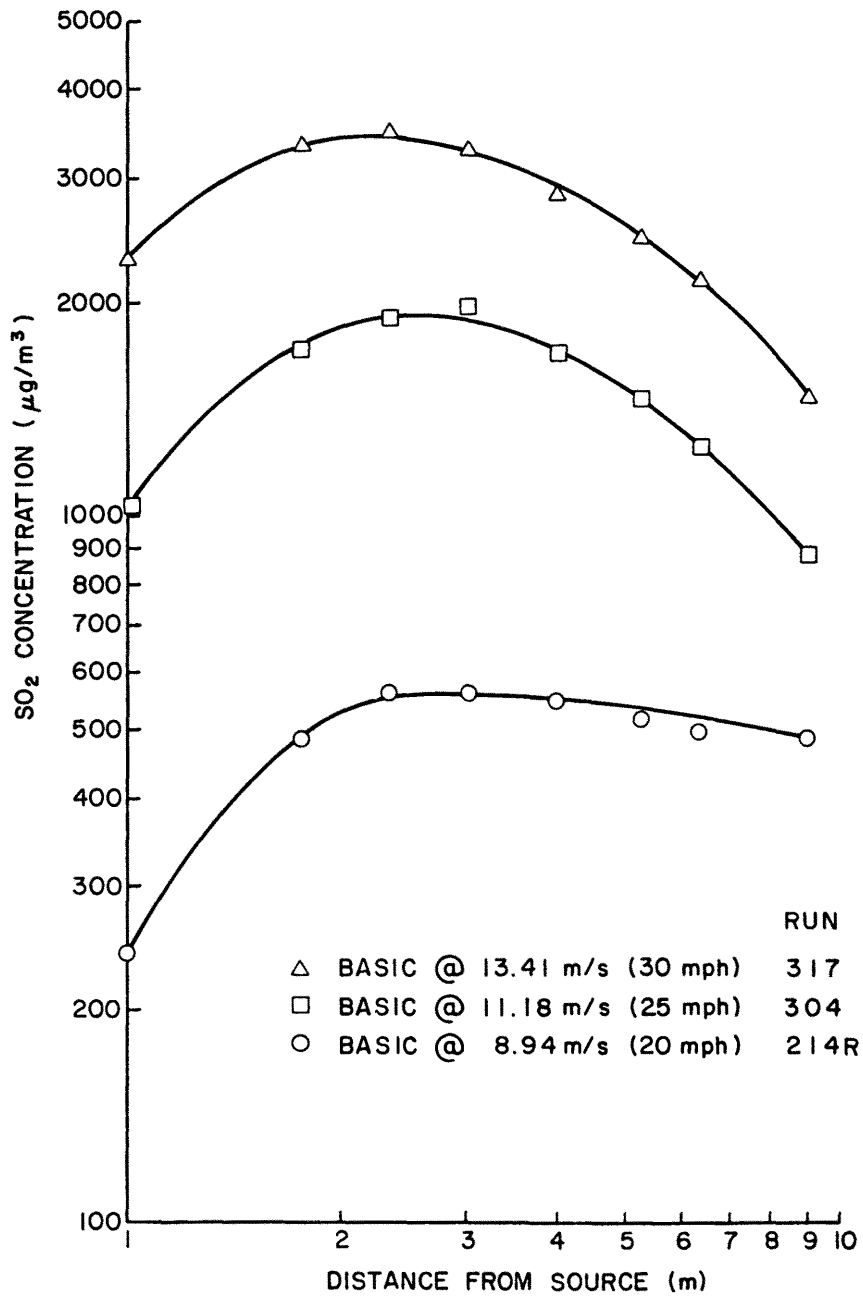


Figure 4-9c. Effect of Wind Speed on Ground-level SO<sub>2</sub> Concentrations Along Plume Centerline with Minimum Power Load for Existing BLES Configuration.

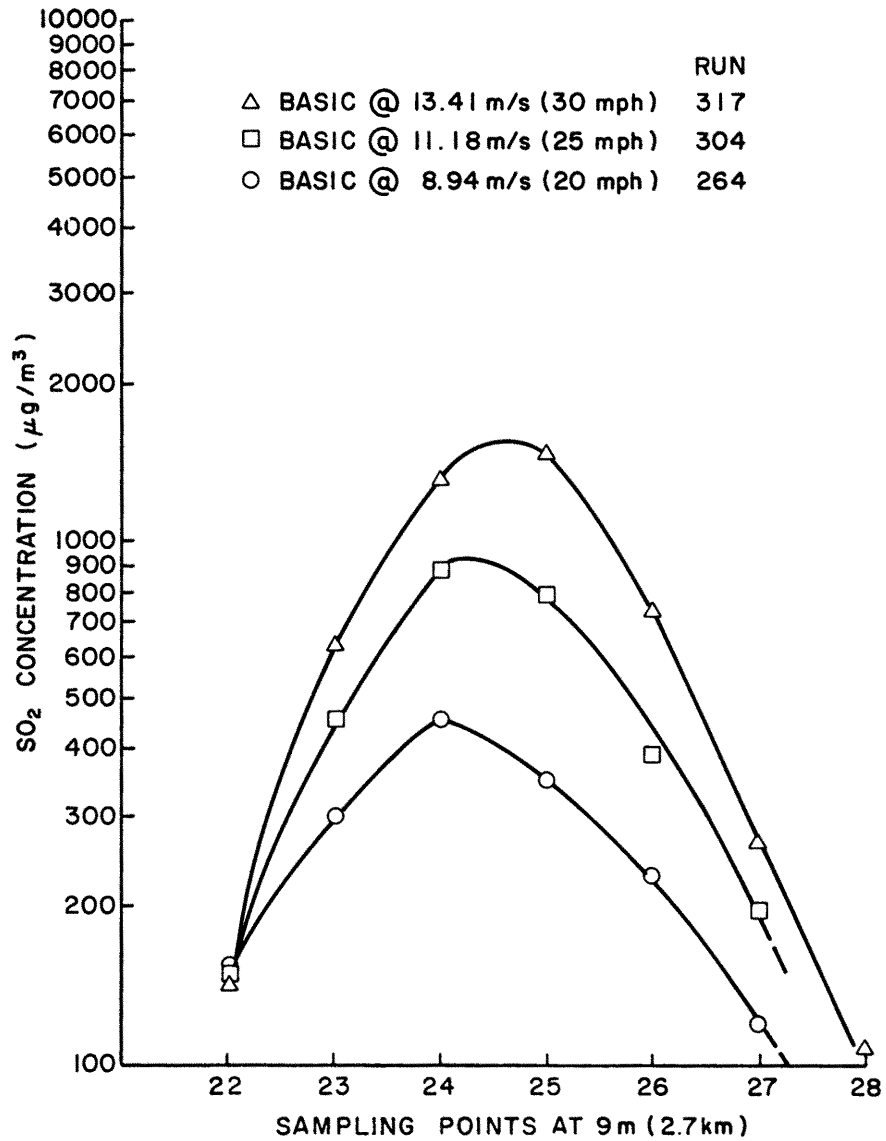


Figure 4-9d. Effect of Wind Speed on Ground-level SO<sub>2</sub> Concentrations at 2.7 km with Minimum Power Load for Existing BLES Configuration.

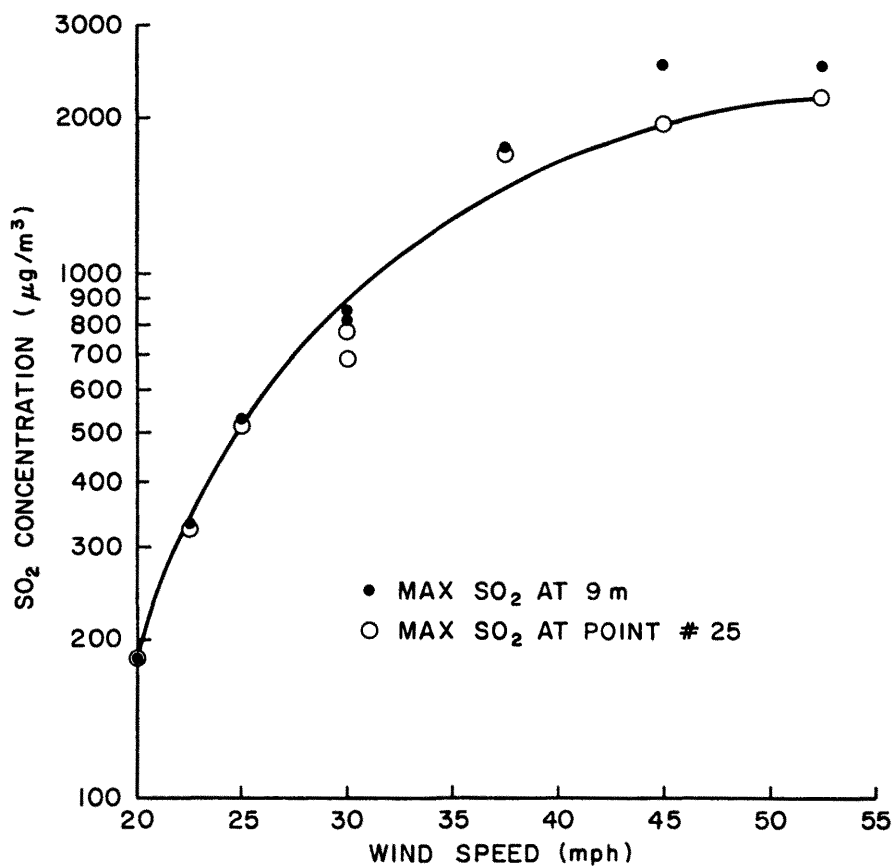


Figure 4-10a. Effect of Wind Speed on Ground-level SO<sub>2</sub> Concentrations at Sampling Point #25 with a Full Power Load.

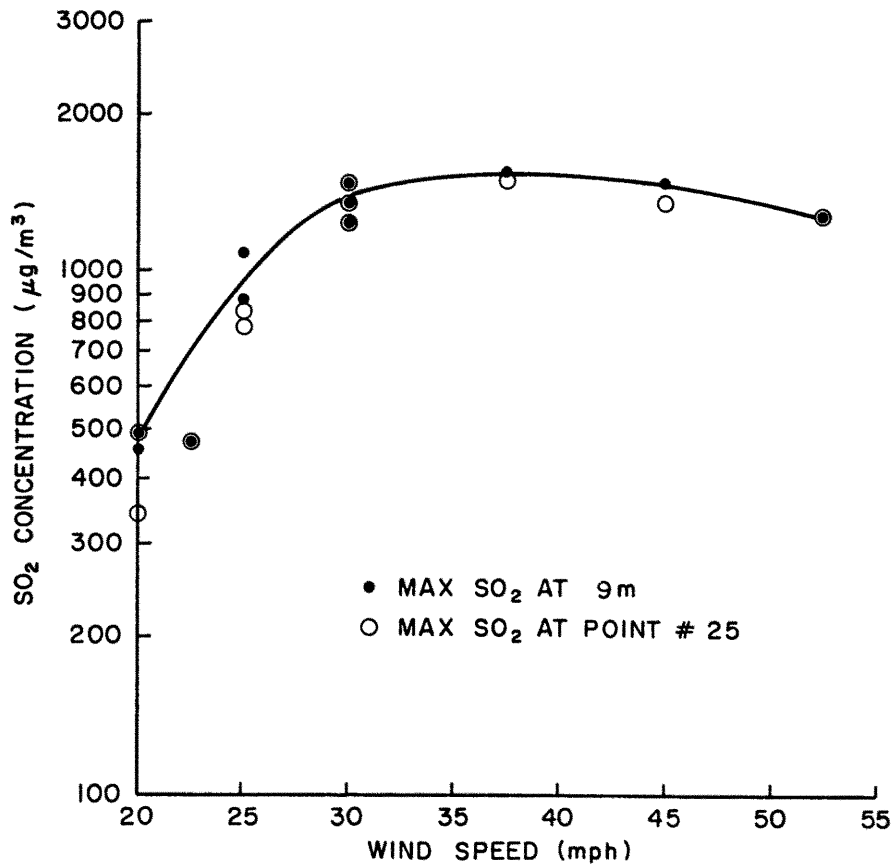


Figure 4-10b. Effect of Wind Speed on Ground-level SO<sub>2</sub> Concentrations at Sampling Point #25 with a Minimum Power Load.

## 5.0 VISUALIZATION STUDY

### 5.1 General

Making the airflow visible can be helpful in understanding flow patterns over, around and in the wakes of buildings and other structures.

Titanium tetrachloride ( $TiCl_4$ ), which readily reacts with water vapor ( $H_2O$ ) in the air to produce titanium dioxide ( $TiO_2$ ) and hydrochloric acid ( $HCl$ ), was used for these studies. The titanium dioxide appears as a white "smoke" discernible to the eye and easily photographed when illuminated.

### 5.2 Visualization Tests

Cotton swabs dipped in  $TiCl_4$  were used during the early part of the visualization tests to observe streamline patterns in the vicinity of the boiler buildings and to note any pattern changes caused by modifications to the building area. Modifications which appeared to affect the airflow were identified for concentration tests, while other suggested modifications were dismissed from further study effort. In particular, the 6.25', 12.5' and 18.75' wide airfoils positioned all along the SW edge of the building roof were rejected as viable solutions in this manner.

Table 5-1 provides a tabulation of specific test parameters/conditions which were documented on film and also serves as a key for relating numbers which appear on the photographs. Run numbers appearing in the pictures may also be correlated with information contained in Table 4-1.

Smoke for the documented photography was obtained by routing a flow of compressed air, regulated with a ball-type flowmeter, through a

supply of  $TiCl_4$  prior to release through the appropriate model BLES stacks. Tunnel speed and volume flow rates were set and monitored during the studies.

A pair of 35 mm Canon F-1 cameras were used to obtain the B&W and slides of the plume visualization study; while a Panasonic Video Recorder in VHS format was used to produce the video tape.

### 5.3 Data Analysis

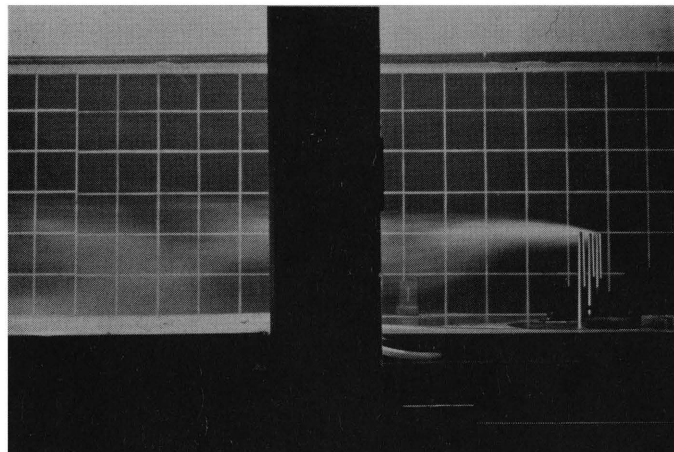
The photographs and video tape reveal some of the effects of stack height, reheat, buildings, power load, wind speed and site modifications upon plume dispersal. Figure 5-1 provides pictorial evidence of the effects of stack extensions and reheat upon the plume for minimum power conditions. Figures 5-2 and 5-3 present similar information for full power load. Figures 5-2a and 5-3b document the building's effect on downwash.

Any assessment of airflow derived from the photos should be treated as qualitative in nature and further substantiation of concentration data.

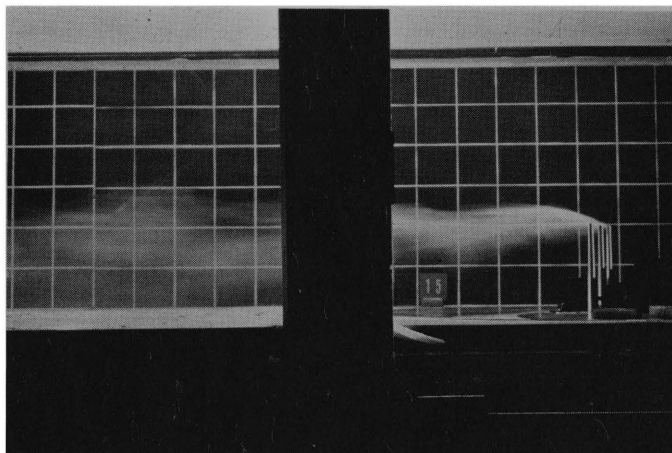
NOTE: Full sets of visualization photographs and video tapes are supplied to the sponsor separately from the formal test report.

Table 5-1. Identification Key for 35 mm Color Slides and Black and White Photos of B. L. England Station Wind-Tunnel Tests

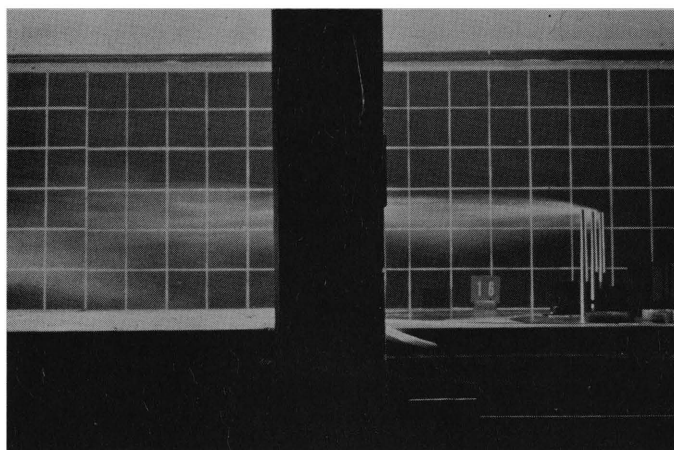
Slide # & B-W#	Description
1	Close-up of model (upwind view)
2	Close-up of model (downwind view)
3	Upwind view of model installed in MWT
4	Lab asst. installing stacks
5	Upwind view of model installed in MWT
6	Lab asst. installing trip and spires for BLES tests
7	Downwind view of vertical plume rake
8	Lab asst. installing vertical rake
9	Close-up of vertical plume rake
10	Close-up of stack, extension, and nozzle
11	Close-up of stacks, extensions, and nozzles
12	Comparison of existing stacks to a 385' comb. stack
13	Comparison of existing stacks to a 425' comb. stack
14-22	Equipment and instruments
1V	Basic configuration at full power w/45 mph wind from 198°, at 260°F
2V	Basic configuration at full power w/22.5 mph wind from 198°, at 260°F
3V	Basic configuration at full power w/67.5 mph wind from 198°, at 260°F
4V	Basic conf. at min power w/45 mph wind from 198°, at 260°F
5V	Stacks align. with wind at full pwr. w/45 mph wind from 315°, at 260°F
6V	Stacks upwind at full power w/45 mph wind from 045°, at 260°F
7V	Stacks w/o bldgs. at full power w/45 mph wind from 198°, at 260°F
8V	50' ext at full power w/45 mph wind from 198°, at 260°F
9V	Nozzles at full power w/45 mph wind from 198°, at 260°F
10V	Basic conf. at full power w/45 mph wind from 198°, at 390°F
11V	Basic conf. at min power w/45 mph wind from 198°, at 390°F
12V	50' ext at full power w/45 mph wind from 198° at 390°F
13V	50' ext at min power w/45 mph wind from 198° at 390°F
14V	50' ext and nozzles at full power w/45 mph wind from 198° at 260°F
15V	125'x275' canopy at full power w/45 mph wind from 198° at 260°F
16V	50'x275' canopy at full power w/45 mph wind from 198° at 260°F
17V	100' vert. vanes at full power w/45 mph wind from 198° at 260°F
18V	60'x300' wall at full power w/45 mph wind from 198° at 260°F
19V	50'H treeline at full power w/45 mph wind from 198° at 260°F
20V	425' comb. stack at full power w/45 mph wind from 198° at 260°F



(a)

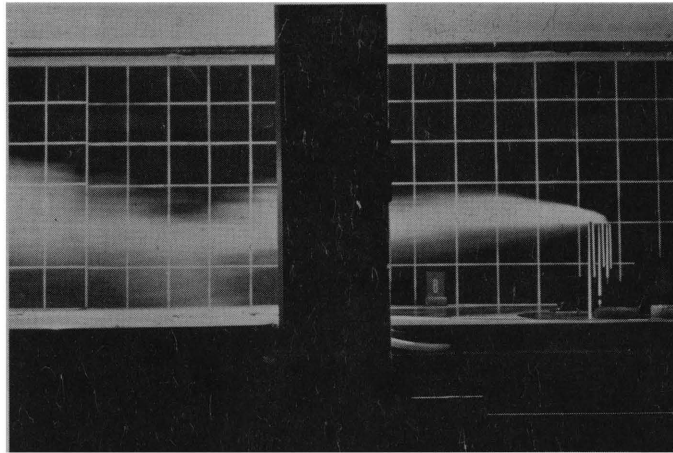


(b)

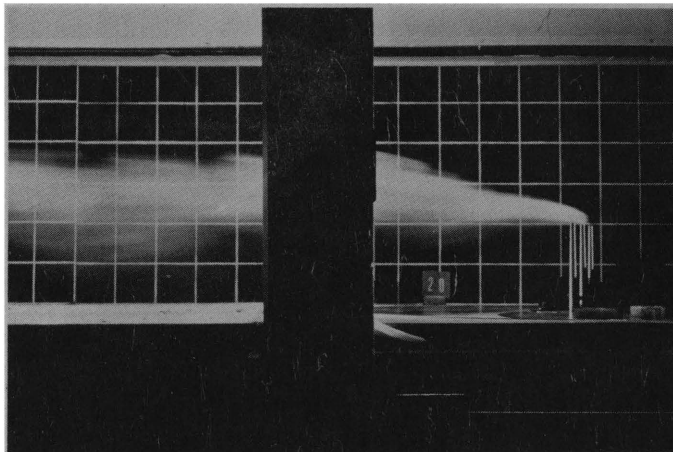


(c)

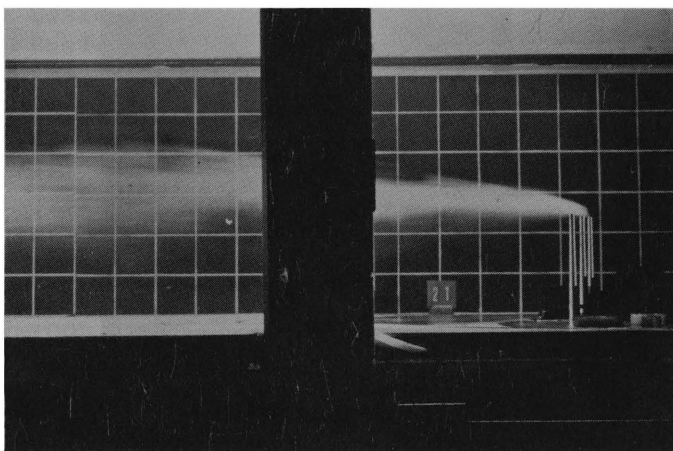
Figure 5-1. Flow Visualization at 45 mph,  $198^{\circ}$  Direction and Minimum Power for: (a) Basic, (b)  $390^{\circ}$  Reheat and (c) 50' Extensions plus  $390^{\circ}$  Reheat Conditions.



(a)

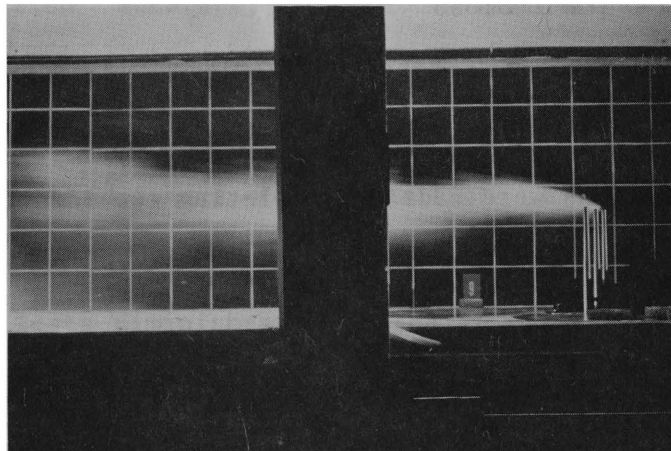


(b)

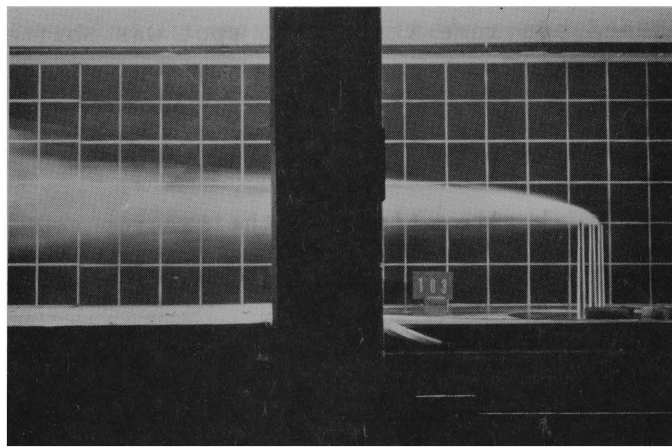


(c)

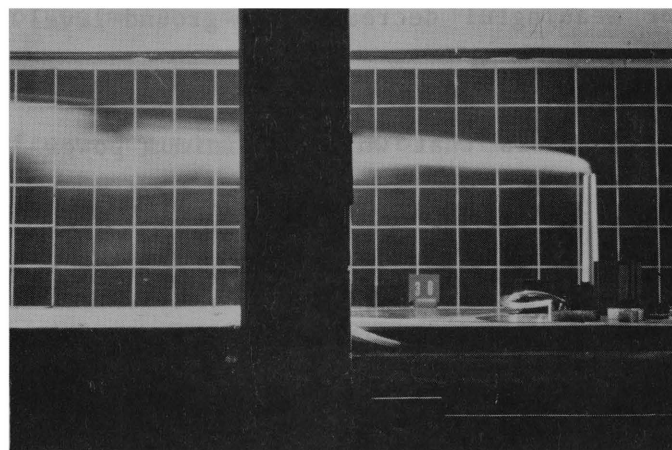
Figure 5-2. Flow Visualization at 45 mph,  $198^{\circ}$  Direction and Full Power for: (a) Basic, (b)  $390^{\circ}$  Reheat and, (c) 50' Extensions plus  $390^{\circ}$  Reheat Conditions.



(a)



(b)



(c)

Figure 5-3. Flow Visualization at 45 mph,  $198^{\circ}$  Direction and Full Power for: (a) 50' Extensions at  $260^{\circ}$ , (b) Basic w/o Buildings and, (c) 425' Multiple Flue Stack.

## 6.0 DISCUSSION AND CONCLUSIONS

Both the concentration and visualization studies provide evidence that the downwash is induced by the boiler building complex. In both studies the comparisons were made by completing two identical tests with the single exception that in one instance the boiler building complex was removed.

Modifications to the building/area, such as roof-mounted airfoils and upwind barriers provided only small changes in near-field diffusion patterns. Such fixes appear to merely shift the area where the plume touches down. Indeed, on some tests that spot was shifted sufficiently downwind to predict an increase in the readings at the Somers Point Monitor. It does not appear that  $\text{SO}_2$  concentrations can be significantly decreased by physical alterations to the station complex, other than to the chimneys.

The downstream (2.7 km) sample points reflected a high degree of correlation with stack height, buoyancy (flue gas temperature), and momentum (stack exit velocity)—all of which elevate the center of mass of the plume—for meaningful decreases in ground-level concentrations (see Table 6-1).

The data also reveals that while a minimum power load diminishes  $\text{SO}_2$  output at the stack, the resultant decrease in flow through the existing stack simultaneously reduces the exit velocity of the flue gas. The resultant change in the velocity ratio,  $V_s/u_s$ , can actually produce increases in ground-level  $\text{SO}_2$  concentrations.

Experience has revealed that for tests performed well within the modelling similarity requirements, data is repeatable to within a  $\pm 10$ -15% range. This percentage encompasses all contributors, i.e.,

instrumentation accuracy, tunnel characteristics, test equipment limitations, dial/gauge settings, and all similar factors, which weigh upon the results of any given test.

As the wind-tunnel test conditions move toward the calculated similarity and physical equipment limitations, the repeatability of individual tests diminishes. For the 20 mph data, the relative size of sample vs. background readings, location of the sampling grid with relation to the plume's boundaries and Reynold's Number limitations, all combined to reduce repeatability. The data recorded at 25 mph, 30 mph, and 45 mph revealed increasingly better repeatability.

The relative changes in concentration in model data can be used with a high degree of confidence in field situations for similar winds. A decrease in concentration levels in the model for a given configuration should produce similar changes in field data when the prototype is similarly reconfigured, for a steady-state, isothermal wind.

Cermak (10) and other references refer to documented studies, wherein model diffusion studies produced good results when compared with direct prototype measurements.

It is recognized that winds in the real atmosphere contain large scale, low frequency perturbations of both velocity and turbulence which can significantly affect dispersion of stack effluents for some time scales. These unmodelled perturbations must be taken into account when converting model results to prototype.

It is reasonable to assume that any decrease in effluent levels observed in the model for different configurations would be maintained approximately for comparable changes to the prototype.

Table 6-1. Tabulation of Percentage Reduction in SO<sub>2</sub> Concentrations for Specified Changes in Stack Operation/Configuration

	20 mph		25 mph		30 mph		45 mph	
Full Power								
	a	b	a	b	a	b	a	b
100,000 cfm air	-45	-29	-17	-30	-29	-26		
390° Reheat	-69	-54	-52	-44	-39	-39	-65	-56
50' Ext.	-66	-49	-77	-63	-55	-34	-56	-33
Ext. & Reheat	-87	-74	-89	-79	-85	-71	-87	-75
New 385' Stack	-	-	-	-	-91	-83	-74	-43
New 425' Stack	-	-	-	-	-92	-84	-90	-79
Min. Power								
100,000 cfm air	-73	-68	-66	-43	-50	-38	-	-
390° Reheat	-64	-56	-63	-41	-39	-27	-23	-14
50' Ext.					-53	-33	-42	-5
Ext. & Reheat					-82	-68	-70	-44
New 385' Stack					-84	-57	-83	-46
New 425' Stack					-90	-69	-89	-57

<sup>a</sup>Sum of Maximum SO<sub>2</sub> at 1.75, 3.0, 5.25 and 9.0 m.

<sup>b</sup>Maximum SO<sub>2</sub> at Somers Point equivalent.

## 7.0 REFERENCES

- (1) Cermak, J. E., "Wind Tunnel Design for Physical Modelling of Atmospheric Boundary Layers," Journal of the Engineering Mechanics Division, ASCE, Vol. 197, No. EM3, Proc. Paper 16340, pp. 623-642, June 1981.
- (2) Cermak, J. E., "Laboratory Simulation of Atmospheric Boundary Layer," AIAA Journal, Vol. 9, No. 9, pp. 1746-1754, September 1971.
- (3) Cermak, J. E., "Simulation of the Natural Wind," Preprint 82-518, ASCE Convention and Exhibit, New Orleans, Louisiana, 25-29 October 1982.
- (4) Halitsky, J., "Gas Diffusion near Buildings," Geophysical Sciences Laboratory Report No. 63-3, New York University, February 1963.
- (5) Martin, J. E., "The Correlation of Wind Tunnel and Field Measurements of Gas Diffusion Using Kr-85 as a Tracer," Ph.D. Thesis, MMPP 272, University of Michigan, June 1965.
- (6) Cermak, J. E. and J. Peterka, "Simulation of Wind Fields over Point Arguello, California, by Wind-Tunnel Flow over a Topographical Model," Final Report, U.S. Navy Contract N126(61756)34361 A (PMR), CER65JEC-JAP64, Colorado State University, December 1966.
- (7) Lord, G. R. and H. J. Leutheusser, "Wind-Tunnel Modelling of Stack-Gas Discharge," Man and His Environment, Vol. 1, (M. A. Ward, Ed.), Pergamon Press, 1970.
- (8) Kothari, K. M., R. N. Meroney and R. J. B. Bouwmeester, "An Algorithm to Estimate Field Concentrations in the Wake of a Power Plant Complex under Nonsteady Meteorological Conditions from Wind-Tunnel Experiments," Journal of Applied Meteorology, Vol. 20, No. 8, August 1981.
- (9) Snyder, W. H. and R. E. Lawson, "Laboratory Simulation of Stable Plume Dispersion Over Cinder Cone Butte," Technical Report by U.S. Environmental Protection Agency, May 1981b.
- (10) Cermak, J. E. and S. K. Nayak, "Wind-Tunnel Model Study of Downwash from Stacks at Maui Electric Company Power Plant, Kohului, Hawaii," CER72-73JEC-SKN28, Colorado State University, March 1973.